

DISSERTATION

MECHANISMS OF PULMONARY FIBROSIS IN PECAM-1 DEFICIENT FVB/N MICE

Submitted by

Marta Lishnevsky

Department of Microbiology, Immunology, and Pathology

In partial fulfillment of the requirements

For the Degree of Doctor of Philosophy

Colorado State University

Fort Collins, Colorado

Spring 2014

Doctoral Committee:

Adviser: Alan R. Schenkel

Steven Dow

Richard Slayden

Christopher Orton

ABSTRACT

MECHANISMS OF PULMONARY FIBROSIS IN PECAM-1 DEFICIENT FVB/N MICE

Idiopathic Pulmonary Fibrosis (IPF) is a fatal disease of the aging population that affects nearly 100,000 Americans, and its incidence has been steadily on the increase.

Patients typically present in late-stage disease, and effective early-stage diagnosis and treatment methods are thoroughly lacking. The cellular and molecular events involved in disease initiation are still unknown. There is increasing evidence that alveolar bleeding and coagulation play an important role in the initiation and progression of IPF, and anti-coagulant therapies have been shown to exacerbate the process of the disease. Most current mouse models have difficulty in reproducing the spontaneous occurrence of the disease. Platelet Endothelial Cell Adhesion Molecule-1 (PECAM-1) deficient mice on the FVB/n background spontaneously develop a fatal chronic pulmonary disease in the absence of a detectable acute inflammatory event. The studies here found that the disease observed in these animals is characterized by alveolar collapse frequently accompanied by extravasated red blood cells in the alveolar space, presence of hemosiderin-positive alveolar macrophages, fibrin deposition, and myofibroblasts in areas of developing collagen deposition. The early events hallmarked by alveolar collapse and extravasated red blood cells in alveoli are of particular importance, as identifying early pathogenic events that lead to the development of fibrotic disease can contribute to the development of preventative, diagnostic, and treatment options for the patient population with IPF.

ACKNOWLEDGMENTS

I would like to extend my heartfelt gratitude to my adviser, Alan Schenkel, who has been a wonderful mentor to me, always there for me in spite of his incredibly taxing schedule. Not only has he provided invaluable guidance, but he has also listened to all my convoluted theories about various mechanisms and provided detailed explanations to all my endless questions. I cannot express enough gratitude for his generosity of knowledge, his enthusiasm for science, and his incredible support and insight in expanding my horizons as a researcher. I cannot imagine a better advisor and hope we collaborate and work together on future projects.

I would like to extend my deepest thanks to my committee - Christopher Orton, Steven Dow, and Richard Slayden for all their encouragement, insightful questions, suggestions for experiments and teaching me how to expand and hone my thinking as an investigator - I cannot thank them enough. This dissertation would not have been possible without all their help, support and input.

A special thank you to our Department Chair, Sandra Quackenbush for her kindness, support, and keeping me afloat financially.

Another special thank you to Bill Wheat for all the encouragement, moral support, and our wonderful discussions.

I would also like to thank all the current and past lab members who have helped me in this endeavor: Merideth Early, Greta Krafur, Sandy Viboolsittisseri, Steven Woods, Lena Young, and Mike DeSarro for all their help with experiments, moral support, and most importantly - their wonderful friendship and camaraderie.

Many thanks go to the wonderful staff at LAR, especially Bianca Junge, Elisa French, and Sheryl Carter for all their help with the maintenance of our colony.

I would like to thank Anne Lenaerts, Gavin Ryan, Mercedes Gonzalez-Juarrero, Emily Driver, and Todd Bass for their incredible generosity with reagents and use of equipment, without which many of my experiments would not have been possible.

My warmest thanks go to Randy Bassaraba and Stephen Groshong for their help, and expertise.

I would like to thank Bill Muller for his generous gift of PECAM-1 deficient FVB/N mice, without which this project would not have existed.

I cannot express enough gratitude for my family: my husband Tomas and my parents Michael and Valentina. Their love, strength, and support are what often kept me going during tough times, and they are a source of inspiration to me.

A very special thank you to my great friends: Fabrizio Pacera, Tatiana Almatoff, and Lobat Asadi for all their moral support, great friendship, and scientific discussion.

Finally, a very, very special thank you goes out to Moshe Solomonow and Karen King - their encouragement, wonderful advice, mentorship, and guidance made graduate studies not only a possibility, but the wonderful experience that it was, and I cannot thank them enough.

DEDICATION

*This dissertation is dedicated to my parents Michael and Valentina,
and my husband Tomas.*

TABLE OF CONTENTS

Abstract.....	ii
Acknowledgments.....	iii
Dedication.....	vi
Table of Contents.....	vii
Chapter 1- Overview and Rationale.....	1
Chapter 2 - Introduction.....	8
2.1 Vascular Endothelium and the Pulmonary Environment.....	9
2.2 Discovery of PECAM-1.....	10
2.3 Structural characteristics of PECAM-1.....	11
2.4 Expression of PECAM-1.....	12
2.5 Ligands of PECAM-1.....	13
2.6 Splice Variants of PECAM-1.....	14
2.7 PECAM-1 Function on Endothelial Cells.....	16
2.8 PECAM-1 Function in Cell Survival.....	18
2.9 PECAM-1 and Signaling.....	19
2.10 PECAM-1 and Inflammation.....	20
2.11 PECAM-1's Role in Platelets.....	22
2.12 PECAM-1 Role in Angiogenesis.....	25
2.13 PECAM-1 and Gene Expression.....	25
Chapter 3 - Non-Invasive Diagnosis of Pulmonary Disease in PECAM-1 deficient FVB/n Mice Using Infrared Pulse Oximetry.....	27

3.1 Summary.....	27
3.2 Introduction.....	27
3.3 Materials and Methods	29
3.3.1 Pulse Oximetry.....	29
3.3.2 Histopathology.....	30
3.3.3 Picosirius Red Assessment of Collagen Deposition.....	31
3.3.4 Statistics.....	32
3.4 Results.....	32
3.5 Discussion.....	36
3.6 Figures and Legends.....	39
Chapter 4 - Microhemorrhage is an Early Event in the Pulmonary Fibrotic Disease of PECAM-1 Deficient FVB/n Mice.....	46
4.1 Summary.....	46
4.2 Introduction.....	46
4.3 Materials and Methods.....	49
4.3.1 Animals.....	48
4.3.2 Disease Stages of PECAM-1 Deficient FVB/n Mice.....	48
4.3.3 Prussian Blue Stain for Hemosiderin-Positive Macrophages in Pulmonary Tissue.....	49
4.3.4 Prussian Blue Stain for Hemosiderin-Positive Macrophages in Bronchoalveolar Lavage (BALFluid.....	49
4.3.5 Russell-Movat Pentachrome Stain for Fibrin Deposition in Pulmonary Tissue.....	50

4.3.6 Anti-Smooth Muscle Actin Stain for Myofibroblasts in Pulmonary Tissue.....	50
4.3.7 IL-10.....	51
4.3.8 Interleukin-10 (IL-10) ELISA.....	51
4.3.9 Tail Bleeding Time Assessment.....	52
4.3.10 Statistics.....	52
4.4 Results.....	53
4.4.1 Presence of Hemosiderin-Positive Alveolar and Interstitial Macrophages Increases in Tissue with the Stage of Disease.....	53
4.4.2 Fibrin Deposition increases in Pulmonary Tissue of PECAM-1 Deficient FVBn Mice with Increasing Disease Stage.....	53
4.4.3 Presence of Myofibroblasts in Pulmonary Tissue of PECAM-1 Deficient FVBn Mice.....	54
4.4.4 IL-10 Expression increases with fibrosis in PECAM-1 deficient mice.....	55
4.4.5 PECAM-1 Deficient Mice in the FVB/n Background Have Increased Bleeding Times.....	55
4.5 Discussion.....	56
4.6 Figures and Legends.....	63
Chapter 5 - Comparative Analysis of Bleomycin in the Lungs of PECAM-1 Deficient and Wild Type FVB/n Mice.....	76
5.1 Summary.....	76
5.2 Introduction.....	76
5.3 Materials and Methods.....	80
5.3.1 Animals.....	80

5.3.2 Bleomycin Delivery.by Intratracheal Instillation.....	81
5.3.3 Blood Oxygen Saturation.....	82
5.3.4 Glutaraldehyde Perfusion.....	82
5.3.5 Prussian Blue Stain for Hemosiderin-Positive Macrophages in Pulmonary Tissue...	83
5.3.6 Russell-Movat Pentachrome Stain for Fibrin Deposition in Pulmonary Tissue.....	83
5.3.7 Statistics.....	83
5.4 Results.....	84
5.4.1 Bleomycin Dosing.....	84
5.4.2 Prussian Blue stain for hemosiderin-Positive macrophages in pulmonary tissue of Bleomycin-treated PECAM-1 deficient and WT FVB/n mice.....	85
5.4.3 Russell Movat Pentachrome Stain for Fibrin Deposition in Pulmonary Tissue.....	86
5.5 Discussion.....	86
5.6 Figures and Legends.....	94
Chapter 6 - Discussion, Troubleshooting, and Future Directions.....	102
6.1 Event Timeline.....	109
6.2 Issues and Troubleshooting.....	112
6.3 Current Projects and Future Directions.....	115
6.3.1 Identification of cell type involvement in initiation and development of spontaneous pulmonary fibrosis in PECAM-1 deficient FVB/n mice.....	115
6.3.2 Examine how PECAM-1 deficient FVB/n mice react to pollution-based pulmonary insult.....	115

6.3.3 Quantification of tissue Evans Blue concentration in lung tissue of PECAM-1 deficient FVB/N mice versus WT FVB/N mice.....	116
6.3.4 Quantification of BAL Evans Blue concentration in PECAM-1 deficient FVB/N mice versus WT FVB/N mice.....	117
6.3.5 Identify coagulation mechanisms active in pulmonary fibrotic development.....	117
6.3.6 Characterizing and quantifying macrophage populations.....	118
6.3.7 Defining the role of M2 macrophages in the pulmonary environment.....	118
6.3.8 Lineage tracing myofibroblast populations.....	119
6.4 Summary.....	120
References.....	121

CHAPTER 1 - OVERVIEW AND RATIONALE

Pulmonary fibrosis is a broad term for a family of diseases where normal lung tissue architecture becomes replaced with scar tissue. They are generally marked by collagen deposition and fibroblast proliferation. Some of these pathologies have known triggers. Heavy metal dusts, some chemotherapeutics, certain mineral agents like silica and malachite dust exposure, and radiation exposure among others can result in fibrotic disease. When the cause is unknown, the disease is termed idiopathic. One of the major forms of these pathologies is Idiopathic Pulmonary Fibrosis (IPF), which strikes about 100,000 Americans per year. It is a disease of the aging, and as the population of this country ages, it will likely increase in prevalence. Currently, the only known cure for IPF is a lung transplant.

One of the problems in treatment of IPF is that patients generally present when they are already in advanced stages. Although the clinical presentation of IPF is established, its stages of trigger, initiation, and progression are still not well defined on a cellular and molecular level [1]. Recent evidence is indicating that bleeding into the alveoli and dysregulated coagulation may be important contributors to the initiation phase of the disease process [2, 3], while Noth et al in a large clinical trial has shown that anti-coagulant therapies have exacerbated the disease process in IPF patients [4].

Current mouse models use triggering agents such as bleomycin or FITC to induce pulmonary fibrosis. The triggering event in IPF is still unknown. Using specific triggering agents that evoke a large-scale inflammatory response may not mimic the events in

spontaneously occurring disease [5]. Importantly, the inflammatory hypothesis of IPF events has not come under scrutiny. If inflammation was driving IPS, there would be an apparent inflammatory infiltrate, which is not seen in IPF. Another important factor is patients' lack of response to immunosuppressive therapies, and indeed immunosuppressive therapies have now come under question of possibly even exacerbating the course of the disease [6]. A murine model with a non-inflammatory profile of spontaneously occurring pulmonary fibrotic disease would therefore be especially useful in mapping out disease events, and contribute to developing new and effective therapies for the human population.

Platelet Endothelial Cell Adhesion Molecule-1 (PECAM-1, CD31) deficient FVB/n strain mice develop a spontaneous fatal pulmonary fibrosis seemingly in the absence of a detectable acute inflammatory event [7, 8]. The earliest events of fibrotic process in these animals appear to be alveolar enlargement and red blood cells in the alveoli. Although PECAM-1 is knocked out systemically, no other organ is involved, and there is no bias for gender. The disease can occur at any age and shows an incomplete penetrance of about 50%, with some cage mates and litter mates developing the disease, while others remain healthy even into advanced age (2 years for mice).

PECAM-1 is an important regulator of endothelial integrity and vascular permeability [9-11]. It is a single-pass transmembrane multifunctional protein that is expressed on all endothelium, platelets, and most leukocytes. It is used for extravasation from blood into tissues by leukocytes [12, 13], to clear dead PECAM-1 positive leukocytes [14, 15], and

for endothelial cell-cell communication and adhesion, and it is used by platelets during thrombosis, where PECAM-1 deficient platelets have larger thrombi and increased thrombus contraction [16].

The spontaneous disease in PECAM-1 deficient FVB/n mice is hallmarked by loss of vascular integrity in pulmonary blood vessels and especially alveolar capillaries, showing microhemorrhages into the alveoli, which eventually result in progressive fibrosis with a consistently fatal outcome. This model can have an important role in elucidating early, middle, and late events of this process, with the early events being of particular importance as potential therapeutic targets for prevention and intervention.

Initially, our a priori hypothesis was that inflammation played a role in the development of disease in these animals. However, over time, an anti-inflammatory profile was observed, marked by increased expression of IL-10, TGF β , presence of FOXP3+ CD4+ T-cells at the later stages of disease progression, and alternatively activated macrophages identified by Ym1 crystals, indicating more in common with a dysregulated repair cycle.

Based on our preliminary data, the central hypothesis for this thesis is that the expression of PECAM-1 is essential to the regulation of vascular integrity of the pulmonary vessels, and to the maintenance of normal coagulation in the lung.

The rationale for this project is that identifying a stepwise progression of events that contribute to the development of spontaneously occurring pulmonary fibrosis in a mouse model may contribute to new diagnostic strategies and therapeutic intervention for human disease, particularly in the early stages of IPF. The long-term goals are to identify the trigger(s) that initiate pulmonary fibrotic events in these animals, and further define the mechanisms used by PECAM-1 to regulate vascular integrity and clotting function.

For Specific Aim 1, the objective was to find the earliest physiologic changes in the spontaneous fibrotic disease of PECAM deficient mice. In order to accomplish that, a reliable and straightforward system for disease scoring and classification needed to be developed. The first step in this development was using the pulse oximetry system which measures arterial blood oxygen saturation. Picrosirius Red stain was used to correlate blood oxygen readings and collagen deposition. This aim is important because it allowed the identification of the stages of disease in a non-invasive manner. These stages of disease could then be confirmed by pathology, showing that early alveolar damage/enlargement occurs prior to actual collagen deposition/fibrosis in these mice. Since this stage does not yet have heavy collagen deposition, it may be the decisive point for pharmaceutical intervention, which could contribute to novel approaches for human pulmonary fibrotic disease.

For Specific Aim 2, the goal was to characterize microhemorrhaging into the alveoli as an essential mechanism in the initiation of spontaneous disease by correlating evidence

for vascular leakage with disease progression using Prussian Blue stain. Additionally, fibrin deposition was evaluated by the use of Russell-Movat Pentachrome stain, IL-10 expression was evaluated by ELISA and IHC, presence of myofibroblasts was evaluated by the use of anti-smooth muscle actin IHC, and clotting time was evaluated by tail nicks in these animals. This aim is important because it shows bleeding and clotting being present in alveolar damage in these animals, which can also be exploited for drug intervention.

For Specific Aim 3, the goal was to test the sensitivity of PECAM-1 deficient mice in the gold standard bleomycin model of pulmonary fibrosis. This was done by using the widely used method of single-dose intratracheal bleomycin instillation.

While we expected PECAM-1 deficient FVB/n mice to be sensitive to the intratracheal bleomycin insult, they have shown to be resistant, with no significant difference in response between the WT and PECAM-1 deficient groups.

In examining the lung pathology of bleomycin treated animals, we saw the presence of heavy inflammatory infiltrate in areas of moderate and heavy fibrosis, which we do not see in untreated PECAM-1 deficient mice in their spontaneously occurring disease. We also detected an unexpected appearance of hemosiderin-positive macrophages, that appeared in their highest numbers at 0.5U, with deposition pattern ranging from diffuse to clumped pockets of cells. PECAM-1 deficient animals had what appeared to be an increased presence of these cells, however that needs to be quantified in future studies with automated imaging software to be confirmed. Fibrin deposition was examined

using Russell-Movat Pentachrome stain, and ranged from pale and clearly visible in areas of preserved lung architecture, to very diffuse and interspersed with deposited collagen in areas of heavy fibrosis.

The importance of this aim lies in showing that PECAM-1 deficient and WT FVB/n mice were virtually identical in their ability to withstand the bleomycin insult even at the highest dose, suggesting that a large-scale inflammatory event is not the cause of spontaneous disease in the PECAM-1 deficient animals. It was also interesting to observe the differences of fibrotic pattern in the treated and untreated PECAM-1 deficient sick mice. Single-dose bleomycin instillation did not mimic the pattern of disease we see in untreated PECAM-1 deficient mice that develop disease. This may be due to intratracheal delivery of bleomycin, which directly targets the epithelium, whereas we believe the events in untreated animals to start with the endothelium. It may also be that the slow and repetitive low-dose intravenous method of bleomycin delivery would better mimic the naturally occurring disease events than a single-dose large scale insult approach.

Contribution to the Field

Spontaneously occurring disease mouse models of IPF are greatly needed to study pathogenic events that are not due to administration of a specifically administered stimulus. This thesis uses the model of PECAM-1 deficient FVB/N mice that do develop a spontaneously occurring pulmonary fibrotic disease, to show that microhemorrhaging into the alveoli is an important event in the initiation and progression of pulmonary

fibrotic disease. We now know that alveolar collapse is an early stage disease event in these animals, and hemosiderin-positive macrophages make an appearance when the animals still show healthy arterial oxygenation, indicating that pathogenic events are already taking place when normal lung structure appears otherwise healthy. We are now able to diagnose disease non-invasively, separate it into stages of pathology, and characterize each stage histologically and on a molecular level, showing that microhemorrhaging is an early stage event that positively correlates with alveolar enlargement, deposition of fibrin, increasing levels of IL-10, appearance of myofibroblasts and collagen deposition. This helps to further characterize microhemorrhaging into the alveoli of PECAM-1 deficient animals, and PECAM-1's role in the initiation and progression pathways of pulmonary fibrotic events, with the goal of contributing to the development of new diagnostic and therapeutic approaches for use in the human patient population.

CHAPTER 2 - INTRODUCTION

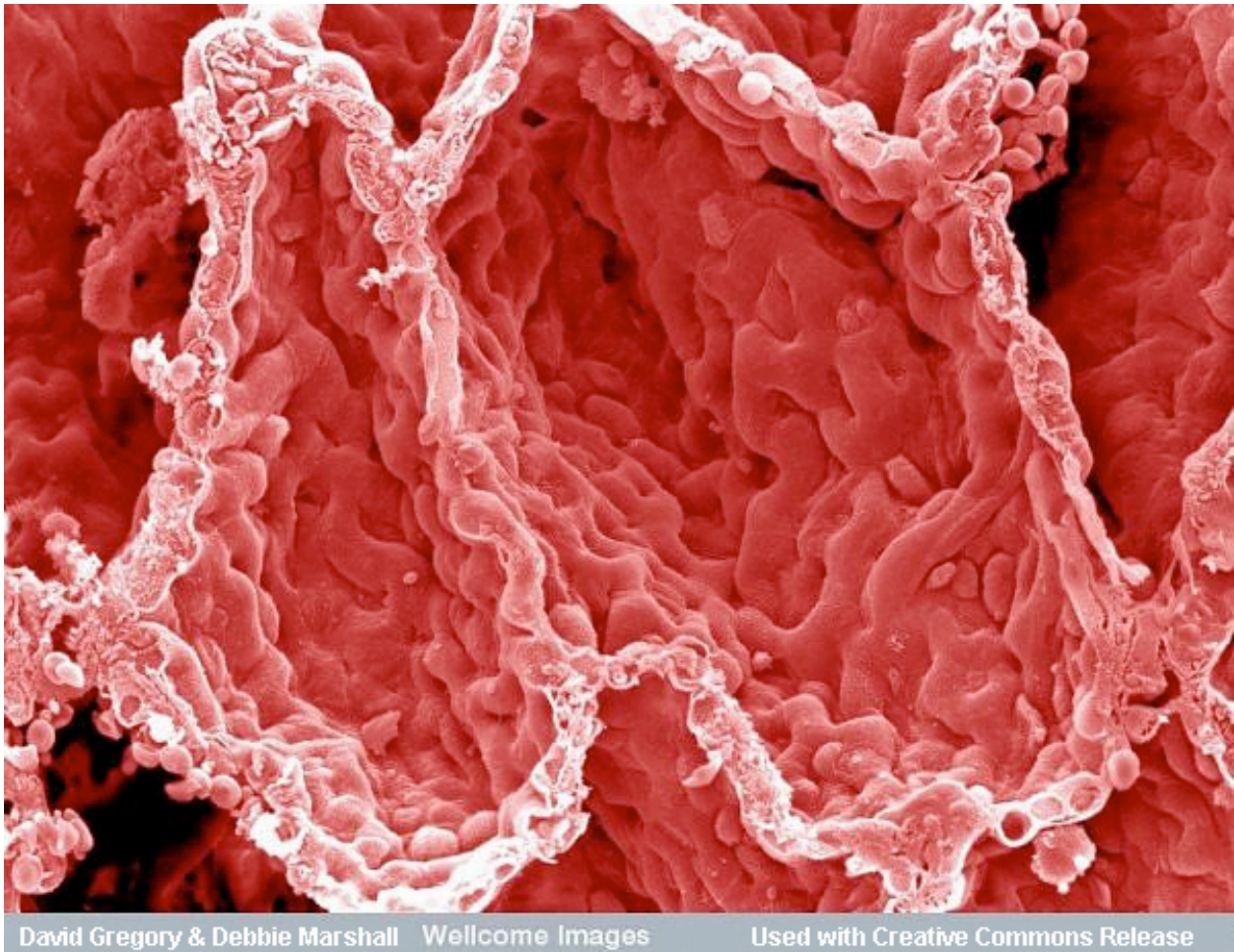


Fig. 2.1. Scanning Electron Microscopy image of alveoli in the lung

The purpose of this thesis project is to study the role of PECAM-1 in the regulation of the pulmonary vascular barrier and clotting function of the lung in pulmonary fibrosis.

This chapter will review the physiologic roles of PECAM-1 in the pulmonary environment and in other functional studies.

2.1 Vascular endothelium and the pulmonary environment

The vascular endothelium is composed of flat cells with a central nucleus, about 1-2 μm thick and 10-20 μm in diameter, that line the insides of vessels. The ones in direct contact with the blood are called vascular endothelial cells, while the ones in contact with lymph are called lymphatic endothelial cells. The junctions between adjoining endothelial cells have overlapping areas that help keep a tight seal on the vessel [17].

Vascular endothelial cells perform multiple tasks. Endothelial barrier function serves to prevent blood components from leaking into the tissues. In maintaining barrier function, the endothelium monitors the passage of white blood cells (WBC's) from the lumen of the blood vessel into tissues. The endothelium is also important in the clotting and fibrinolysis function, and under normal conditions maintains a non-thrombogenic microenvironment. Endothelial cells activate and recruit leukocytes in the process of inflammation, and direct leukocytes from the lumen of the blood vessel into tissues in the process of extravasation. The endothelium is also a critical component in the control of functions such as vascular tone, vasculogenesis and angiogenesis, and gas exchange. The capillary endothelium of the lung is made up of very thin endothelial cells that rest on a thin basement membrane. The intercellular junctions of capillary endothelial cells form a tight barrier between the blood and tissue. The molecules on the surface of endothelial cells act as receptors, docking and communication sites. The ones that control the communication and junction integrity between endothelial cells are particularly important for continued performance of barrier function [17-21]. Knowledge about their structure and function is important for possible therapeutic approaches.

2.2 Discovery of PECAM-1

Platelet Endothelial Cell Adhesion Molecule 1 (PECAM-1) was discovered in the late 1980's as a marker of differentiation for myeloid cells [22]. Concurrently, antibodies were being developed for endothelial cell integral membrane protein, which at the time was being called EndoCam [23, 24]. These antibodies were found to cross-react with transmembrane glycoprotein expressed on both platelets and endothelial cells. The two studies collaborated as CD31, EndoCAM, and the platelet/endothelial cell glycoprotein were found to be the same molecule [23, 25]. For ease of nomenclature, it was renamed Platelet Endothelial Cell Adhesion Molecule 1 (PECAM-1).

PECAM-1 is a single-pass glycoprotein of 130-kDa, that is differentially glycosylated involving N-linked and O-linked glycosylation sites. It is comprised of six C2-type Ig-domains, a transmembrane region and a cytoplasmic tail. PECAM-1 is differentially expressed on tissues, having higher expression in the lung, kidney, and heart, and less so in the liver and brain [26]. PECAM-1 is expressed on all vascular endothelium, with the highest density in the junctions of adjoining endothelial cells (10^6 copies per cell). It is expressed by macrophages, neutrophils, monocytes, mast cells, natural killer cells, naive T cells, naive B cells and platelets. It is not expressed by fibroblasts, epithelial cells, red blood cells, and is cleaved from the surface of activated lymphocytes [27].

PECAM-1 functions include leukocyte extravasation, mediation of integrin-mediated cell adhesion, angiogenesis, apoptosis, cell migration, negative regulation of immune cell

signaling, autoimmunity, macrophage phagocytosis, IgE-mediated anaphylaxis and thrombosis [27].

2.3 Structural characteristics of PECAM-1

PECAM-1 has six extracellular Ig-like domains, a transmembrane domain and a cytoplasmic tail [25]. Extracellular domains 1 and 2 are used for PECAM-1 to PECAM-1 homophilic interactions while domains 1, 2, and 6 are involved in homophilic and heterophilic interactions with PECAM-1 and other ligands [28].

The cytoplasmic tail of PECAM-1 has two immunoreceptor tyrosine inhibitory motifs, which is what reassigned it from the CAM subfamily to the immunoglobulin gene superfamily that is characterized by such domains on the cytoplasmic portions [29]. Upon activation, the tyrosine residues of the ITIM motif get phosphorylated and can then serve as docking stations for the SH2-domain holding signaling molecules. SHP-2 was the first SH-2 domain molecule shown to communicate with PECAM-1 [27], while other SH2 domain containing molecules such as She, Grb2, Src, PI3 Kinase, and Crk-L were also found to interact with PECAM-1 [30, 31], impacting signaling mechanisms that regulate such functions as the migration, adhesion, and survival of endothelial cells [27, 31].

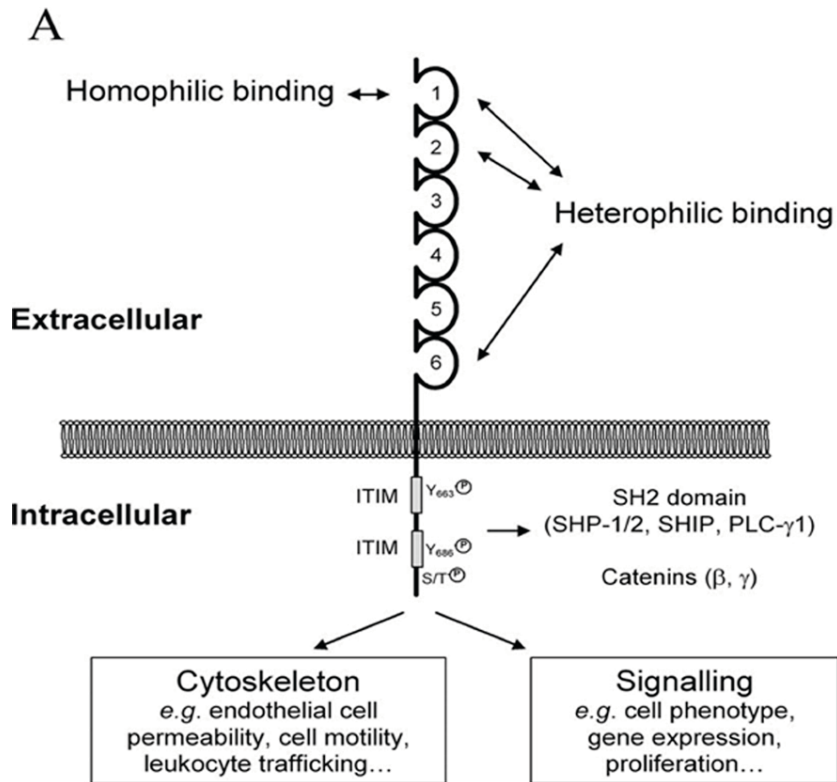


Fig. 2.2. Structure of PECAM-1 [32].

2.4 Expression of PECAM-1

PECAM-1 is expressed to a high extent in the lungs, kidney, and heart, and less so in the liver and brain. PECAM-1 gene is a single allele that encodes a single molecule of mRNA. The transmembrane or cytoplasmic domain of the mRNA molecule can be alternatively spliced to generate multiple isoforms of PECAM-1. Expression of PECAM-1 appears to be species-specific, tissue-specific, and cell-specific.

Humans mainly express the full-length PECAM-1, but do express alternative isoforms on endothelial cells - Δ -exon 14 form and Δ -exon 13, and a soluble form of PECAM-1

that is made by splicing out the transmembrane exon 9 being examples of alternative splicing in humans.

Mice express very little full-length PECAM-1. Mouse PECAM-1 gets highly spliced, especially at exons 12, 14, and 15, which give the eight endothelial isoforms [26, 33, 34].

In mice, isoforms with exons 14 and 15 spliced out (A14&15) appear to be the primary endothelial forms used. In the mouse heart, the isoform with exon 15 spliced out (A15) is the primary form used. Other forms commonly used by mice are A12&14, A12&15 and A12,14&15. The A13 isoform that is predominant in humans, is absent in mice entirely [26], and the consequences of these variants are still under question.

2.5 Ligands of PECAM-1

PECAM-1 mediates endothelial cell-cell adhesion by homophilic interactions, when PECAM-1 on one endothelial cell binds PECAM-1 on an adjacent endothelial cell. PECAM-1 extracellular domains 1 and 2 are used for homophilic interactions, while domain 6 and also domains 1 and 2 serve for heterophilic interactions by binding ligands such as $\alpha_v\beta_3$, CD38, 120-kDa ligand on T cells and heparin-dependent proteoglycans. Domains 3, 4, and 5 are as of yet undefined. CD38 is surface marker for lymphocytes and its interaction with PECAM-1 is thought to be important in the leukocyte's signaling and adhesion, while interaction between PECAM-1 and integrin $\alpha_v\beta_3$ affects integrin activity [35-38].

In their 1992 study, Tanaka et al challenged resting peripheral human T-cells with PECAM-1 antibodies and saw that by increasing integrin activity, it increased their adhesion to the integrin ligands vascular cell adhesion molecule 1 (VCAM-1) and fibronectin. This was blocked by antibodies to integrins [39]. This shows that PECAM-1 may mediate integrin activity. In other studies, antibodies that mimicked ligand binding to PECAM-1 were shown to cause change in β -integrins, leading to increased adhesion of lymphocytes to endothelial cells [38, 40].

Several studies implicate PECAM-1 in interacting with integrin, thereby affecting cell-cell and cell-matrix adhesion, an affect that seems to involve only the β 2 integrins. Yet more studies indicate that antibodies to PECAM-1 can activate β 2 and β 3 integrins found on other cells [41-43]. Studies that looked at dimerization and oligomerization of PECAM-1 by the use of a dimerizer show it affecting integrin activity, increasing adhesion to fibronectin [44]. The modulatory effect PECAM-1 appears to have on integrin function could play an important role in EC cell-cell and matrix adhesion, EC migration, leukocyte extravasation, and contact apoptosis [35, 36, 39, 42, 44-46].

2.6 Splice variants of PECAM-1

How PECAM-1 interacts with its ligands may be controlled by which splice variant it is. Some isoforms may be predisposed towards homophillic binding and others towards heterophillic, with cells expressing isoforms on need to need basis. A transfection of full-length PECAM-1 into a murine fibroblast cell line (L cells) induced heterophillic binding, but a systematic deletion of its cytoplasmic tail affected cell aggregation. PECAM-1

isoforms without exon 14 promoted aggregation through homophilic binding. Isoforms that included exon 14 promoted heterophilic binding. Analysis of exon 14 showed that the switch between homophilic and heterophilic preference resides in the presence and phosphorylation of the tyrosine residue of exon 14 [33, 47-50]. Alternative splicing would help explain the multifunctional nature of PECAM-1, as the organism controls which splice variants to express, how many, and on which cells and/or tissues in order to gain the most impact with the least energy expenditure.

During their differentiation, leukocytes express PECAM-1 that they do not express in resting state. Isoforms without exon 14 are generally present at the stage of hematopoietic activation. This may be because the regulatory mechanism for homophilic interaction is needed for aggregation and extravasation [31].

Additionally, subsets of T-cells and B-cells express PECAM-1. It is noted in downgrading the signaling of the T-cell receptor (TCR) [51, 52]. Crosslinking of TCR or PECAM-1 on the surface of T-cells induces PECAM-1 to phosphorylate, leading to the interaction with SHP-2 and subsequent downregulation of calcium release from intracellular stores - an action that depends on the ITIM motif being present for SHP-2 docking. This may be why when leukocytes activate, they isotype switch or downregulate the PECAM-1 they express, as it may be inhibitory to activation. In a similar manner, PECAM-1 can also dampen B-cell receptor activation, which is also dependent on the ITIM domain being available for SHP-2 docking [51].

Determining the properties of PECAM-1 isoforms and their function is important for deciphering which species and cell types selectively express which isoforms and why.

2.7 PECAM-1 function on endothelial cells

PECAM-1 expression on vascular endothelial cells is at approximately one million copies per cell [53]. PECAM-1 involvement in the maintenance of vascular permeability barrier has been shown in formation and maintenance of cell-cell contact and adherence, where it is concentrated in the lateral junctions of endothelial cells. It has also been shown to be involved in endothelial cell migration [54, 55]. Cultured PECAM-1 deficient endothelial cells show increased permeability when challenged with histamine, in comparison to PECAM-1 reconstituted endothelial cells [9].

The connection between PECAM-1 and endothelial cell migration was made in 1992 by Schimenti et al. when they found that the expression of the full-length PECAM-1 promoted cell adhesion while reducing migration, while endothelial cells with PECAM-1 knocked out lacked adhesion and were more prone to migration [54]. Bovine aortic endothelial cells (BAEC) express high levels of PECAM-1. Overexpression of PECAM-1 in this cell line did not affect migration, indicating that enhanced expression did not affect function [56, 57]

On the other hand, PECAM-1 deficient endothelial cells also show reduced capillary morphogenesis, paralleling vascular development defects such as reduced vascular density and increased vessel dilation that has been observed in PECAM-1 deficient

mice. Studies have shown that PECAM-1 deficient mice cannot mount a neovascular response to hypoxic or inflammatory challenges, as is consistent with endothelial cell migratory defects. DiMaio has shown that that re-expression of PECAM-1 in PECAM-1 deficient endothelial cells restored their migratory and capillary morphogenesis defects in an isoform-specific manner [58]. The differences in migrational behavior in PECAM-1 deficient endothelial cells may also be due to their behaving differently in vivo rather than in vitro.

Sheibani et al and Wang et al indicate that PECAM-1 regulation of cell adhesion and cell migration could be isoform-dependent [31, 59]. Phosphorylation of exon 14 tyrosine (Y686 of human PECAM-1) could be a decisive factor in how PECAM-1 maintains cell adhesion, and PECAM-1 appears to lose its cell-stabilizing effect if mutated at that position. Dephosphorylation by SHP-2 on tyrosine 686 causes PECAM-1 to distribute diffusely rather than concentrate at endothelial cell-cell junctions, which is how the tyrosine residue of exon 14 may be mediating cell stability. PECAM-1 communication with β -catenin may be mediating β -catenin's level of phosphorylation and translocation to nucleus [60]. In endothelial cells, PECAM-1 that was mutated at tyrosine 686 or had its cytoplasmic-domain deleted (hence could not be phosphorylated), induced phosphorylation of β -catenin and promoted cell migration [55-57]

Additionally, PECAM-1 needs endothelial cell-cell contact in order to keep itself localized to the lateral junctions of endothelial cells. Without cell-cell contact, PECAM-1

diffusely distributes within the membrane of endothelial cells, until it comes in contact with its homophilic ligand PECAM-1 on a neighboring cell [61].

2.8 PECAM-1 function in cell survival

There is evidence that PECAM-1 plays an anti-apoptotic role by blocking mitochondrial-dependent apoptosis in endothelial cells. Noble et al saw that when monocytes adhere to endothelial cells during serum-induced starvation, apoptosis of endothelial cells did not occur [62]. This protective effect was eliminated by antibody-blocking PECAM-1's homophilic interactions.

PECAM-1 may act suppressively to BAX-mediated apoptosis. Endothelial PECAM-1 deficient cells appeared more susceptible to apoptosis when challenged with stimuli that are known to induce mitochondria-dependent apoptosis [63]. Additionally, when PECAM-1 expressing kidney endothelial cells were challenged with the overexpression of the pro-apoptotic protein Bax, PECAM-1 was observed to prevent mitochondrial release of cytochrome c and caspase activation. This anti-apoptotic property of PECAM-1 was traced to its ITIM domain but not to anti-apoptotic gene upregulation [63].

In macrophage-mediated apoptosis, the macrophage engages the other cell through homophilic PECAM-1 interactions. If the cell is healthy, signaling through the linked PECAM-1 receptors leads to the two cells being repelled from each other. In a dying cell undergoing apoptosis, signaling through PECAM-1 appears to be altered, the

macrophage and the dying cell are not repelled from each other, which is thought to engage the macrophage phagocytosis receptors [64, 65].

2.9 PECAM-1 and signaling

The cytoplasmic tail of PECAM-1 enables it to act as a signaling molecule by means of exons that contain serine, threonine, and tyrosine residues that can be phosphorylated. In 1992, Newman et al showed that PECAM-1 on resting platelets could be phosphorylated on its serine residues upon platelet activation [66]. Serine phosphorylation of PECAM-1 occurs in hypoxic endothelial cells or upon simulation of hypoxia, and in monocytes stimulated with TGF β [67, 68].

Shear and oxidative stress or exposure to anti-PECAM-1 crosslinking monoclonal antibodies can trigger tyrosine phosphorylation [43, 69]. Once phosphorylated, the residues can then be docking sites for src homology 2 (SH2) containing signaling molecules. In that way, tyrosine phosphorylation of PECAM-1 regulates signaling events downstream of PECAM-1.

The delivery of 'outside-in' (inhibitory) input to PECAM-1 is needed to mediate PECAM-1's tyrosine phosphatase dependent inhibitory signaling. Input of "outside-in" signaling appears to be dependent on co-engagement of ITAM-mediated signaling (such as BCR, Fc receptor, or platelet Fc receptor) with ITIM-mediated signaling [27]. For this, the cytoplasmic tail of PECAM-1 needs to have intact ITIM domains, and interaction with specific tyrosine phosphatases [51]. Although not yet determined, the

extracellular homophilic-binding domains of PECAM-1 play a role in “outside-in” signaling [27]. Additionally, it appears that PECAM-1 dimers but not oligomers perform well in PECAM-1 homophilic binding involved in “outside-in” signaling. However, oligomerization of PECAM-1 in the plane of the membrane appears to be required for it to modulate integrin adhesive function [44].

2.10 PECAM-1 and inflammation

During inflammation, circulating leukocytes become activated by inflammatory cytokines and chemokines, and start the process by using selectins to adhere to the endothelium. That slows the leukocyte down, and it begins the process of “rolling” or “walking” along the endothelium. Getting closer to the region of inflammation, leukocytes slow down further by forming stronger attachments to the endothelium through VCAM-1 and ICAM-1, and eventually begin extravasating, which is mediated by multiple molecules such as VCAM-1, ICAM-1, and especially PECAM-1 [13, 28].

PECAM-1 is important to leukocyte extravasation, as antibodies to PECAM-1 have been shown to block extravasation of monocytes, neutrophils, and natural killer cells [12, 13, 28], which may be partially because the engagement of PECAM-1 on endothelium and leukocytes triggers a signaling pathway that activates leukocyte integrins [41, 45]. Also noted is the defect in the inflammatory response of PECAM-1 deficient mice, in which the numbers of circulating peripheral leukocytes tend to be the same as wild type mice, PECAM-1 deficient mice show a “pooling” of leukocytes at endothelial cell junctions, unable to get across. Neutrophils in PECAM-1 deficient mice can attach to and migrate

through endothelium, but appear to become trapped between the endothelium and basement membrane [70, 71].

PECAM-1 interactions between endothelial cells and neutrophils may regulate integrin expression of neutrophils, thereby leading to changes in the adhesion of neutrophils to the basement membrane [45]. Interestingly, the regulation of neutrophil migration by PECAM-1 is cytokine dependent, suggesting there are multiple mechanisms regulating leukocyte transendothelial migration [71]. However, in a mouse model of experimental autoimmune encephalomyelitis (EAE), PECAM-1-deficient mice show an early onset of inflammation, increased leukocyte extravasation, and longer lasting vascular permeability [9]. This might be due to the type of inflammation. EAE produces a chronic inflammation rather than the acute, and the process of inflammation is started by antigen-specific T-cells that have low to no PECAM-1 expression. Additionally, differences between mouse strains can have different compensatory mechanisms when it comes to PECAM-1 deletion. C57/BL/6 strain, for example, can uniquely compensate, generating a near-normal inflammatory response as opposed to other strains [8]. Supporting this notion are the polyvinyl acetyl sponges. When implanted subcutaneously in wild type and PECAM-1 deficient mice, PECAM-1 deficient mice initially show a lower neutrophil infiltration. However, after two weeks, when inflammation becomes more chronic, neutrophil infiltration increases [72]. Neutrophil infiltration is dependent on PECAM-1 expression by endothelial cells, however, there are probably compensatory mechanisms that get activated after a certain point, if inflammation persists.

2.11 PECAM-1's role in platelet function

Balanced hemostasis and thrombogenesis is maintained by the normal function of platelets. When a blood vessel is broken, platelets need to adhere and aggregate to the wall of the injured endothelium to form a hemostatic plug, which also involves von Willebrand factor (VWF), collagen, receptors glycoprotein Ib/IX/V (GPIb/IX/V) complex, integrins $\alpha_{IIb}\beta_3$, integrin $\alpha_2\beta_1$ and collagen GPVI. The initial attachment of platelets starts when VWF interacts with amino-terminal of the GPIba subunit under conditions of high shear stress, which in turn activates integrin $\alpha_{IIb}\beta_3$ that causes a stable platelet adhesion to the endothelial surface. The reason for that stable adhesion is that interacting with integrin $\alpha_{IIb}\beta_3$ causes platelets to restructure their cytoskeleton, giving them a better ability to spread, aggregate, and thereby form a thrombus [73].

Agonist-induced activation of integrin $\alpha_{IIb}\beta_3$ induces its receptor to undergo a conformational change, changing it from a low-affinity resting form to the high-affinity active form, in which it can bind fibrinogen, which is a ligand made by the liver. Having been bound, fibrinogen is used in the capacity of “glue” by the aggregating platelets, although it is now implicated in their activation as well, putting out additional signaling that enhances their spreading and aggregating capacity. In this way, integrin $\alpha_{IIb}\beta_3$ mediates irreversible and stable platelet adhesion through their cytoskeletal rearrangement needed for spreading, aggregation, and thrombus formation [44, 46].

PECAM-1 may be an important regulator of integrin $\alpha_{IIb}\beta_3$ activation. In in vitro models where PECAM-1 was cross-linked with bivalent anti-PECAM-1 Abs on cellular surface,

upregulation of β_1 , β_2 , and β_3 integrin function was observed, indicating that PECAM-1 might have a role in these events, however it was unclear if this regulation involved integrin conformation switching or its clustering functions [46].

Wee and Jackson used platelets from PECAM-1 deficient mice to examine how PECAM-1 might influence integrin function. They used terminally differentiated anucleate platelets to specifically examine integrin $\alpha_{IIb}\beta_3$ clustering (“outside-in”) versus integrin $\alpha_{IIb}\beta_3$ conformational changes (“inside-out”), simplified by excluding nuclear signaling. There seemed to be no apparent abnormality in integrin activation of PECAM-1 deficient murine platelets, however, the defect was observed in the “outside-in” signaling events of integrin $\alpha_{IIb}\beta_3$ complex tied to actin-myosin cytoskeletal proteins. Stunted filopodia, inhibited spreading on integrin $\alpha_{IIb}\beta_3$ –dependent matrix (immobilized fibrinogen), and slower clot retraction pointed to a malfunction of cytoskeletal rearrangement in platelets. However, integrin $\alpha_{IIb}\beta_3$ did normally activate, and robust platelet aggregation to PAR-4 among other factors suggest that PECAM-1 is not involved in platelet integrin $\alpha_{IIb}\beta_3$ “inside out” functioning (affinity), but rather influences its clustering (avidity) [46].

Additionally, numerous studies show that dimerization of PECAM-1 extracellular portions on surfaces of neutrophils, NK cells, platelets, and lymphocytes leads to upregulation of integrin adhesive function. Wee and Jackson saw an upregulation in T-cell binding to immobilized β_1 integrin substrates including fibronectin ($\alpha_5\beta_1$) and vascular cell adhesion molecule 1 (VCAM-1; $\alpha_4\beta_1$) by inducing dimerization with the

addition of bivalent anti-PECAM-1 mAB fragments. They also noticed an increase in β_2 integrin function on neutrophils, ligand-induced binding site (LIBS) exposure, and increased integrin β_3 platelet adhesion [46].

PECAM-1 was shown to act as a negative regulator of platelet-collagen interactions, acting to limit the growth of thrombi on collagen surfaces. PECAM-1 is inhibitory to platelet hyperaggregation and PECAM-1 deficient platelets form larger thrombi and show increased thrombus contraction. In models of static platelet adhesion, PECAM-1 deficient platelets demonstrated an increase in adhesion to immobilized collagen compared to WT platelets. They also showed a preference for collagen, as they did not demonstrate increased adhesion to fibrinogen or bovine vWF matrix compared to WT platelets. When perfused over a collagen matrix under flow, platelets isolated from PECAM-1-deficient mice also formed larger thrombi compared to WT platelets [74]. It is possible that PECAM-1 acts as a negative regulator to hyperaggregation and possibly limits adhesion by negatively modulating ITAM-related signaling, such as signaling through collagen receptor GPVI/FcR- γ chain and Fc γ RIIA-mediated signaling, promoting a more anti-thrombotic environment [27].

The Duncan study showed that PECAM-1 deficient mice have normal megakaryocyte and platelet production [70], indicating that the defect was not in generation of platelet numbers. However, PECAM-1 deficient mice do show an increase in bleeding time, which we have also shown. This appears to be due to a vascular weakness and not to inability of platelets to aggregate, as under condition of being PECAM-1 deficient, they

should theoretically aggregate more aggressively. Mahooti has shown that irradiation of PECAM-1 deficient mice and subsequent reconstitution of them with PECAM-1 competent platelets did not correct their increased bleeding propensity, indicating that the defect comes from the endothelium [10].

2.12 PECAM-1 role in angiogenesis

In vitro studies of endothelial cell behavior has shown that when endothelial cells are plated on Matrigel, they tend to conglomerate into networks of capillary-like assemblies that resemble the later stages of angiogenesis. Antibodies to PECAM-1 have been shown to block this process. Antibodies to PECAM-1 have also been demonstrated by DeLisser et al to inhibit angiogenesis in in vivo mouse corneal studies [75, 76]. Studies using bEND.3 cells that normally express high PECAM-1 levels showed that when PECAM-1 was deleted, bEND.3 cells were unable to organize into capillary-like networks, while cells that had PECAM-1 downregulated (but were still expressing it, albeit at reduced levels) did retain the ability to organize into networks. Using polyvinyl acetyl sponges, Duncan et al has shown that PECAM-1 deficient mice do have vascular and angiogenesis defects, where PECAM-1 deficient mice showed a lack of sponge-penetrating angiogenesis compared to PECAM-1 competent mice [70].

2.13 PECAM-1 and gene expression

It is still undetermined if PECAM-1 has any functionality as a gene expression regulator. Microarrays analyzing wild type and PECAM-1 deficient endothelial cells show that large numbers of genes involved in vascular homeostasis, angiogenesis, and vascular

development are influenced by the presence or absence of PECAM-1 [58]. DiMaio examined two genes in particular - connective tissue growth factor and endoglin, both of which encode for proteins involved in the TGF β ₁ signaling pathway. Since this pathway is important in vascular development and angiogenesis, it may be that impaired expression of these two genes would have functional consequences. Endoglin heterozygous mice show vascular defects that are similar to PECAM-1 deficient mice, suggesting that PECAM-1 may affect endoglin expression, however the details of these similar vascular defects would have to be better understood [58].

CHAPTER 3 - NON-INVASIVE DIAGNOSIS OF PULMONARY DISEASE IN PECAM-1 DEFICIENT FVB/N MICE USING INFRARED PULSE OXIMETRY

3.1 Summary

Pulse oximetry is a common tool for detecting reduced pulmonary function in human interstitial lung diseases. It has not previously been used in a mouse model of interstitial lung disease. Further, Platelet Endothelial Cell Adhesion Molecule deficient mice rarely show symptoms until disease is advanced. Using blood oxygen saturation, different stages of disease could be identified in a non-invasive manner. These stages could be correlated to pathology. Collagen deposition, using Picrosirius Red, did correlate with blood oxygen saturation. These studies are the first to show the use of an infrared pulse oximetry system to analyze the progression of a fibrotic interstitial lung disease in a mouse model of the human diseases. Further, these studies show that an early alveolar damage/enlargement event precedes fibrosis in this mouse model. This stage does not yet have extensive collagen deposition. Most importantly, targeting this earliest stage of disease for therapeutic intervention may lead to novel treatment for human disease.

3.2 Introduction

Pulse oximetry is a commonly used, non-invasive method for monitoring oxygen levels that is being delivered to tissues on hemoglobin molecules of red blood cells [77]. This method allows for a non-invasive method of monitoring hemoglobin saturation while the mice are alive. 97% of oxygen is carried on hemoglobin, thus allowing for a good assessment of arterial O₂ levels. A sensor is placed on the tail, the back paw, or around the neck of the mouse. Light of two wavelengths passes through the tissue to a

photodetector. Arterial O₂ saturation is directly measured using two different light wavelengths, one of which is visible red, and the other is infrared, not visible to the naked eye. How much light is absorbed changes depending on how much oxygen is bound to hemoglobin. Light absorption that reaches the sensor oscillates with the pulse of the heart, and since the pulse is very diffuse in capillary beds, it is best detected in the arteries. The software measures the changing absorbance at each of the wavelengths due to pulsing arterial blood, excluding venous blood, skin, muscle, fat, bone, and fur (StarrLife Sciences). Pulse oximetry system monitors pulse (beats per minute, bpm), arterial oxygen saturation (SpO₂, % in Figure 1), pulse and breath distention, and breath rate [77].

Human studies of interstitial lung disease (ILDs) have shown that patients have a marked reduction in arterial blood oxygen saturation (SpO₂) while even in resting state [78-80]. In this aim, a rodent pulse oximetry monitoring system was successfully used to non-invasively diagnose and monitor disease in PECAM-1 deficient FVB/n mice. PECAM-1 deficient mice in the FVB/n background show histological similarities to the human IPF, such as alveolar collapse, airway expansion, fibroblastic hyperplasia, collagen deposition, interstitial thickening, and a fibrotic pattern that starts at the bottom and peripheral regions of the lung [8]. PECAM-1 is important for leukocyte extravasation, apoptosis and cell signaling [8, 11, 13, 22, 52, 63, 64, 81, 82].

As is the case with human IPF, the main issue was our inability to non-invasively and consistently diagnose disease, until the mouse would be in advanced stages and in

visible respiratory distress, which also presented problems of unexpected mortality before tissue could be harvested. Much like the human patients, mice do not show any outward signs of the disease until it reaches the advanced stages, which made studying disease progression dependent on random culling of valuable, difficult to breed animals. Pulse oximetry has made it possible to monitor the colony twice per week to diagnose disease at its earliest stages and to monitor its progression. Pulse oximetry has also allowed us to collect specimen at different stages in the disease process, allowing us to examine cellular and molecular events per stage of disease.

3.3 Materials and methods

All animals used were housed under the care and supervision of the Laboratory for Animal Research. FVB/n strain wild type and PECAM deficient mice (a generous gift from Dr. William A. Muller, Northwestern University) were raised in one room together. All procedures were reviewed and approved by the CSU research institutional Animal Care and User Committee.

3.3.1 Pulse oximetry

Non-anesthetized mice were used to test the Mouse Ox System (Starr Life Sciences, Oakmont, PA). The animals were held in dorsal recumbency using one hand, which is performed by using the thumb and forefinger to scruff the mouse, while securing the tail between the forth and fifth fingers. The back of the hand can be stabilized against a flat surface such as a table. The probe is placed on the left rear foot of the animal, aiming to have the middle of the foot in the clamp groove. It is best to exclude the hock and to

have the toes securely out of the probe. The black portion of the probe needs to be in steady contact with plantar surface to ensure consistency. The mouse needs to be held steady to minimize movement, as that can cause movement of the probe and affect the reading. Likewise, the cord should be secured and stationary, so as to not pull on the probe. The probe, however, should not be hand-held in place, as that also interferes with accurate measurement and can disrupt the signal. If the room where the measurements are being conducted has fluorescent lighting, a light blocker should be placed over the probe in order to block the fluorescent light, as that can also disrupt the readings.

3.3.2 Histopathology

After the animals were humanely euthanized, the pulmonary cavities were dissected opened, and the aorta was cut in the peritoneal cavity to prevent blood pooling in the pulmonary cavity. Lungs were dissected out and fixed in IHC Zinc formalin-free Fixative (BD Pharmingen, San Diego, CA, proprietary formulation) for 48 hours at 4 degrees C for histology. Lungs were then washed in 1X PBS, standardly processed and embedded in paraffin. Blocks were sectioned at 7 um on a standard microtome and slides were baked on slide heater at 50 degrees C until adherence, then de-waxed in Xylene (2 baths, for 3 minutes each), and rehydrated in an ethanol gradient by submerging for 3 minutes in 100%, 100%, 96%, and 70% ethanol solutions.

For Hematoxylin and Eosin staining, slides were immersed in Hematoxylin (Surgipath, Richmond, IL) for 5 minutes, washed with DI water, then incubated in defining solution

and bluing buffer (Surgipath). Slides were then immersed in 96% ethanol for 1 minute and immersed in Eosin Y (Surgipath) for 3 minutes. Slides were then washed with 96% ethanol and mounted with Permount mounting media (Fisher Scientific, Pittsburgh, PA).

3.3.3 Picrosirius Red stain and assessment of collagen deposition

Protocol by J. A. Kiernan protocol was used to assess the extent of collagen deposition [83]. Slides were de-waxed and rehydrated as described above. Slides were then stained with Vector's formulation of Mayer's Iron Hematoxylin (catalog no. H-3404; Vector Laboratories, Burlingame, CA) for eight minutes at room temperature, then rinsed under tap water until water ran clear. Slides were submerged in a covered bath of 0.1% Sirius Red in saturated Picric Acid (catalog no. 26357-02, Electron Microscopy Sciences, Hatfield, PA) for 1 hour at room temperature in the chemical hood. It is important to keep the bath closed to prevent any evaporation and crystal deposition of Picrosirius Red. Post incubation, slides were washed for two minutes in two changes of acidified water (5 ml Glacial Acetic Acid per 1 liter distilled water). Slides were then dehydrated for three minutes in 70% isopropanol, three minutes in 96% isopropanol, two changes of three minutes in 100% isopropanol baths, and cleared for two changes of three minutes in xylene. The slides were then mounted with Permount mounting media (Fisher Scientific, Pittsburgh, PA).

Sections were imaged using birefringence at 4X magnification on an Olympus IX-71 microscope using two circular polarizing filters. The viewing software used was Q Capture Suite using a Q Color digital camera (Qimaging, Surrey, BC, Canada). Images

were taken and analyzed using Nikon NIS-Elements software (Nikon Instruments Inc., Melville, N.Y.) computer-assisted image analysis. Each image was cropped to an area of 1,125,000 pixels, then thresholding function was used to assess the extent of Picrosirius staining on tissue in each cropped area, after which the automeasure was used to numerically assess the degree of stain. Data was exported in an Excel spreadsheet for quantitation.

3.3.4 Statistics

The statistics software package JMP (SAS, Research Triangle, NC) was used to analyze all data. Differences in means were tested using the Tukey-Kramer HSD (honestly significant difference) test between each group. Correlation, linear fit, and the Receiver Operating Characteristic tests were also done using JMP. Error bars shown are the standard error of the mean for each group.

3.4 Results

Pulse oximetry system was used to diagnose disease in conscious, non-anesthetized PECAM-1 deficient mice in the earliest possible stages. The system was tested in PECAM-1 deficient and wild type animals. Mice were monitored in time periods between 30 second and 2 minutes, taking several consistent measurements at points when the mouse was calm and not moving (Figure 1). Attempts were made to use the ear and tail, but the rear left foot pad proved to be most consistently reliable option and was used to all recorded measurements. The Pulse-Ox system monitors pulse (beats per minute, bpm), arterial oxygen saturation (SpO₂, % in Figure 1), pulse and breath

distention, and breath rate. While published pulse rates in resting mice tend to be around 400-600 bpm [84, 85], the pulse rate in our mice averaged between 650-700 bpm and could be due to the animals being somewhat stressed during handling. Other parameters were found to be difficult to consistently monitor on conscious and restrained animals.

Three data set examples are shown in Figure 1: wild type mouse (SpO₂ average 92%, Fig. 1A), healthy PECAM deficient mouse (SpO₂ average 93%, Fig 1B), and two mice significantly below the average (SpO₂ average 85%, Fig. 1C, average 77% Fig. 1D). The Pulse Ox system needs adequate time to acquire a signal, followed by signal optimization and then acquisition of usable data, for which the animal needs to be still and calm. Some mice continuously move, which disturbs the sensor and extends handling time, which can present difficulties. If an animal is visibly stressed, it needs to be placed back in its cage and another reading can be attempted after the mouse has calmed down.

Established baselines in wild type mice averaged from about 92% to 93% (Figure 2) after weekly monitoring. Some wild type readings went as low as 87% and as high as 94%, usually for only one observation point. Healthy PECAM-1 deficient mice averaged at 89-91%, diseased PECAM-1 deficient mice averaged around 80% in the early stages. Mice at 89 and above were classified as healthy, 88% to 85% were classified as early borderline, 85% to 75% as moderate, and below 75% as severe for the disease process. In week three of the study, diseased mice dropped to 75% and had to be

euthanized for humane care reasons, as well as to examine pulmonary pathology. In the previously borderline PECAM-1 deficient group, several dropped to around 85% SpO₂ and were euthanized for pathology examination.

The primary goal of this aim was to test the sensitivity of pulse oximetry in non-invasively diagnosing disease onset in its earliest stages. Thirteen mice from each group, PECAM deficient mice and wild type controls, were examined (Fig. 3). Wild type mouse lungs showed no signs of disease (Fig. 3A). PECAM-1 deficient mice presented with a range of pathology (Fig. 3B-D): fibroblast proliferation and collagen deposition was found in advanced lesions, moderate alveolar enlargement was seen at SpO₂ levels around 82% (Fig. 3B-C). More severe disease was observed in PECAM-1 deficient mice that had SpO₂ levels slightly above 75% (Fig. 3D).

Mice with extensive fibrosis were not used due to sacrificing the animals before SpO₂ levels dropped below 75% for humane reasons. Based on SpO₂ levels and consequent histological assessment, a general scoring system was established for each group (Table 1). Comparing SpO₂ levels and histology will lead to a more detailed assessment of cellular and molecular events during each disease stage.

Two statistical tests were performed to examine this scoring system: a simple correlation analysis between SpO₂ levels and pathology, and a Receiver Operating Characteristic (ROC) test (Figure 4). The ROC test has been established to identify accuracy rate between false positives and false negatives in a scoring system. Based

on this data alone, the correlation coefficient was 0.79 (Figure 4A). ROC analysis also indicated that this system is sensitive and accurate, and all three groups were correctly classified by testing SpO₂ levels alone (Fig. 4B)

Collagen deposition is a critical event in the fibrotic process. Dr. Cory Hogaboam [86] recommended using Picrosirius Red as a useful method not only for staining collagen, but also for differentiating the age of deposited collagen and for quantitative assessment. It is important to use circular polarizing filters in order to visualize all of the fibers [83]. Picrosirius Red Stain is intended for use in the histological visualization of collagen I and III fibers. This method exploits the enhancement of birefringence of collagen fibers, which is largely due to co-aligned molecules of Type I collagen [87]. Picrosirius Red intercalates into the tertiary grooves of types I and III collagen. When viewed under bright-field microscopy, collagen is dark red on a pale yellow background, with cell nuclei in black. When viewed through the crossed polars, the older, larger collagen fibers are bright orange, the younger thinner ones are yellow to pale green. The birefringence is very specific for collagen [88, 89], and all fibers can be brought into view by equipping the microscope for use with circular rather than plane polarized light [90, 91]. It is also important to mark and use the same light intensity and the same parameters when imaging and scoring the images. Several materials such as type 4 collagen, some mucus, and keratohyaline granules also stain red, but are not birefringent. For our purposes, Picrosirius Red was used to quantify the deposited collagen for the stages of disease, and to draw the correlation between the value of SpO₂ readings and the intensity of Picrosirius Red on the lung tissue of each animal.

The stain can be used for quantitation using images captured with the 4X objective (Fig. 5), which correlated with blood oxygen saturation ($R^2 = 0.57$ with wild type mice; $N = 7$ wild type mice and 13 PECAM-1 deficient mice; ANOVA of linear regression, $p < 0.0001$). Importantly, the earliest stage of disease at $>85\%$ SpO₂ levels does show alveolar enlargement, but does not show significantly higher amount of fibrosis in large areas of the lung (Fig. 5C), which is similar to the baseline amount of collagen normally found around blood vessels and bronchioles of wild type mice (Fig. 5A-B). The developing lesions of PECAM-1 deficient mice do contain collagen (Fig. 5D). It is only as lesions develop that fibrosis becomes evident (Fig. 5E-F), and this leads to some of the variability in the linear regression. The stain should be used at full strength. Scoring of all slides with NIS Elements should be done on the same day to minimize variation in thresholding.

3.5 Discussion

The most important finding of this aim is that the earliest stage of disease in PECAM-1 deficient mice has alveolar damage/enlargement before lesion formation and collagen deposition begins to take place. Some literature mentions a similar stage of disease in human familial IPF [92]. This is clearly a critical event in the disease process. The cellular and molecular events that occur at this stage are the focus of our current studies and underline the value of complimentary animal models of disease because it is not feasible to study, or even currently diagnose these early events in the human population.

This specific aim demonstrates that PulseOx system was used to accurately identify decreased arterial oxygen saturation in diseased mice and to correlate the extent of disease with SpO₂ levels. This system is sensitive enough to diagnose the earliest stages of disease and it appears that we are the first to employ this system to diagnose and monitor disease progression in a murine model of pulmonary fibrosis. In pulse oximetry studies of human interstitial lung disease, SpO₂ levels that drop below 90% during exercise are considered at highest risk [78-80]. As the mice in this study are not truly at rest, since a conscious mouse being held is never truly at rest, the substitution of this method as a surrogate of moderate exercise has sufficient predictive value. It might be ideal to use active exercise routines for the mice, similar to the treadmill tests for humans, but the cost and time may outweigh any benefit when screening a fairly large mouse colony two times per week on a consistent basis. The data here shows sufficient sensitivity currently for the purposes of this study.

This assay is minimally stressful to the mouse and eliminates the need for unnecessary culling. It may be useful in a variety of animal models. Most importantly, determining stages of disease is critical for examining the pathology on a cellular and molecular level.

Recently, the tail/paw clip has been upgraded to a collar based system. The collar is small and light, unstressful to the mouse, and measures blood oxygen from the carotid artery. This upgrade came out after this study, but has the advantages of improved sensitivity and eliminates the restraint, allowing the mouse to freely roam its cage during

measurements and improving accuracy. The tail/paw clip can still be used on obese mice, as their neck often gets too large in circumference for the collar to fit comfortably.

We have shown here that SpO₂ measurements can be used to identify stages of disease, allowing for examination of cellular and molecular events early in the development. Alveolar enlargement occurs before collagen deposition, while Picrosirius red stain can be used as an independent quantitative analysis of collagen deposition. Examining molecular and cellular events at the earliest stages of disease will be the focus of future studies, as it is now possible to select mice from each respective disease stage. Examining each stage of disease is important for identifying events involved in the fibrotic development, which can lead to novel approaches to diagnosis and therapeutics in human pulmonary fibrotic disease.

3.6 Figures and legends

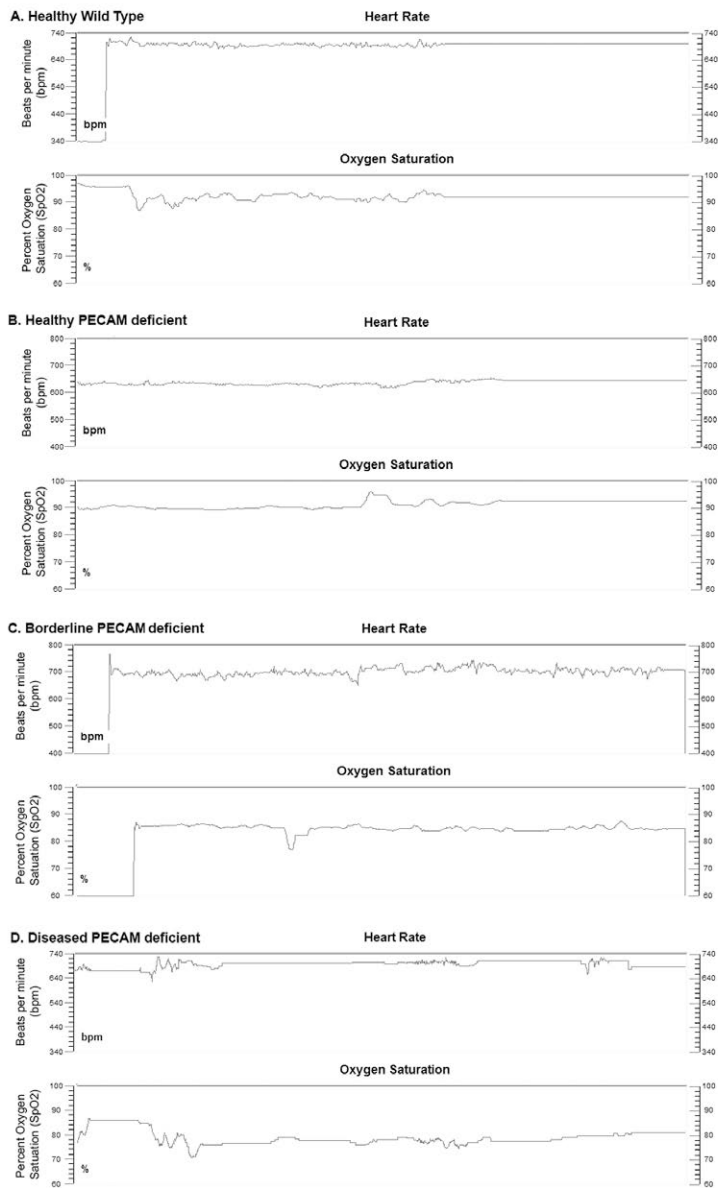


Fig. 3.1.

Examples of typical output readings from the MouseOx system on awake mice. A. Wild type mouse, average SpO₂ = 94% B. PECAM deficient healthy mouse, average SpO₂ = 92%. C. PECAM deficient mouse, borderline, average SpO₂ = 87%. D. PECAM deficient mouse, diseased, average pO₂ = 72%

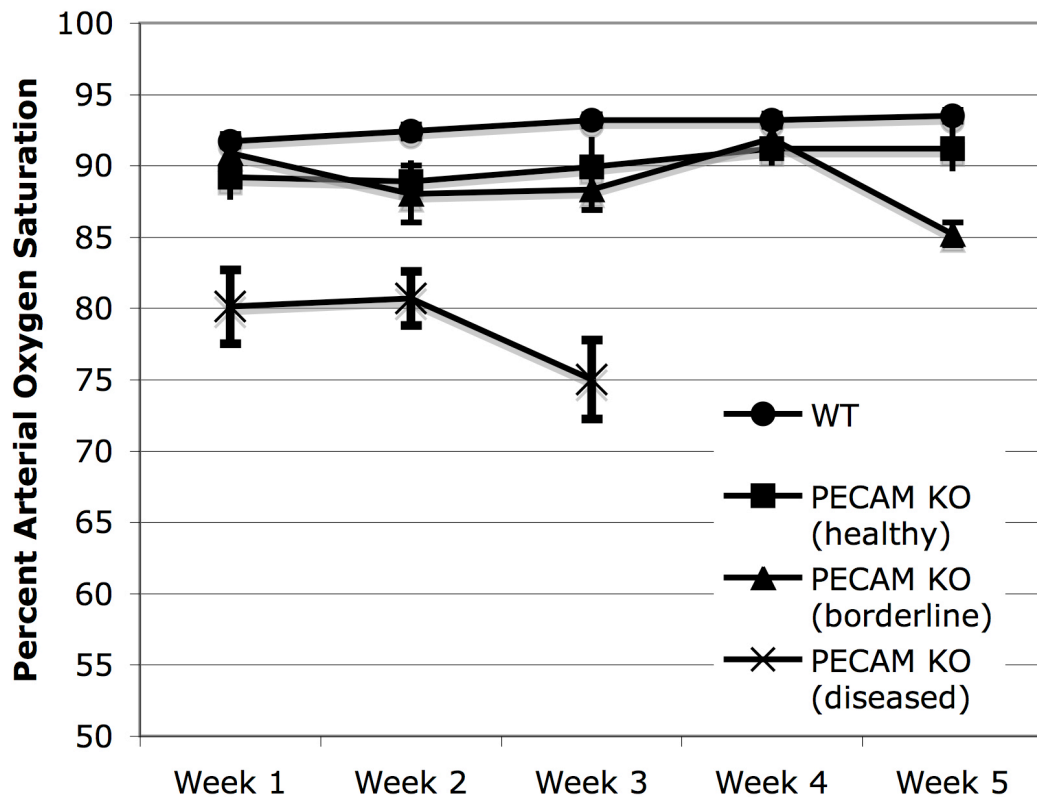


Fig. 3.2.

Percent arterial oxygen saturation data over time. Healthy wild type and PECAM-1 deficient FVB/n mice were measured over 3-5 weeks. Diseased mice (SpO₂ < 85%) were sacrificed at week 3 due to humane care requirements. Borderline mice (~90%) showed no significant difference until week 5, and then showed a significant drop in SpO₂ (Tukey-Kramer HSD, $p < 0.01$). All measurements of the diseased mice were significantly lower than both wild type and healthy PECAM-1 deficient FVB/n mice (Tukey-Kramer HSD, $p < 0.01$). Wild type mice ($n = 24$), healthy PECAM-1 deficient mice ($n = 5$), borderline PECAM-1 deficient mice ($n = 4$), diseased PECAM-1 deficient mice ($n = 7$). Error bars shown are the standard error of the mean.

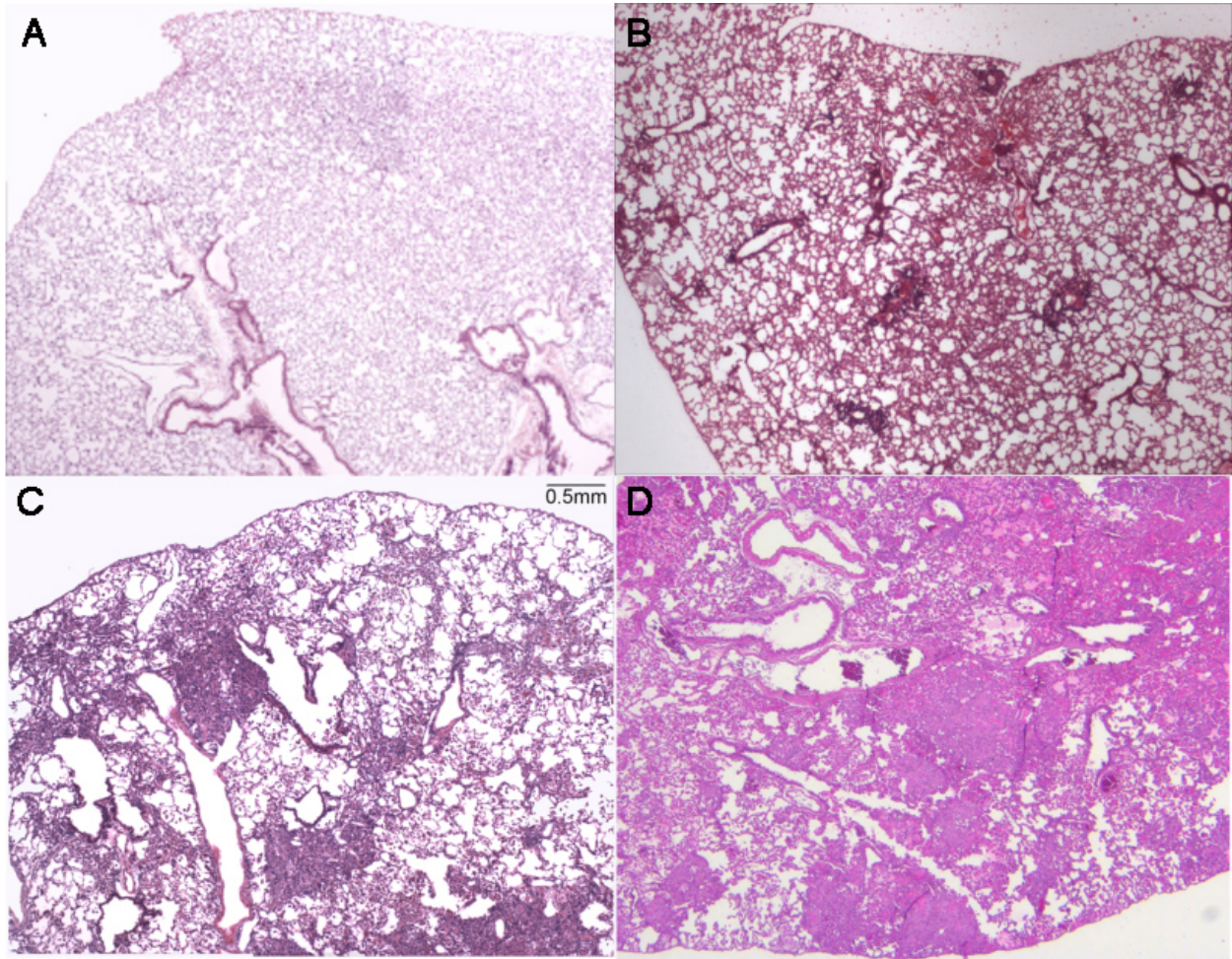
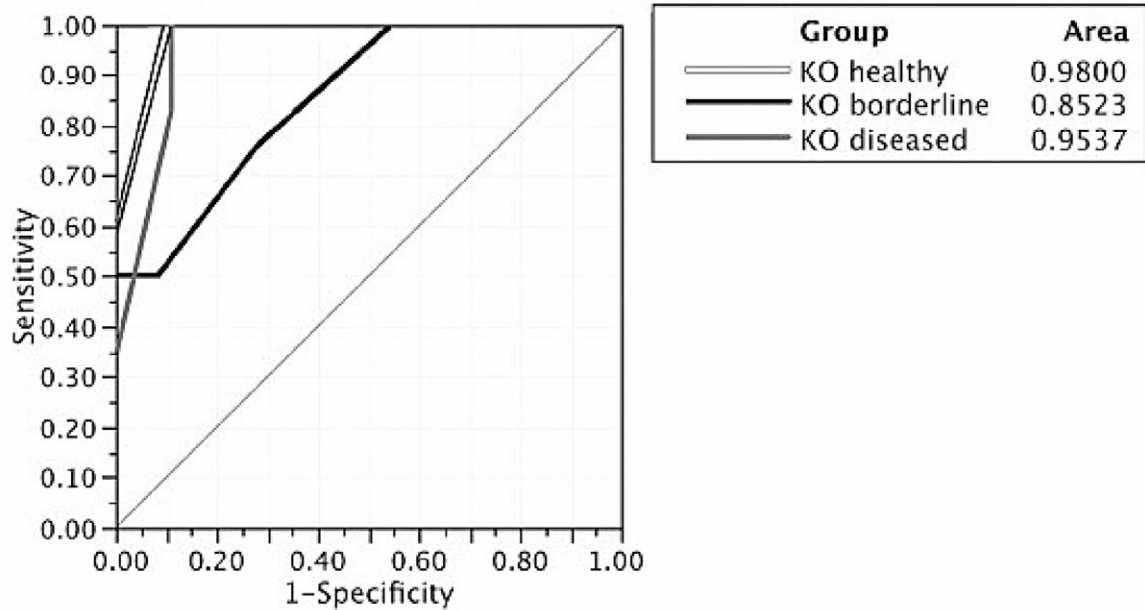


Fig. 3.3.

Histology of lungs at different blood oxygen saturation levels Low magnification images showing disease in lungs A. Wild type lung, average SpO₂ = 91% (2X magnification). B. PECAM deficient mouse, average SpO₂ = 82% (2X magnification). C. PECAM deficient mouse, average SpO₂ = 73% (2X magnification). D. PECAM deficient mouse, average SpO₂ = 67%(2X magnification).

Receiver Operating Characteristic SpO2 Levels by Group



Bivariate Fit of Last Recorded SpO2 by Pathology Score

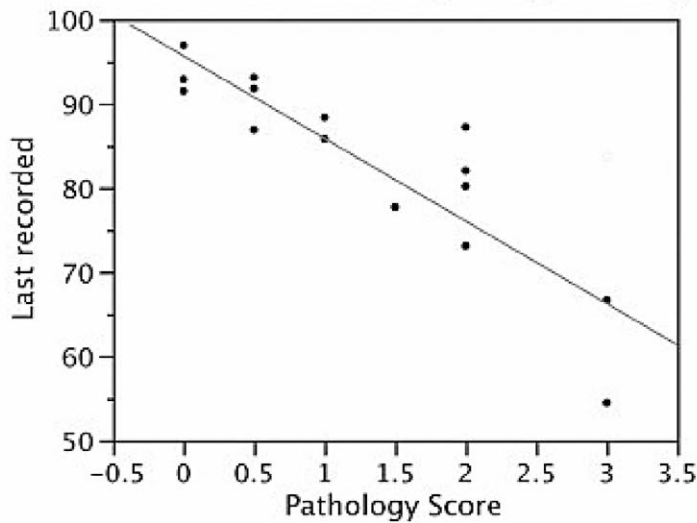


Fig. 3.4.

Correlation and Receiver Operating Characteristic (ROC) tests on the data in this study.

A. The correlation coefficient based on the linear fit was 0.79. B. The ROC analysis classified by testing SpO2 levels alone. The white line is mice classified as healthy, black line is mice classified as borderline, and grey is mice classified as diseased. In

this analysis, the area of the curve should be greater than 0.5 and as close to 1.0 as possible.

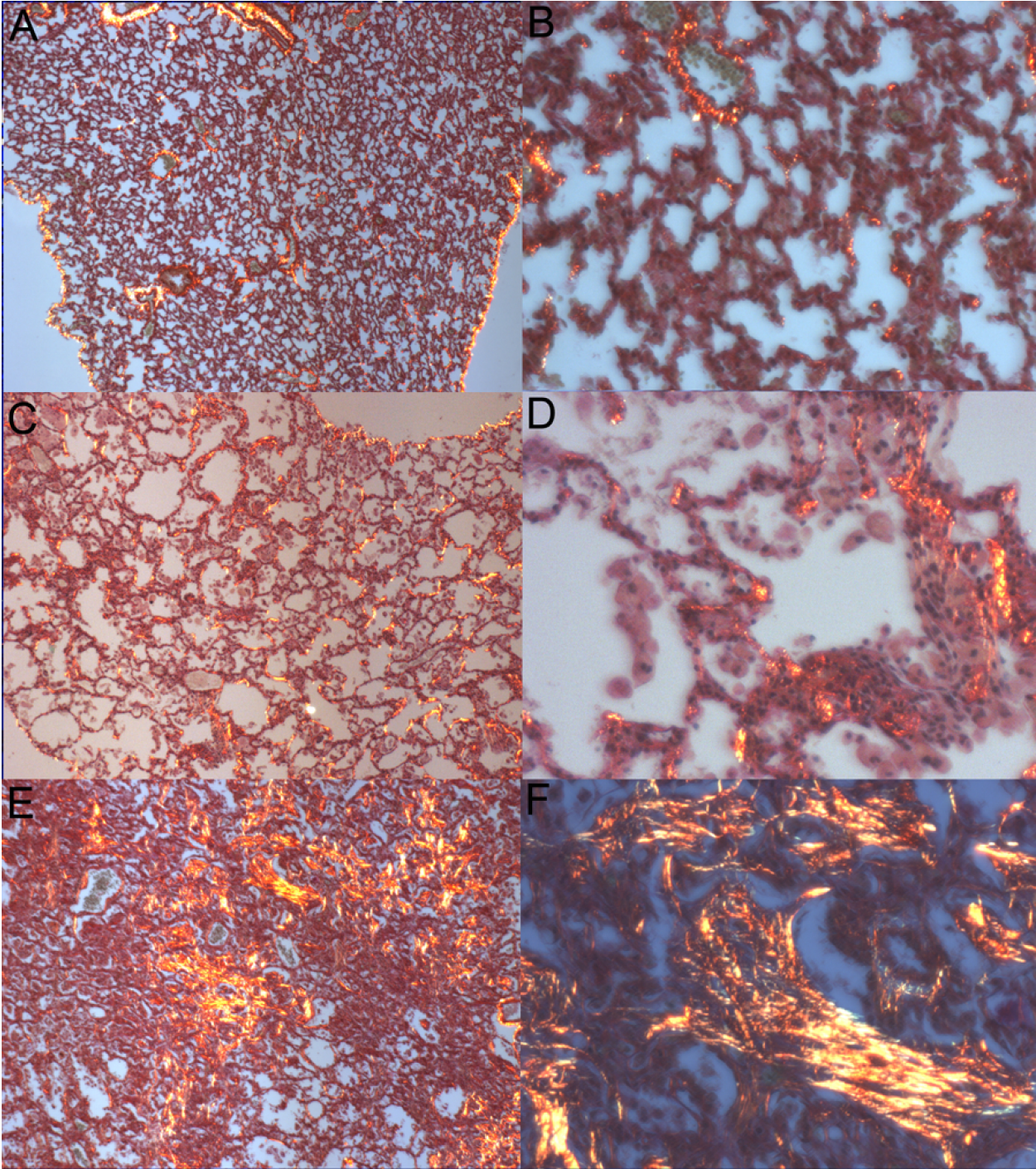


Fig. 3.5.

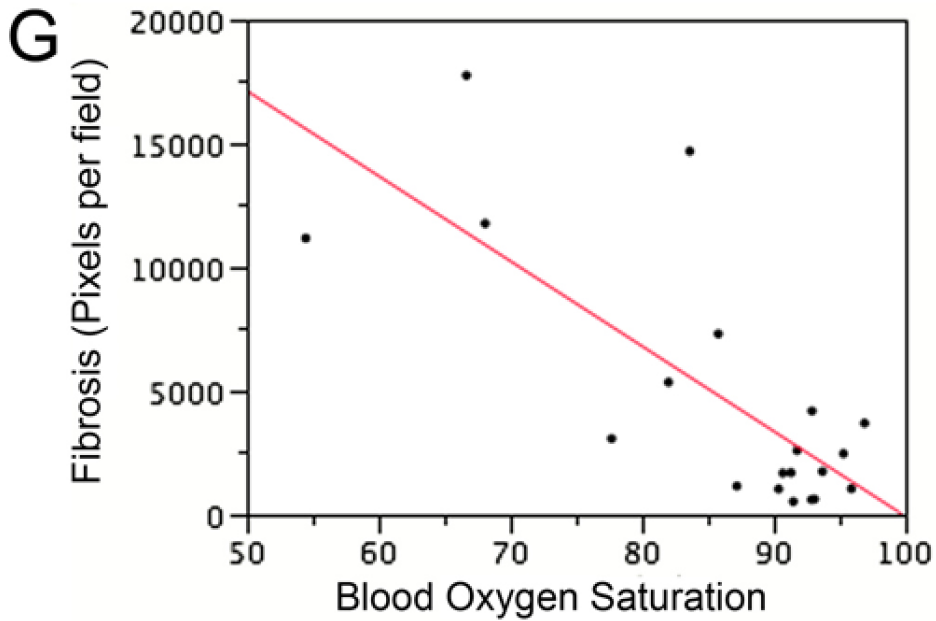


Fig. 3.5 continued.

Picrosirius Red Stain to quantitate fibrosis. A. Wild type lung (4X magnification). C, PECAM deficient mice with borderline SpO₂ (84%; 4X magnification). D. PECAM deficient mice with borderline SpO₂ (84%; 40X magnification) E, PECAM deficient mouse with average SpO₂ = 68%. (4X). F. PECAM deficient mouse with average SpO₂ = 68%. (40X) F. Multivariate analysis between blood oxygen saturation and stain intensity.

Table 1. Grouping of disease in PECAM deficient mice

Group	SpO₂ range (3+ observations)	Pathology scoring
Healthy	89-94	None
Early/borderline	88-85	Focal, small lesions and alveolar enlargement
Moderate	85-75	Many lesions, early fibrosis
Late	<75, often cyanotic	Large lesions, extensive fibrosis

Disease stages of PECAM-1 deficient FVB/n mice classified by SpO₂ readings.

CHAPTER 4 - MICROHEMORRHAGE IS AN EARLY EVENT IN THE PULMONARY FIBROTIC DISEASE OF PECAM-1 DEFICIENT FVB/N MICE

4.1 Summary

Platelet Endothelial Cell Adhesion Molecule 1 (PECAM-1) deficient mice in the FVB/n strain exhibit fatal chronic pulmonary fibrotic disease. The illness occurs in the absence of a detectable pro-inflammatory event. PECAM-1 is vital to the stability of vascular permeability, leukocyte extravasation, clotting of platelets, and clearance of apoptotic cells. We show here that the spontaneous development of fibrotic disease in PECAM-1 deficient FVB/n mice is characterized by early loss of vascular integrity in pulmonary capillaries, resulting in spontaneous microhemorrhages. Hemosiderin-positive macrophages were found in interstitial spaces and bronchoalveolar lavage (BAL) fluid in relatively healthy animals. We also observed a gradually increasing presence of hemosiderin-positive macrophages and fibrin deposition in the advanced stages of disease, corresponding to the accumulation of collagen, IL-10 expression, and myofibroblasts expressing alpha smooth muscle actin (SMA). Together with the growing evidence that pulmonary microhemorrhages and coagulation play an active part in human pulmonary fibrosis, this data further supports our hypothesis that PECAM-1 expression is necessary for vascular barrier function control and regulation of homeostasis specifically, in the pulmonary environment.

4.2 Introduction

Platelet Endothelial Cell Adhesion Molecule (PECAM-1, CD31) is a 130 kDa transmembrane adhesion and signaling glycoprotein. It belongs to the Ig superfamily of

cell adhesion molecules. It is concentrated at endothelial cell–cell junctions in highly vascularized regions and is expressed by the majority of leukocytes with the exception of activated lymphocytes [25, 28, 93-95]. PECAM-1 is important to the integrity of the vascular permeability [9-11], leukocyte extravasation [12, 28], control of thrombus activation and contraction [16], and apoptotic cell/debris clearance [14, 15]. Six Ig-like homology domains make up the extracellular domain of PECAM-1, followed by a 19-residue transmembrane domain, and a 118-residue cytoplasmic tail [25]. The residues of the N-terminal extracellular Ig domain-1 are required for mediating homophilic PECAM-1–PECAM-1 interactions that direct PECAM-1 to localize to endothelial cell–cell junctions [50, 96-98].

Idiopathic Pulmonary Fibrosis (IPF) affects nearly 100,000 Americans. It is progressive and fatal in the absence of a lung transplant [99]. PECAM-1 plays a vital role in the regulation of vascular stability, and there is growing evidence that alveolar bleeding and coagulation play essential roles in the development of IPF, especially at initiation phases. The current hypothesis is that the formation of a clot in the lung, followed by activation of protease activated receptors (PAR1 and PAR2) leads to the fibrotic response [2, 3]. A recent clinical trial using warfarin to treat IPF found that this treatment was detrimental [4]. This indicates that coagulation does indeed play a role in the diseases like IPF.

We previously showed that PECAM-1 deficient FVB/n strain mice spontaneously develop a fatal chronic pulmonary disease with some similarities to that seen in patients with IPF, including the absence of a detectable acute inflammatory event and the

accumulation of collagen in lesions [1, 7]. We have established a disease monitoring system for these animals using pulse oximetry to detect reduced pulmonary function while the animal is conscious, alive, and unrestrained [7]. The most important finding of our earlier study [7] was that the earliest occurring disease stage in the PECAM-1 deficient FVBn mice is alveolar collapse, before any actual lesion formation, collagen deposition, and fibrosis occurs. Here we show that the early stages of disease process in PECAM-1 deficient FVBn mice are hallmarked by increased numbers of hemosiderin-positive macrophages and fibrin deposition, which increase as the disease progresses. This supports the hypothesis that pulmonary microhemorrhaging and coagulation may play a role in human fibrotic diseases [2, 3, 92].

4.3 Materials and Methods

4.3.1 Animals

PECAM-1 deficient and wild type FVB/n mice were housed at Colorado State University Laboratory Animal Resources. Veterinary care and pulse oximetry were done under protocols approved by the Colorado State University Animal Care and Use Committee.

4.3.2 Disease stages of PECAM-1 deficient FVB/n mice

MouseOx system (Starr Life Sciences Corp., Allison Park, PA) was used to noninvasively assess disease state in PECAM-1 deficient FVB/n mice as described in [7], with the disease stages outlined in Table 1.

4.3.3 Prussian Blue stain for hemosiderin-positive macrophages in pulmonary tissue

Mouse lungs were fixed using formalin-free IHC zinc fixative (BD Pharmigen, Cat. # 550523). Antigenic epitopes are masked, and can undergo degradation by 10% formalin fixation. In the case of non-infectious tissue, a gentle fixative such as zinc preserves the integrity of the epitopes and eliminates the need for antigen retrieval. From here on, the use of this fixative is referred to as “zinc-fixed” unless specified otherwise. Lungs were fixed for 8 hours as per fixative protocol, then, transferred to 1X PBS before routine processing and paraffin embedding. Paraffin-embedded tissue was sectioned on a standard microtome at 7 μ m and rehydrated to dionized (DI) water. Slides were immersed in equal parts 0.2% hydrochloric acid and 0.2% potassium ferrocyanide solution for 1 hour at room temperature (RT). Slides were counterstained in 0.2% solution of Safranin Orange for 2 minutes, washed in 1% aqueous acetic acid, dehydrated and mounted in synthetic resin. Hemosiderin appears in blue, nuclei in red, and background in pink.

4.3.4 Prussian Blue stain for hemosiderin-positive macrophages in bronchoalveolar lavage (BAL) fluid

After humane euthanasia, trachea was exposed and lavaged with sterile saline using an 18-gauge feeding needle attached to a 1-cm³ syringe. Then 500 μ l of BAL fluid from each animal was applied to each slide. After centrifugation (Cytospin, Shandon Southern Instruments, Runcorn UK) for 2 minutes at 90Xg, a cell pellet was obtained. Slides were air-dried, fixed in methanol, immersed in methyl blue followed by eosin red,

and hemosiderin-positive macrophages were detected with Prussian blue stain. At magnification of 16X, alveolar macrophages were examined for the number of cells positive for Prussian blue stain, and the total cell number was counted.

4.3.5 Russell-Movat Pentachrome stain for fibrin deposition in pulmonary tissue

Zinc-fixed paraffin-embedded tissue was sectioned on a standard microtome at 7 μ m and rehydrated to DI water. Staining was performed as per the kit protocol (American Master Tech Catalog No. KTRMP), however, due to the porosity of the sections, Verhoeff's Elastic stain was omitted. Resulting stain shows collagen in greenish-yellow depending on the age of deposition, muscle in red, mucins in blue to green, and fibrin in pale red.

4.3.6 Anti-Smooth Muscle Actin stain for myofibroblasts in pulmonary tissue

Zinc-fixed paraffin-embedded tissue was sectioned on a standard microtome at 7 μ m and rehydrated to DI water. Since a monoclonal primary anti-smooth muscle actin antibody was used on mouse lung sections, the staining was performed as per the Vector Mouse-On-Mouse (M.O.M) staining protocol (VECTOR® M.O.M.™ Immunodetection Kit BASIC Catalog No. BMK-2202). Vector diaminobenzidine was used as substrate as per kit protocol (VECTOR® DAB Substrate Kit for Peroxydase Catalog No. SK-4100), counterstained with iron hematoxylin QS (Vector® Hematoxylin QS Catalog No. H-3404), dehydrated and mounted in synthetic resin. The resulting stain shows myofibroblasts in brown, nuclei in blue.

4.3.7 IL-10

Zinc-fixed paraffin-embedded tissue was sectioned on a standard microtome at 7 μm . The slides were then re-hydrated for 5 minutes in 100%, 90%, 85% and 70% in ethanol solutions, followed by DI water for 3 minutes. Endogenous peroxidase was blocked with a solution of methanol containing 0.3% H_2O_2 for 20 min at room temperature (RT). Nonspecific binding was blocked in 3% bovine serum albumin (BSA) in PBS for 30 min at RT, and this solution was used to wash between subsequent steps. Slides were incubated overnight at 4°C with a primary antibody for IL-10 (Santa Cruz cat. # 1783). The slides were then washed and incubated with the secondary antibody for 1 hour at RT. Slides were washed and specific antibody binding reaction was amplified with Vectastain ABC system (Vector Laboratories, Burlingame, CA). Slides were washed and incubated again for 5 min with at RT with 3-amino-9-ethylcarbazole (AEC) (Vector Laboratories). Finally the slides were counter-stained with Hematoxylin QS (Vector Laboratories) and mounted.

4.3.8 Interleukin-10 (IL-10) ELISA

After the mice were humanely euthanized, pulmonary cavities were opened. The aorta was severed in the peritoneal cavity to minimize blood pooling in the pulmonary cavity. To collect bronchoalveolar lavage fluid (BALF), an 18-gauge gavage needle was used. The trachea was cannulated, and 1 ml of PBS was slowly injected into the lungs and then withdrawn. Samples were collected and frozen at 20°C . IL-10 was measured from previously frozen mouse bronchoalveolar lavage fluid samples using the eBioscience Mouse IL-10 Ready-SET-Go! ELISA sandwich kit with precoated plates. (eBioscience

#88-7904). Briefly, the standard curve range was 2000pg/mL to 0 pg/mL of cytokine, and was generated by the frozen standard. The plate with standards and samples was incubated for 2 hours at room temperature, washed, and secondary detection antibody was applied and allowed to incubate for one hour at room temperature. After washing, Avidin-HRP was linked to the detection antibody and incubated for 30 minutes in darkness. A final wash was performed, and wells were developed with color substrate (TMB) solution for 12 minutes in darkness before stopped with acidic stop solution. The plate was read on a microplate reader (BioRad Model 680) at 450nm.

4.3.9 Tail bleeding time assessment

Tail-bleeding times were assessed by nicking the tail vein at the tip of the tail and then allowing mice to freely move about the cage on clean paper towels, until bleeding stopped without any human assistance or mouse grooming.

4.3.10 Statistics

JMP software (SAS, Cary, NC) was used for comparison between multiple groups of uneven sample size, using Tukey Kramer Honestly Significant Difference (HSD) test as indicated in the figure legends. Bleeding time comparisons between wild type and PECAM-1 deficient mice was compared with the Student's T test.

4.4 Results

4.4.1 Presence of hemosiderin-positive alveolar and interstitial macrophages increases in tissue with the stage of disease

Using a mouse pulse oximetry system to monitor the state of disease in our animals, we classified the state of disease into 4 stages (Table 1) and [7], with alveolar collapse and fibrotic lesions getting more extensive as the disease progresses. Prussian blue staining confirmed the increased presence of hemosiderin-positive macrophages in sick mice compared to healthy mice (Fig. 1). The number of hemosiderin-positive macrophages in tissue increased with each stage of disease (Fig. 1-2). However, in the highly fibrotic areas of the severe stage the numbers of hemosiderin-positive macrophages became more dispersed, indicating that perhaps microhemorrhaging is no longer as intense in those areas (Fig. 1I-L). We have observed the hemosiderin-positive macrophages in the lungs of our animals to be present in the alveoli, as well as in the interstitium. BAL fluid of PECAM-1 deficient FVB/n mice also showed increased presence of alveolar hemosiderin-positive macrophages (Fig. 3).

4.4.2 Fibrin deposition increases in pulmonary tissue of PECAM-1 deficient FVBn mice with increasing disease stage

Russell Movat Pentachrome Stain was used to detect deposition of fibrin as the disease progressed (Fig. 4). Fibrin stains as light, transparent pink in the healthy mice, intense pinkish-red in the borderline moderate animal, and diffuse pink in the severe animal, probably due to macrophage clearance of the fibrin. Fibrin deposition was observed to

increase as disease pathology progressed, but in the severe, highly fibrotic areas it was not as intense, which may be due to the macrophage clearance of fibrin deposits, however significant hyaline membrane (fibrin polymers) formation were not found. That may be due to the fact that mice are euthanized for humane care considerations once they fall below 65% blood oxygen saturation, which does not allow enough time for the membranes to form. Another possibility is that where hyaline membranes are a typical presence in acute lung injury, the injury in PECAM-1 deficient animals consists of chronic and slow microhemorrhages, which may account for a different response.

4.4.3 Presence of myofibroblasts in pulmonary tissue of PECAM-1 deficient FVBn mice

In order to determine the phenotypic characteristics of the interstitial fibroblasts, antibody against α -Smooth Muscle Actin (SMA) was used to detect the presence of myofibroblasts, and has shown a strongly increased presence of myofibroblasts in areas of fibrotic lesion formation (Fig. 5). Animals in the moderate disease stage were stained for α -SMA and show developing lesions with the characteristic swarming “swimming fish” pattern of myofibroblasts, clearly visible in brown. The presence of fibroblasts expressing smooth muscle actin is indicative of type I collagen secretion, an increase in the deposition of extracellular matrix and an increase in the contractile function of the pulmonary parenchyma, all of which contribute to the development of fibrotic foci [100]. We've previously shown the deposition of collagen in lesions of these mice [7].

4.4.4 IL-10 expression increases with fibrosis in PECAM-1 deficient mice

IL-10 is reported to be an anti-inflammatory cytokine and new evidence is coming forward that in some cases it may actually play a pro-fibrotic role [101]. We expected the levels of IL-10 to increase with the disease progression in our animals. Both Wild type and Healthy PECAM-1 deficient mice showed significant difference from Borderline PECAM-1 deficient mice (Fig. 6). WT and Healthy PECAM-1 deficient mice did not differ significantly from each other. Borderline and Moderate PECAM-1 deficient mice also did not differ significantly from each other. Only one mouse classified as Severe was available for analysis and included for comparison. Qualitative evaluation of IL-10 expression per disease stage by immunohistochemistry (Fig. 7) indicated that IL-10 was present in greater amount in fibrotic lung tissue and increased as disease stage progressed. IL-10 was detected mainly around and in the fibrotic lesions, supporting the assumption that erythrocytosis and consequent iron release by macrophages, together with the hypoxic environment, may be contributing greatly to increased expression of IL-10. We did see IL-10 expression around major airways in both control and diseased lungs, possibly expressed in the airway smooth muscle or airway fibroblast populations [102, 103].

4.4.5 PECAM-1 deficient mice in the FVB/n background have increased bleeding times

PECAM deficient FVB/n mice demonstrated significantly increased bleeding times. Average bleeding time of wild type mice was approximately 4 minutes (Fig. 8). In PECAM-1 deficient mice, the average bleeding time was 8.6 minutes. This result agrees

with Mahooti et al, who suggests this may be due to the overall vascular weakness in the PECAM-1 deficient mice, and that it may be endothelial PECAM-1 and not PECAM-1 on platelets that is mainly responsible for normal thrombotic functioning in this case [10].

4.5 Discussion

Our current working hypothesis is that pulmonary fibrosis in PECAM-deficient FVB/n mice is a result of alveolar collapse and bleeding, which is controlled by PECAM-1 dependent mechanisms, regulated by PECAM on platelets and/or endothelial cells. These mechanisms may include vascular integrity, thrombus activation, and endothelial cell survival. There is increasing evidence that vascular microinjury and coagulation are instrumental in the development of pulmonary fibrotic disease. Magro et al. has shown the role of vascular microinjury by anti-endothelial cell antibodies, extravasated red blood cells in alveoli and interstitia, and hemosiderin-positive alveolar and interstitial macrophages in IPF [104]. In 2012, Noth et al. assessed the role clotting plays in IPF by showing in a large clinical trial that anti-coagulant therapies exacerbated the process in IPF patients [4]. Several studies show that components of the pro-coagulant and anti-coagulant pathways, such as Tissue Factor upregulation, decreased anticoagulant Protein C, and thrombin generation are instrumental in fibrotic events [105]. The current coagulation hypothesis in human interstitial lung disease is that the formation of a clot in the lung, followed by activation of protease activated receptors (PAR1 and PAR2), leads to the fibrotic response. One of the immediate consequences of pulmonary microhemorrhages is the deposition of fibrin in the interstitia and alveoli. While a normal,

uninjured lung has an environment that is antithrombotic and pro-fibrinolytic, a chronic, repetitive injury appears to shift the balance towards procoagulant and anti-fibrinolytic events. In such an environment, fibrin deposition following repeated injury could be contributing to activating protease-activated receptors (PARs) and consequent pro-fibrotic events mediated by Transforming Growth Factor β . The increased microhemorrhages promote alveolar and interstitial fibrin deposition, forming a provisional matrix and thereby substantially contributing to lung fibrosis. Moreover, several procoagulant serine proteases such as Tissue Factor/ factor X and thrombin induce fibrotic events via the Protease Activated Receptors PAR-1 and PAR-2. In response to the activation of this G-protein coupled receptor, increased ECM production and secretion and induction of profibrotic growth factors such as TGF β and Platelet Derived Growth Factor (PDGF) are probably being produced [2, 3].

Duncan et al. discovered that vascular development and function is largely normal in PECAM-1 deficient mice [70], however since then, numerous studies have demonstrated that the stability of the endothelial cell junctions in the blood vessels of these animals is far easier to disrupt when these animals are subjected to physiological stress [69, 106]. PECAM-1 is also important for vascularization and alveolarization. Anti-PECAM-1 antibody treatment of rat pups inhibited endothelial cell (EC) migration but not proliferation or survival in vitro, thereby disrupting the development of normal alveolar septae without reducing the actual EC content. Subsequent three-dimensional reconstruction of the lungs showed that blocking of PECAM-1 caused a remodeling of proximal branches, producing large, tubular airways. Following studies in PECAM-

deficient C57 mice showed impaired alveolarization in spite of unaffected EC content, proliferation, or survival, while EC migration had shown to be reduced. Taken together, these studies provide evidence that it is the inhibition of EC function rather than loss of ECs that inhibits alveolarization in PECAM-1 deficient C57 mice [107]. Grasser et al. provided evidence on the significance of PECAM-1's role in the regulation of endothelial cell barrier function. Re-establishment of a vascular permeability barrier is delayed in the vessels of PECAM-1-deficient mice in skin exposed to histamine, and in the brain microvasculature of mice suffering from experimental autoimmune encephalomyelitis [9]. In 2005, two studies provided striking evidence of the effect of PECAM-1 deficient endothelial cell junctions in the events of septicemia, where PECAM-1-deficient mice proved to be far more susceptible to lipopolysaccharide (LPS)-induced septic shock than the WT controls [11, 69]. The two groups demonstrated, that when challenged with LPS, the blood vessels of PECAM-1-deficient mice showed increased permeability and a much increased loss of blood volume, with the resulting lethal drop in blood pressure, which, like the previously mentioned increased bleeding time phenotype, correlates particularly with the expression and non-expression of PECAM-1 on endothelial cells [11, 69]. Privratsky et al. found that unlike PECAM-1-deficient endothelial cells, PECAM-1 competent endothelial cells show increased barrier stability and quickly regain barrier integrity after challenging them with a thrombin-induced disruption to the monolayer[106]. PECAM-1 control of barrier maintenance was localized to its homophilic cell–cell junctions localization, as tested by a homophilic binding-crippled mutant of PECAM-1, which was not able to maintain barrier integrity in endothelial cells. PECAM-1 mutants deficient in residues specializing in PECAM-1-mediated signal

transduction did maintain adequate barrier integrity [106]. The prolonged tail-vein bleeding times in PECAM-1 deficient mice points towards the function of the vascular endothelium, rather than circulating platelets [10], although we are examining the role PECAM-1 in the functioning of platelets as well. Considering these previous findings, our studies here support the notion that PECAM-1-mediated adhesion and/or signaling contributes appreciably to vascular integrity and maintenance of a stable vascular permeability barrier, especially following disrupting stimuli, and the absence of PECAM-1 is leading to increased vascular permeability and subsequent pulmonary microhemorrhages in these mice.

In contrast to diseases like Diffuse Alveolar Damage (DAD) or Idiopathic Pulmonary Hemosiderosis (IPH), we see a relatively mild bleeding and alveolar collapse that eventually manifests into a chronic fibrosis, although DAD and IPH do involve fibrosis. Additionally, one of the hallmarks of our model is the relative absence of a pro-inflammatory cell infiltrate (such as neutrophils), and indeed our animals exhibit an anti-inflammatory profile. Based on other murine models of pulmonary fibrosis [5] our *a priori* hypothesis for this study was that inappropriate inflammation played a major role in disease initiation. One of the inflammatory cell types commonly present in an inflammatory response is the cells of the monocyte/macrophage line. Macrophages are noted for their plasticity, and can respond to their surroundings with numerous different types of polarized activation, such as the classically activated pro-inflammatory M1 type, the alternatively activated pro-repair M2 type, and the anti-inflammatory regulatory macrophages, to mention just a few examples [108-112]. The M1 type are activated by interferon gamma and tumor necrosis factor (TNF alpha), and manufacture inducible

nitric oxide synthase and IL-12. Once activated, they are effector phagocytes that specialize in microbicidal and tumoricidal activity [108-112]. The M2 type is activated by IL-4, IL-13, CCL2, and IL-6. They express arginase-1 (Arg-1), Fizz1, chitinase-3-like-3 (Ym1), and mannose receptor C-type lectin-1 (35-39). The M2 type has been associated with profibrotic and angiogenic conditions, especially in the pulmonary environment (35-39). Another subtype of regulatory macrophages is marked by the high production of IL-10 and low IL-12, and their immunosuppressive qualities [108-112]. Of particular interest to us are the M2 and the regulatory types having a possible function overlap. In moderate-severe stages of fibrotic disease of our PECAM deficient mice, we previously found high numbers of Ym1 positive M2 macrophages [8]. In this study, we found increased IL-10 levels, both in BAL and in the tissue of these animals, which would suggest that the M2 and the regulatory types are present in these animals, with possible overlap. One of the contributing factors could be that animals are experiencing hypoxia as the disease progresses, and there is current evidence that hypoxia leads to an accumulation of alternatively-activated alveolar macrophages that occurs prior to the development of pulmonary hypertension [113]. Indeed, the hypoxic environment is thought to polarize macrophages towards the M2 and regulatory pro-fibrotic phenotype [113]. However, extravasated red blood cells and iron can also polarize macrophages towards a M2 or repair phenotype [114]. This likely contributes to the accumulation of Ym1-positive alternatively activated macrophages that were found in our first examination of the fibrotic disease in PECAM-1 deficient mice [8]. Interestingly, corticosteroids have also been found to polarize macrophages towards the M2

phenotype, which might explain why these drugs have been found ineffective against fibrotic disease [115].

Hemosiderin is an iron-storage complex composed of ferritin, denatured ferritin and other material, located exclusively within cells. The iron it contains is not a readily-available source for supply iron, if needed. Hemosiderin is often found in macrophages after a hemorrhage [116, 117]. After blood exits a compromised blood vessel, the red blood cells die, releasing their hemoglobin. Macrophages phagocytose the hemoglobin and degrade it into hemosiderin and biliverdin [116, 117]. In an inflammatory response, pro-inflammatory M1 macrophages take up and use the iron bacteriostatically.

Alternatively activated M2 macrophages exhibit high numbers of scavenger receptors (CD163). These CD163 receptors play a dual role: they let the M2 macrophages take up iron very rapidly, and they allow the M2 macrophages to maintain a ferritin^{low}/ferroportin^{high} phenotype that allows the M2 macrophages to donate iron to their immediate surroundings [114]. Additionally, the M2 macrophages make anti-inflammatory mediators through the heme-oxygenase-dependent heme catabolism. Finally, the M2 phenotype is suspected of providing iron to fibroblasts for collagen synthesis, thus contributing to inappropriate tissue repair in the context of microhemorrhages [114]. We found that iron-positive macrophages increased as disease progressed, however, we then observed a slightly lessened but continued presence in the severe disease areas of dense fibrosis (Fig. 1). This would indicate that the microhemorrhages are no longer as intense in areas of dense fibrosis.

We conclude that this data supports the notion that PECAM-1-mediated adhesion and/or signaling contributes appreciably to vascular integrity and maintenance of a stable vascular permeability barrier, especially following disrupting stimuli, and that the absence of PECAM-1 is leading to increased vascular permeability and subsequent pulmonary microhemorrhages in these mice. Although the DeLisser study demonstrated transiently-delayed alveolarization in the PECAM-1 deficient C57 mice [107], we have not yet performed these studies in FVB/n PECAM-1 deficient mice partially due to breeding difficulties with this strain. We find that heterozygous breeding yields on average 10% FVB/n PECAM-1 deficient pups rather than the expected 25%, indicating that there may be potential embryonic lethality at vascularization and/or alveolarization stages phases of development. These questions will be the focus of future studies.

4.6 Figures and legends

Table 1. Grouping of disease in PECAM deficient mice

Group	SpO₂ range (3+ observations)	Pathology scoring
Healthy	89-94	None
Early/borderline	88-85	Focal, small lesions and alveolar enlargement
Moderate	85-75	Many lesions, early fibrosis
Late	<75, often cyanotic	Large lesions, extensive fibrosis

Disease stages of PECAM-1 deficient FVB/n mice classified by SpO₂

readings, using the MouseOx system by StarrLife Sciences. Redrawn from previous similar figure appearing in (7).

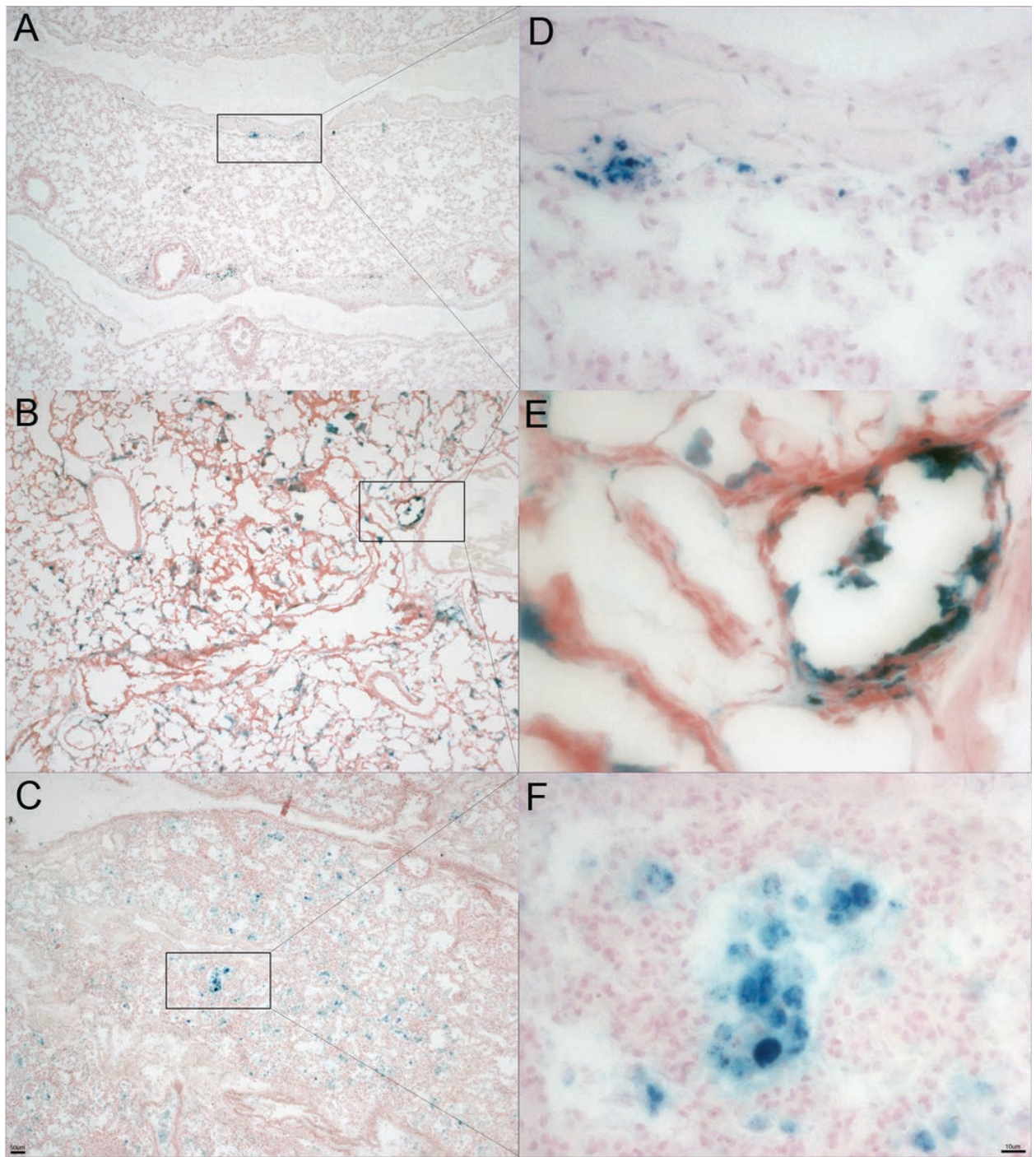


Fig. 4.1.

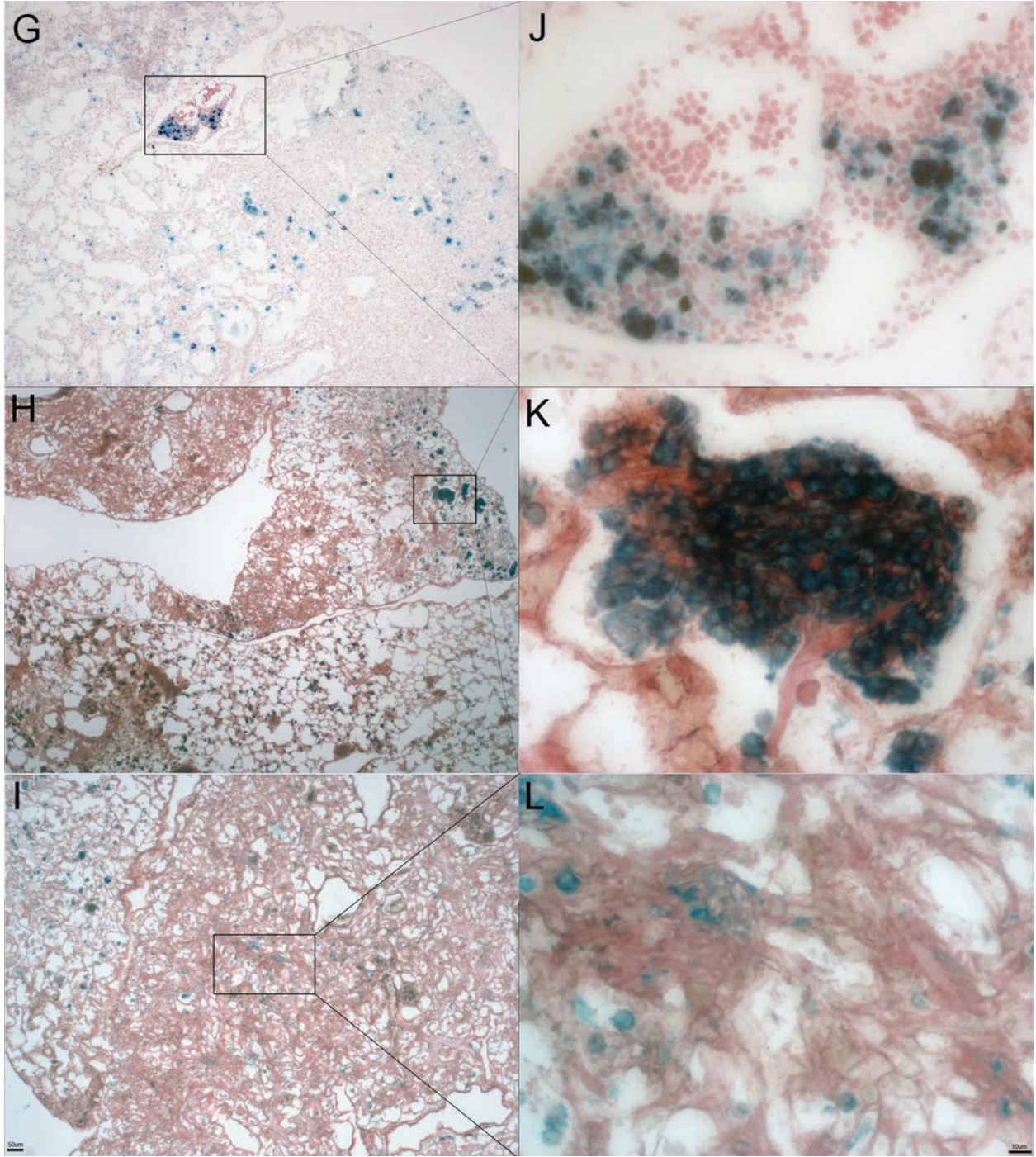


Fig. 4.1 continued.

Figure 4.1 continued: Prussian blue stain in healthy and diseased lung. A, D. Healthy PECAM-1 deficient mouse with sporadic iron-positive macrophages (4X and 32X). B, E, C, F. Borderline disease PECAM-1 deficient mice showing an increase in iron positive macrophages around vasculature, lesions, and in the interstitia and alveoli (4X and 32X). G, J. Moderate disease PECAM-1 deficient mouse showing a progressively increasing presence of iron-positive macrophages, with far more extensive regions of fibrosis (4X and 32X). H, K, I, L. Severe disease PECAM-1 deficient mouse, showing a heavy infiltration of iron-positive macrophages. The areas of dense fibrosis appear to be less permeated by these cells than areas of still somewhat retained lung architecture (4X and 32X).

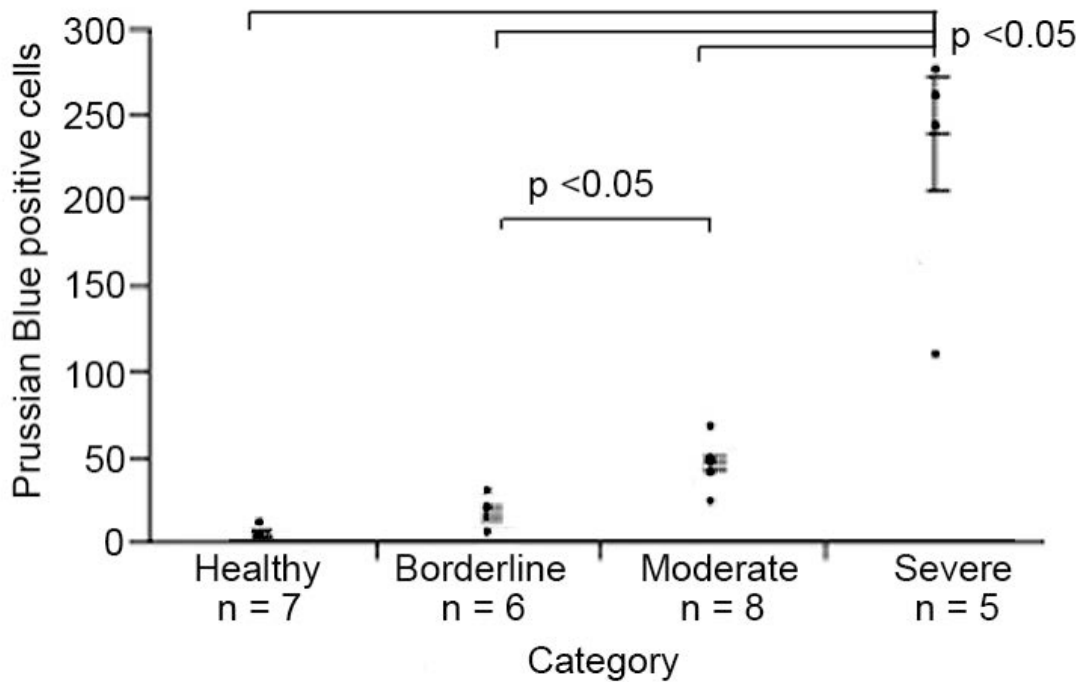


Fig. 4.2.

Figure 4.2 continued: Graph illustrating the increase of iron-positive macrophages in healthy and diseased lung. Group sizes (n = 4 wt; n = 7 healthy; n = 6 borderline; n = 7 moderate; n = 5 severe). Differences: what groups are different from what groups. $p < 0.05$ Tukey Kramer Honestly Significant Difference (HSD) test. Error bars indicate standard error.

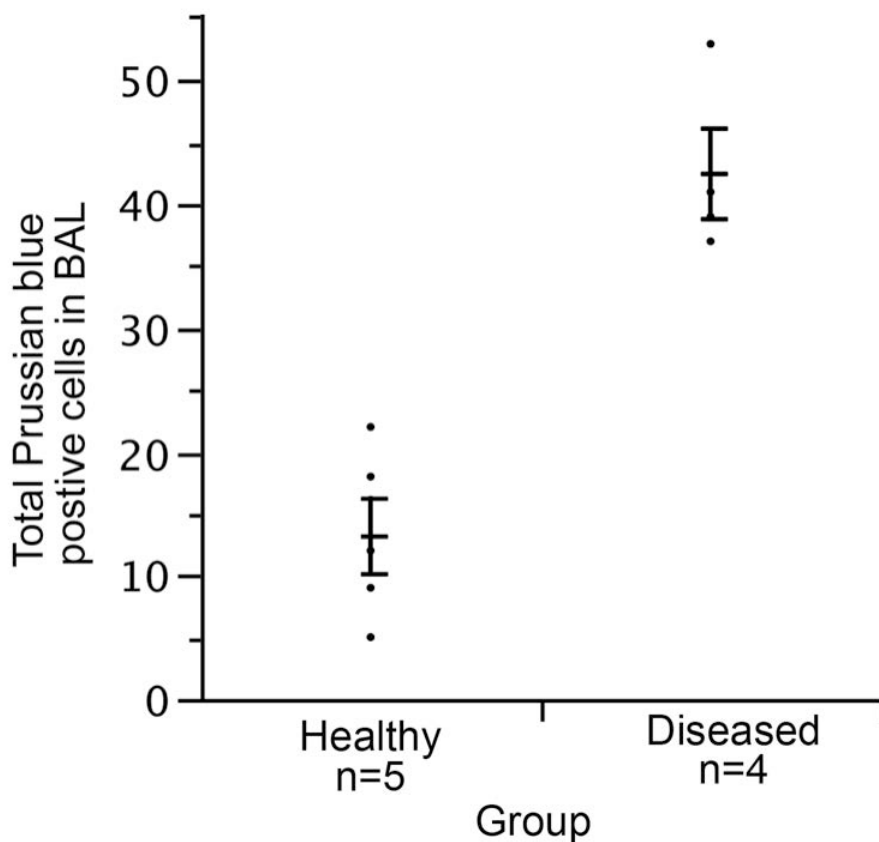


Fig. 4.3: Quantification of Prussian blue stain of bronchoalveolar lavage in healthy and diseased lung shows an increase in the presence of iron-positive macrophages with the progression of disease. Group sizes (n = 17 wt; n = 5 healthy; n = 5 moderate; n = 6 unknowns). Due to limited numbers of PECAM-1 deficient mice, we used most for histological analysis and did not do broncho-aleveolar lavages (BAL) in order to

maintain lung architecture. We did have frozen BAL samples from earlier studies before we had blood oximetry data, and we performed cytopins on five healthy and four diseased samples (confirmed by pathology), stained them with Prussian blue, and looked for hemosiderin-positive macrophages and red blood cells. We were unable to find red blood cells probably due to the freezing and thawing of the samples but did note significantly higher numbers of hemosiderin-positive macrophages in BAL from diseased mice ($p < 0.05$, Tukey Kramer HSD). Error bars indicate standard error.

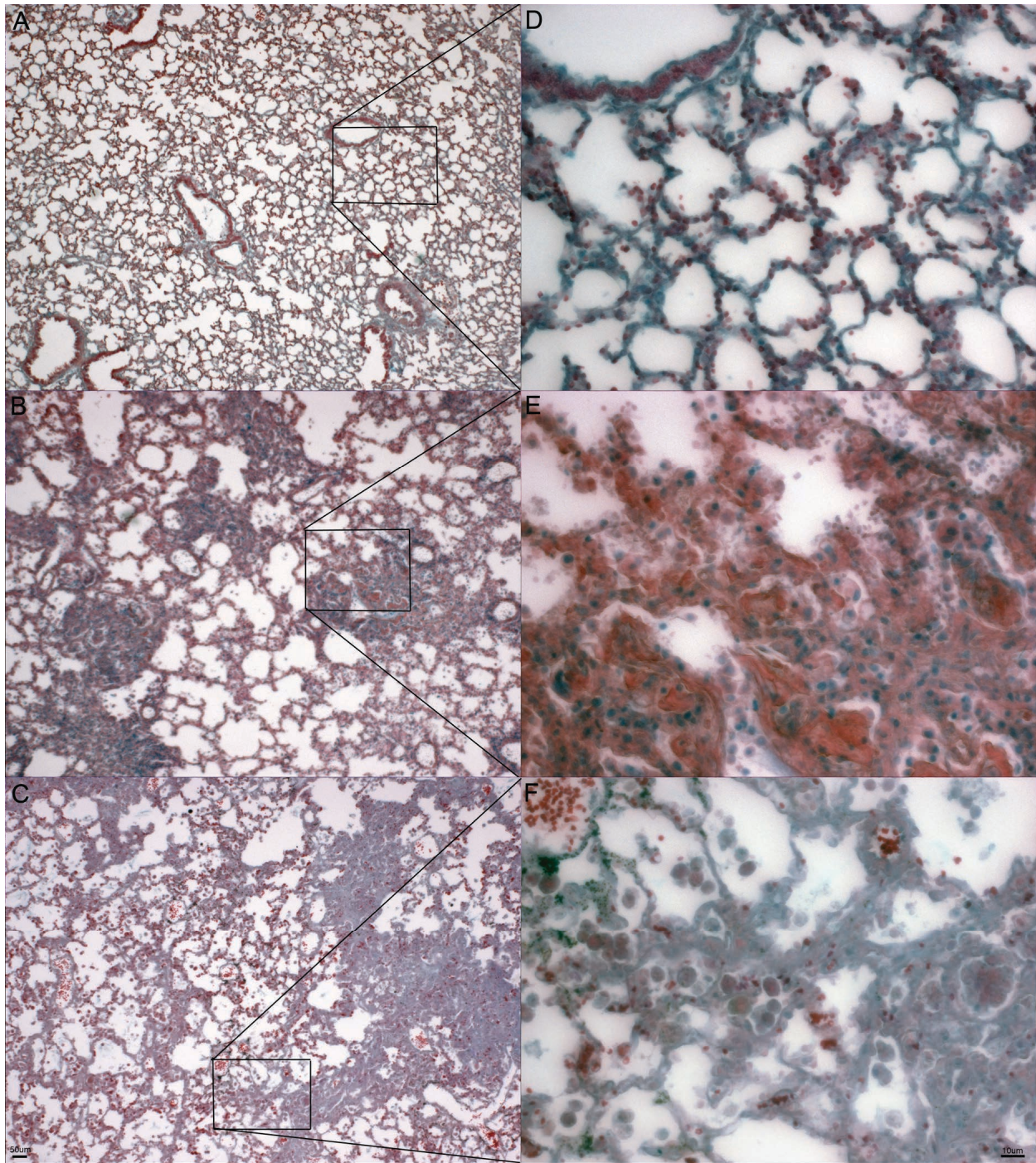


Fig. 4.4: Russell Movat Pentachrome stain for fibrin deposition in healthy and diseased lung. A, D. Healthy PECAM-1 deficient mouse with very minimal to no fibrin deposition (pinkish-red stain) around alveoli and interstitia (4X and 32X). B, E. Borderline

PECAM-1 deficient mouse showing an increase in fibrin deposition in the fibrotic lesions (pink-red stain) (4X and 32X). C, F. Severe PECAM-1 deficient mouse showing further fibrin deposition (pink-red stain), which appears to be less intense in the areas of dense fibrosis and more pervasive in the areas of still somewhat retained lung architecture.

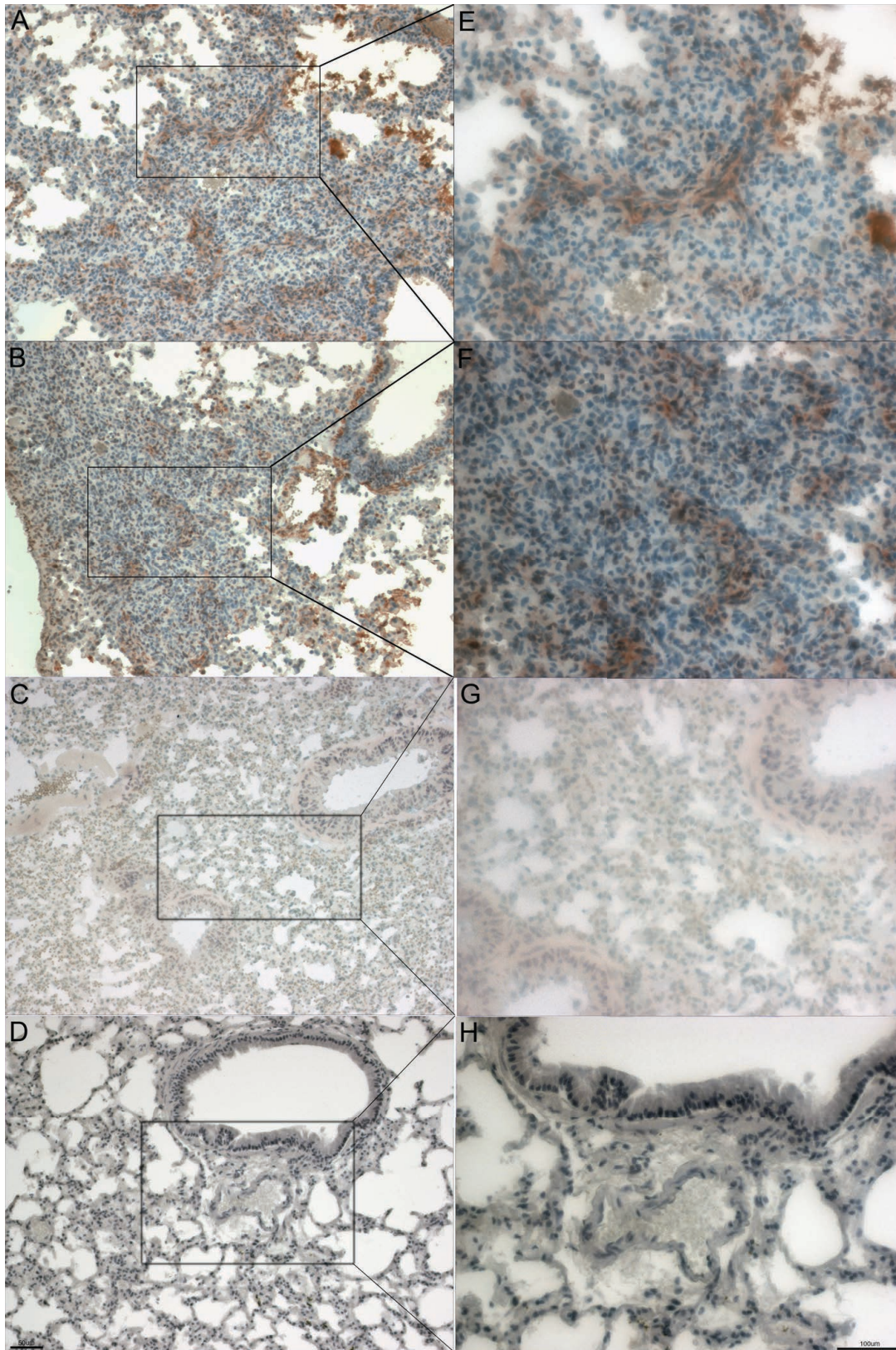


Fig. 4.5.

Figure 4.5 continued: Anti-smooth muscle actin stain in diseased PECAM-1 deficient mouse lung and wild type FVB/n lung. A, E, B, F. Moderate-severe PECAM-1 deficient mouse lung showing a heavy presence of myofibroblasts (brown stain) in a characteristic swarming swimming fish pattern around areas of collagen deposition (10X and 20X). C, G. Wild type FVB/n mouse was used as control. Some background staining is present in light brown around the interstitia and vasculature (10X and 20X). D, H. Tissue from a borderline PECAM-1 deficient mouse was used as a negative control due to shortage of tissue on the moderate-severe blocks (10X and 20X).

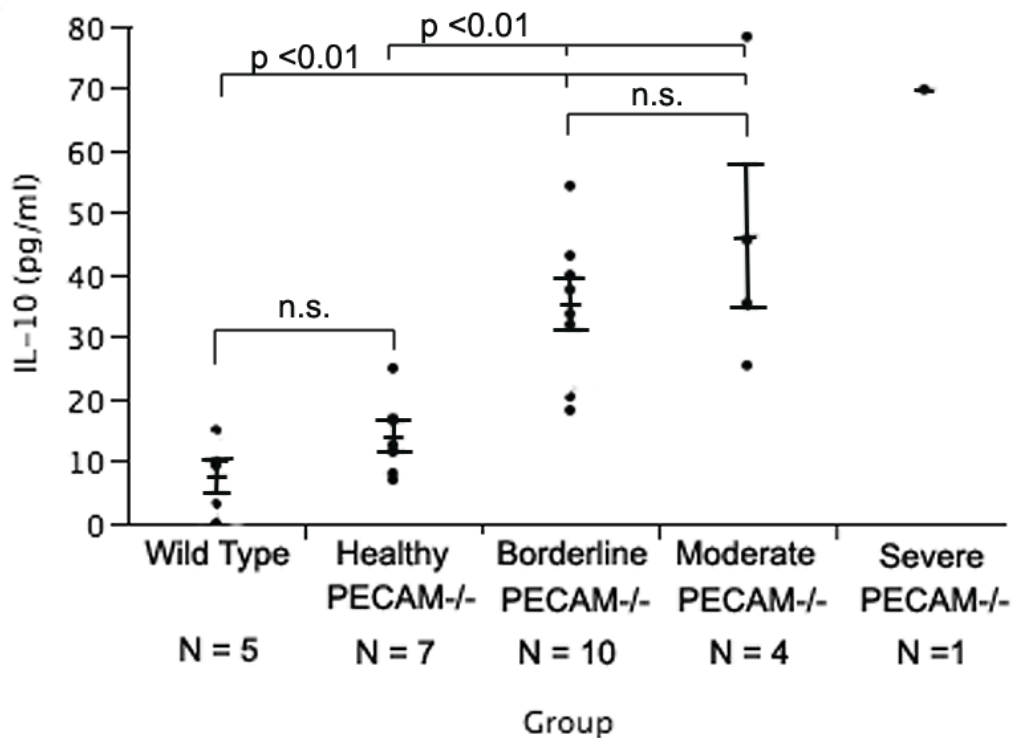


Fig. 4.6: IL-10 concentrations from lung lysates of both Wild type and Healthy PECAM-/- mice was significantly different from Borderline PECAM-/- and Moderate PECAM-/- mice ($p < 0.01$, Tukey-Kramer HSD). Wild type mice were not significantly different from healthy PECAM-/- mice. Borderline PECAM-/- mice were not significantly different from Moderate PECAM-/- mice. Unfortunately, only one mouse could be classified as Severe, but its data is shown here for comparison.

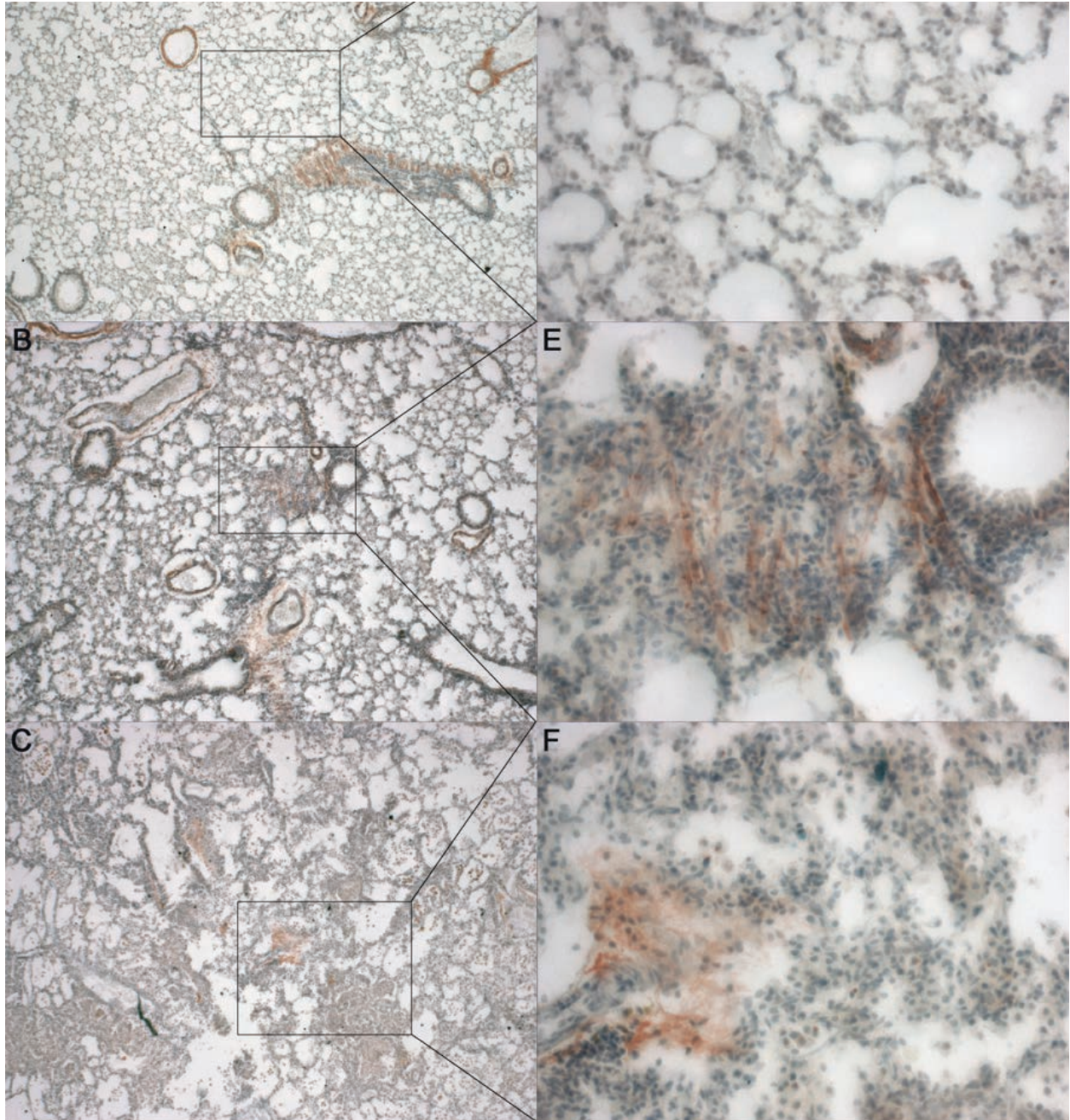


Fig. 4.7: IHC for IL-10 expression in healthy and diseased lung. A, D. Healthy PECAM-1 deficient mouse with minor IL-10 expression deposition (reddish-brown color) around alveoli and interstitia (4X and 20X). B, E. Borderline-Moderate PECAM-1

deficient mouse showing an increase in IL-10 expression in the fibrotic lesions (reddish-brown color) (4X and 20X). C, F. Moderate-Severe PECAM-1 deficient mouse showing further increase in IL-10 expression (reddish-brown color), visible more intensely around developing lesions and more diffuse in areas of existing dense fibrosis.

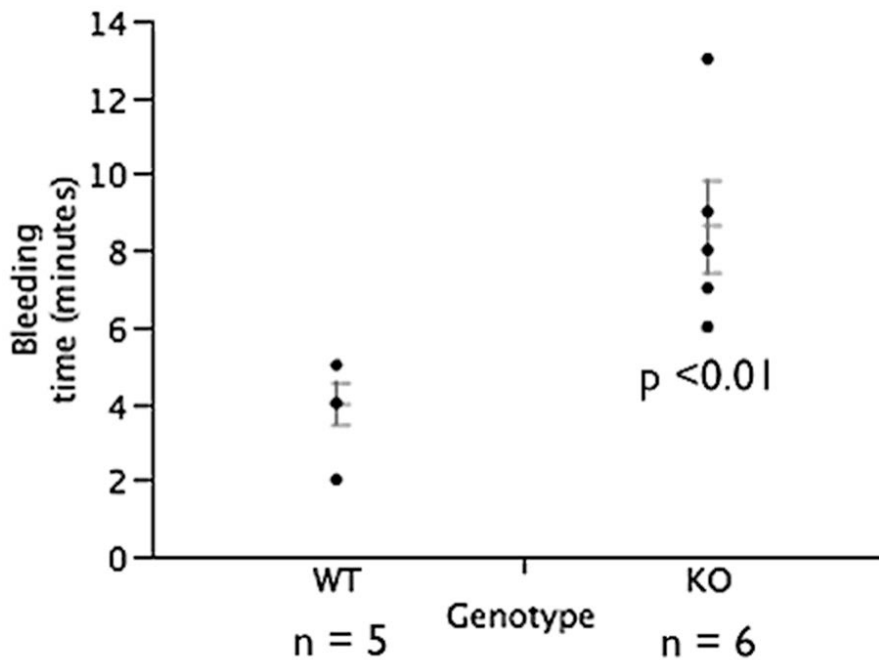


Fig. 4.8. Increased bleeding times in PECAM-1 deficient FVB/n compared to wild type control FVB/n mice.

CHAPTER 5 - COMPARATIVE ANALYSIS OF BLEOMYCIN IN THE LUNGS OF PECAM-1 DEFICIENT AND WILD TYPE FVB/N MICE.

5.1 Summary

Platelet Endothelial Cell Adhesion Molecule (PECAM/CD31) deficient mice in the FVB/n background spontaneously develop a chronic interstitial pneumonia. It has similarities to human interstitial pneumonia, including early alveolar collapse, subsequent development of fibrosis, and proliferation of myofibroblasts. This disease affects mice of all ages but is not fully penetrant, developing in about 40% of the mice. We show here that there appears to be leakage of blood into the lungs of affected mice. This implies that these mice would be susceptible to pulmonary insults. Bleomycin was used to try to induce lung injury and subsequent fibrotic disease in PECAM deficient and wild type mice in order to compare the disease process in this well-characterized model of pulmonary fibrosis. The FVB/n strain proved highly resistant to bleomycin, paradoxically suggesting that rather than being more susceptible to damage, these mice may have highly active but improper repair mechanisms that may contribute to subsequent fibrosis.

5.2 Introduction

PECAM-1 deficient mice on the FVB/n background spontaneously develop a fatal chronic pulmonary fibrotic disease that has similarities to the human IPF. One of the important aspects of the murine pathology is the absence of a detectable acute inflammatory event and absence of inflammatory infiltrate. One of the earliest disease events in these animals are alveolar collapse and red blood cells in the alveoli, which

we explain as the loss of vascular integrity in pulmonary and alveolar capillaries, with subsequent spontaneous pulmonary microhemorrhages into the interstitial and alveolar spaces. These occurrences would essentially be a repetitive sort of a pulmonary micro-hematoma. The alveolar space is currently thought to be an anti-inflammatory microenvironment, and the immune response to such a micro-hematoma in the lung is presently not well defined [3]. As consequence of microhemorrhages, these animals also show fibrin deposition into the interstitia and alveoli. In a normal lung where the microenvironment is pro-fibrinolytic and anti-thrombotic, a fibrin deposit would get dissolved and cleared, but in a chronically injured lung, the microenvironment may shift to pro-coagulant and anti-fibrinolytic, where fibrin deposits may remain, leading to increased protease receptors (PARs) activity, upregulation in Transforming Growth Factor β (TGF β), deposition of provisional matrix and consequent fibrosis [1, 2, 4, 105].

The bleomycin model of pulmonary fibrosis is currently the gold standard murine model of pulmonary fibrosis and intratracheal administration of it to mice is believed to be a faithful reproduction of histological fibrotic events that take place in humans [5, 118]. Bleomycin is a chemotherapeutic that was isolated from a strain of *Streptomyces verticillus* in 1966 [5, 119]. As a side effect of the treatment, it was discovered that bleomycin was able to cause irreversible interstitial pulmonary fibrosis in up to 10 percent of patients [5, 118]. It induces damage by the production of single- and double-strand scission by complexing itself with ferrous ions and molecular oxygen [5, 118]. The bleomycin model is considered the Gold Standard model of pulmonary fibrosis, although pulmonary fibrosis comes in many forms and bleomycin model most closely

mimics the features of acute lung injury (ALI) [5, 120]. Bleomycin complexes with oxygen and Fe²⁺, leading to formation of oxygen radicals, DNA breaks, and cell death. The enzyme that inactivates it is bleomycin hydrolase (cysteine protease), which is expressed in varying levels in different species, tissues, and cells. Of all organs, the lungs have the lowest levels of bleomycin hydrolase, and are thus susceptible to bleomycin. However, rabbits have sufficiently high amounts to be quite resistance to bleomycin. In mice, while C57BL6 mice are particularly sensitive, the Balb/c and C3H mice are resistant. Not much literature is available on the sensitivity of the FVB/n mice to bleomycin [5, 120].

Administered systemically, bleomycin does elicit lung inflammation that can progress to irreversible pulmonary fibrosis in humans and reversible fibrosis in rodents, due to inactivating effects of bleomycin hydrolase. Bleomycin hydrolase in human lungs and skin is far less active than in the lungs and skin of the rodent species, thus accounting for the reversibility of bleomycin-induced pulmonary fibrosis in rodents. In the human lung particularly, where bleomycin hydrolase is practically absent the effect of bleomycin is especially pronounced, and indeed different mouse strains show different levels of this enzyme, thus accounting for varying strain susceptibility to the bleomycin insult [121-127].

Bleomycin causes pulmonary injury and resultant fibrosis in a variety of species including mice, and is effective in a range of doses and delivery methods such as intraperitoneal (IP), subcutaneous (SC), intratracheal (IT) or intravenous (IV) [5].

Although the IV administration has its advantages in that it more closely resembles human exposure to bleomycin and targets the endothelium first, the disadvantage is that not all animals will develop fibrosis, and the time frame for development is quite long [128]. The delivery of bleomycin by IT (generally 1.25–4 U/kg) generally produces lung injury and resultant fibrosis in rodents with a single instillation [5].

The process starts with an initiation phase, which is marked by production of chemoattractant agents that emanate from the injured pulmonary tissue, inflammatory cytokines and resultant increase in the presence of inflammatory cells such as macrophages, granulocytes, and lymphocytes [120, 129]. Within 24 hours after a single-dose IT instillation, there is an increase in BAL neutrophils which plateaus around day 11. The lymphocytic influx starts around day 7 and has been seen to persist on day 11. TNF- α , IL-1 β , and IL-6 have been observed to be of particular importance, as their neutralization studies have shown a decrease in permeation of inflammatory cells and resultant fibrosis [130]. After that, alveolar inflammatory cells are cleared, fibroblast proliferation expands, and extracellular matrix is deposited [120, 130]. The fibrotic response can be seen in the lungs on day 11 and continues till around day 20 [5]. After 28 days, however, the response varies, with some earlier reports noting that IT bleomycin causes progressive or persistent fibrosis for 60–90 days, while others report a self-limiting response with a resolution phase at 60-90 days [120, 130].

In this study, a single dose intra-tracheal delivery of bleomycin was used to induce lung injury and subsequent disease in PECAM-1 deficient and wild type mice in order to test

sensitivity of the PECAM-1 deficient mice as compared to WT mice, to establish dose response, and to observe differences in pathology between the treated animals, and the spontaneous disease in untreated PECAM-1 deficient FVB/n mice. The mice were challenged with doses in the range of 0.01, 0.03, 0.05, 0.1 and 0.5 U. Surprisingly, both PECAM-1 deficient and WT FVB/n mice proved to be resistant to single-dose intra-tracheal delivery of bleomycin, demonstrating over 6 months survival. Only very high doses were able to cause a drop in blood oxygen levels. Lower doses caused dose dependent changes, but these were minor and PECAM deficient mice were able to fully recover from all but the highest doses. The ability of FVB/n mice to withstand all but the highest doses may point to highly active repair mechanisms that may be contributing to the spontaneously occurring pulmonary fibrosis seen in untreated PECAM-1 deficient FVB/n mice.

5.3 Materials and methods

5.3.1 Animals

PECAM-1 deficient and wild type FVB/n mice were housed at Colorado State University Laboratory Animal Resources. Veterinary care and pulse oximetry were done under protocols approved by the Colorado State University Animal Care and Use Committee. All animals used were under the care and supervision of the Laboratory for Animal Research. FVB/n strain wild type and PECAM deficient mice (a generous gift of Dr. William A. Muller, Northwestern University) were raised in the same rooms. All

procedures were reviewed and approved by the CSU research institutional Animal Care and User Committee.

5.3.2 Bleomycin delivery by intratracheal instillation

We tested doses 0.01, 0.03, 0.05, 0.1 and 0.5 Units per mouse. Bleomycin was delivered by intrapulmonary aerosol delivery using a microspray device (MicroSprayer, model IA-C; PennCentury, Philadelphia, PA) attached to an FMJ-250 high pressure-syringe device (PennCentury). Briefly, mice were first lightly anesthetized in a sealed vessel containing Isoflorane (5% isofluorane in oxygen 4L/min; VIP 3000 isofluorane vaporizer). When the animal became anesthetized it was removed and placed on its abdomen with head elevated, on the 45° angle wedge-shaped block, unrestrained. Heads of animals were suspended up with an incisor loop located on block attachment. During the intubation the mouse was on continued isofluorane anesthesia via a nose cone. The mouth was opened and with help of a cotton tip, the tongue was extended in an outward rolling motion. To focus on the trachea, we used a binocular optivisor, x 5 magnificent (Thomas Scientific, Swedesboro, NJ). The same operator performed all the instillations in these studies. Then, the MicroSprayer™ tip was inserted into the trachea and the formulation was sprayed. The mouse was placed in its cage until it woke from the anesthesia (2-3 minutes). All the animals were monitored for regular breathing and behavior post treatment.

5.3.3 Blood oxygen saturation

Blood oxygen saturation was monitored as described previously in [7].

5.3.4 Glutaraldehyde perfusion

Lungs were glutaraldehyde perfused post sacrifice, processed, and sectioned at 7 μ m on standard microtome. A column of 8% EM grade glutaraldehyde was suspended about 20 cm above work surface using tape. An extension tube was connected from the column to a blunt 20 gauge needle. The tubing was primed before inflation so no air passed into the lungs. The mouse was humanely euthanized using carbon dioxide. The mouse was placed on a dissection board in a supine position and limbs were pinned to secure positioning. The abdominal cavity was opened and the mouse was additionally exanguinated by cutting the abdominal aorta. The thoracic cavity was cut open carefully to avoid cutting the lungs or any vessels, and the trachea was revealed. A small incision was cut in the trachea making sure not to cut it in half completely. The 20 gauge needle was inserted into the trachea and secured with a piece of suture. The board was then raised upright, placing the mouse in an upright position. Glutaraldehyde was allowed to flow slowly into the lungs under the force of gravity, until the lungs were fully inflated. The lungs were tied off with a piece of suture to prevent glutaraldehyde from escaping, and then were dissected out in one piece and placed in additional glutaraldehyde for 24 hours. After 42 hours, the lungs were placed in 70% ethanol, until ready for processing.

5.3.5 Prussian Blue stain for hemosiderin-positive macrophages in pulmonary tissue

Zinc-fixed paraffin-embedded tissue was sectioned on a standard microtome at 7um and rehydrated to dionized (DI) water. Slides were immersed in equal parts 0.2% hydrochloric acid and 0.2% potassium ferrocyanide solution for 1 hour at room temperature (RT). Slides were counterstained in 0.2% solution of Safranin O for 2 minutes, washed in 1% aqueous acetic acid, dehydrated and mounted in synthetic resin. Hemosiderin appears in blue, nuclei in red, and background in pink.

5.3.6 Russell-Movat Pentachrome stain for fibrin deposition in pulmonary tissue

Zinc-fixed paraffin-embedded tissue was sectioned on a standard microtome at 7 um and rehydrated to DI water. Staining was performed as per the kit protocol (American Master Tech Catalog No. KTRMP), however, due to the porosity of the sections, Verhoeff's Elastic stain was omitted. Resulting stain shows collagen in greenish yellow depending on the age of deposition, muscle in red, mucins in blue to green, and fibrin in pale to intense red.

5.3.7 Statistics

Tukey-Kramer Honestly Significant Difference T test was used for comparison between blood oxygen levels at each timepoint.

5.4 Results

5.4.1 Bleomycin dosing

Single dose intra-tracheal delivery of bleomycin was used to induce lung injury and subsequent disease in PECAM-1 deficient and wild type mice in order to compare the disease process in this well-characterized model of pulmonary fibrosis. The mice were challenged with doses in the range of 0.01, 0.03, 0.05, 0.1 and 0.5 U.

At 0.01U: n = 3 PECAM-1 deficient mice; n = 5 WT mice

At 0.03 U: n = 3 PECAM-1 deficient mice; n = 2 WT mice Note: one of the 0.03 knockouts was instilled with an additional 0.1U at a second timepoint.

At 0.05 U: n = 3 PECAM-1 deficient mice; n = 3 WT mice Note: two of the 0.05 knockouts were instilled with an additional 0.1U each at a second timepoint.

At 0.1 U: n = 2 PECAM-1 deficient mice; n = 4 WT mice

At 0.5 U: n = 4 PECAM-1 deficient mice; n = 5 WT mice

Both PECAM-1 deficient and WT FVB/n mice were resistant to single-dose intra-tracheal delivery of bleomycin at doses from 0.01U to 0.1U, demonstrating over 6 months survival. Sporadic deposition of hemosiderin-positive macrophages was seen ranging from single cells to small pockets of clumped cells at 0.01U, along with appearance of separate fibrotic foci (Fig. 2). Hemosiderin positive macrophages were seen at 0.5U, present mainly in the highly fibrotic regions of PECAM-1 deficient animals

in a spread-out pattern, and in clumped, peripheral clusters in wild type animals (Fig. 3-4).

Out of the four PECAM-1 deficient mice at 0.5U, two of the PECAM-1 deficient mice did show falling SpO₂ levels, and two remained at around 87% SpO₂. Upon examining their lungs for histology, all 4 mice did have areas of fibrosis. The lungs of one mouse that did show a drop in blood oxygen did not show extensive hemosiderin-positive infiltration, although it also had areas of fibrosis (data not shown). This mouse started out with SpO₂ levels of 98% at its time of treatment, and retained its level of around 87% at week 2.5.

Similarly, at 0.5U the wild type mice had half the mice show falling SpO₂ levels, and half the mice not show any drop. The lungs of all WT mice showed some infiltration of hemosiderin-positive macrophages into the heavily fibrotic areas, less so than the PECAM-1 deficient mice.

5.4.2 Prussian Blue stain for hemosiderin-positive macrophages in pulmonary tissue of bleomycin-treated PECAM-1 deficient and WT FVB/n mice

Due to limited samples, only 0.01U and 0.5U tissue was available for histology for the Prussian Blue staining. At very low doses (0.01U), both PECAM-1 and WT FVB/n mice showed separate foci of fibrosis as well as predominantly areas of still retained lung architecture. The hemosiderin-positive macrophage infiltration ranged from a widespread pattern to pocketed clusters of cells, which appeared to be similar in both

PECAM-1 deficient and WT animals. Hemosiderin positive macrophages were seen at 0.5U. The pattern of deposition in PECAM-1 deficient mice ranged from spread out to small clusters of cells predominantly in fibrotic areas. The pattern in WT mice presented less cells, but they appeared mainly as single cells rather than clumps in fibrotic areas.

5.4.3 Russell Movat Pentachrome stain for fibrin deposition in pulmonary tissue

Due to limited samples, only tissue of .01U, .03U, and 0.5U was available for fibrin staining with Russell-Movat Pentachrome. Fibrin deposition at 0.01U and 0.03U was pale pink but visible with a steady presence. At 0.5U, the stain increased in intensity, but appeared interspersed in areas of fibrosis. It differed from the pattern of deposition we see in spontaneously occurring disease, which may be due to intratracheal delivery of bleomycin, which directly targets the epithelium, whereas in the spontaneously occurring disease on untreated PECAM-1 deficient FVB/n mice, the events start with the endothelium. It may also be due to the single-dose of bleomycin approach, which delivers the robust insult once. Rather than a repetitive series of smaller insults - reoccurring microhemorrhages leading to fibrin deposition again and again, it is a one-time event with bleomycin, where hemorrhage occurs, fibrin deposition takes place, after which debris clearance begins.

5.5 Discussion

Our primary intention for conducting a study with bleomycin was to test the sensitivity and long-term survival of PECAM-1 deficient mice. We were also interested in how the spontaneously occurring disease would compare to the events induced by a single dose

IT bleomycin. We show here that there appears to be leakage of blood into the lungs of affected mice. This implies that these mice would be susceptible to pulmonary insults. The lungs are known for having a predisposition towards an anti-inflammatory microenvironment. Deletion of PECAM-1 in an FVB/n mouse may be skewing it further towards anti-inflammatory events. We aimed to establish dose effectiveness and assess response in PECAM-1 deficient and wild type FVB/n mice to the well-established bleomycin-driven inflammatory model of intra-tracheal instillation.

Both PECAM-1 deficient and wild type FVB/n groups showed resistance to bleomycin. We tested doses at 0.01, 0.03, 0.05, 0.1 and 0.5 U. All five doses resulted in survival for over 6 months. We were able to induce a drop in SpO₂ levels only at 0.5U and only in half of the animals per group. Most importantly, PECAM-1 deficient mice were virtually identical to wild type mice in their ability to withstand such a high dose.

Different mouse strains do show a varied response to bleomycin, likely due to differences in the levels of bleomycin hydrolase expression [124]. The resistance both PECAM-1 deficient and the wild type FVB/n mice had demonstrated in our study suggests higher levels of bleomycin hydrolase in the FVB/n strain. Before any further studies with bleomycin, assessment of bleomycin hydrolase expression in FVB/n strain should be done.

Additionally, prostaglandins (PG), which have both pro and anti-inflammatory properties, may be involved in protecting against bleomycin-induced injury, PGE₂ being of

particular interest. Kolodsick shows that PGE₂ can inhibit proliferation of fibroblasts and thereby dampen collagen deposition, and inhibit fibroblast to myofibroblast transition induced by TGFβ [131]. Oppenheimer-Marks shows that PGE₂-treated animals show a reduced lymphocyte population in damaged pulmonary tissue, while numerous studies demonstrate that PGE₂ is vital in lymphocyte influx regulation and differentiation in bleomycin injury [132] Given the gene expression variations between mouse strains, this could offer a partial explanation for the resistance we observed in our study.

At 0.5U we observed areas of alveolar hemorrhage in bleomycin-treated PECAM-1 deficient and WT FVB/n mice. These areas were infiltrated by hemosiderin-positive macrophages, which indicate a chronic pulmonary bleeding, and are known to secrete matrix metalloproteases (MMPs). MMPs have been found in lungs of humans with Idiopathic Pulmonary Fibrosis (IPF) and diffuse alveolar damage. In particular, MMP-2 (gelatinase A) and MMP-12 (macrophage metalloelastase) levels have been found to be higher in the acute phase of bleomycin induced injury in rodents [120]. MMP-12 is secreted by activated macrophages and is converted to active form in pulmonary tissue - an event that studies show to be an early event shortly after bleomycin treatment, while the macrophages levels are at their peak. MMP-12 is particularly effective at elastin and collagen IV degradation, which are structurally important to the basement membrane. Several studies with MMP-12 deficient mice have shown that MMP-12-deficient macrophages are less able to degrade extracellular matrix and cannot penetrate the basement membrane [5, 120]. Studies have shown that mice respond to acute pulmonary insult such as bleomycin by increasing numbers of macrophages,

activation of metalloproteases, basement level degradation and formation of leaky capillaries [5].

The initial response of the lung to single-dose IT delivery of bleomycin is hallmarked by severe inflammation. Chemoattractants emanating from the injured lung tissue recruit an influx of inflammatory cells into the alveolar spaces. An increase in the permeability of pulmonary epithelium and endothelium allows for extravasation of plasma proteins such as fibrinogen, which leads to fibrin clots in the alveoli [5, 120].

Fibrin in the intra-alveolar spaces and interstitia was analyzed in bleomycin-treated PECAM-1 deficient and WT animals. The extent and pattern of deposition of fibrin in the lungs of these mice were examined at 0.01, 0.03, and 0.5 U. Pale but clearly visible deposits were observed in the lungs of 0.01 and 0.03 instilled PECAM-1 deficient and WT animals. 0.5 U showed a more diffuse deposition interspersed in areas of fibrosis. For this diffuse pattern of deposition, our method of Russell Movat Pentachrome stain is not optimal and does not provide distinct visualization. For future fibrin visualization, a fibrin(ogen) antibody will be used, and morphometric quantification could be used to compare fibrin deposition with more precision.

Hemosiderin-positive macrophages in bleomycin-treated mice were an unexpected find. Interestingly, most single-dose IT bleomycin studies in mice do not show the presence of hemosiderin-positive macrophages. One study that did show a presence of these cells was done by Swaisgood et al in 2000, and used the C57BL6/129 strain of mice,

with 0.075 U bleomycin administered IT single-dose. Mice were sacrificed 14 days post treatment, with some animals showing early mortality. Swaisgood et al used Prussian Blue to track hemorrhages by hemosiderin-positive macrophages. The experimental groups were:

- plasminogen-deficient mice
- plasminogen +/- mice
- urokinase-deficient mice
- urokinase receptor-deficient mice
- tissue plasminogen activator-deficient mice
- control wild type mice

Upon examination, it was observed:

- WT mice showed the most significant hemorrhages
- plasminogen +/- mice showed mixed phenotype of hemorrhage and fibrosis
- tissue plasminogen activator-deficient showed mixed phenotype of hemorrhage and fibrosis

Hemorrhagic phenotypes correlated with early deaths in these animals. The other experimental groups showed collagen buildup with no hemorrhages detected by Prussian Blue. Higher levels of macrophages and activation of MMP-12 were found in the lungs of mice with hemorrhagic phenotype [120].

Swaisgood et al speculates that the intra-alveolar hemorrhages may be due to cell-mediated basement membrane degradation through cell-mediated urokinase activation

of plasminogen with possible involvement of matrix metalloproteinases. Macrophages, especially when stimulated with a toxin, have been shown to secrete macrophage plasminogen activator, however for that, plasminogen needs to be present in the system. Plasminogen can serve as an attractor for greater numbers of macrophages, which leads to greater levels of MMP-12 production, degradation of the ECM, and eventual endothelial cell damage, leading to hemorrhages.

The highest numbers of hemosiderin-positive macrophages were observed at 0.5U concentration, in the highly fibrotic areas of PECAM-1 deficient mice. These hemosiderin-positive macrophages may belong to the M2 phenotype as it scavenges red blood cells and tries to initiate repair. The reason we see more of these cells in the PECAM-1 deficient mice compared to the wild types, may be that PECAM-1 deficient mice are predisposed towards trying to reestablish an anti-inflammatory environment and in doing so generate higher numbers of these cells.

Mechanistically, in spontaneous disease we see a PECAM-1 based endothelial dysregulation, which leads to chronic, repetitive micro-hemorrhages, generating an ongoing cycle of repair, fibrin deposition, provisional matrix deposition, collagen deposition, and resultant fibrosis. We believe the damage in this model to start from the endothelial cells and show fibrin deposition as one of the later steps.

In single-dose IT bleomycin instillation, we see a single time robust insult that begins with the endothelium, an inflammatory response and edema leading to plasma protein

leakage and fibrin deposition due to that leakage. In this model of injury, we probably see a mixed M2/M1 macrophage population. The M1 may be present in the initial inflammatory phase, secreting MMP-12 which would lead to ECM degradation and subsequent damage to the endothelium. Red blood cell leakage may be due to this resultant damage and possibly apoptosis of endothelial cells. Once there is blood cell leakage, it is possible that the M2 is generated in greater numbers, as it would need to scavenge extravasated red blood cells and initiate repair.

In this regard, it is possible that in the model of spontaneously occurring disease, we see hemosiderin-positive macrophages in the earliest stages, even in animals that are still showing healthy SpO₂ readings, because the microhemorrhage in that model is a starting event (whether triggered by an externally inhaled or an internal trigger) that precipitates the cascade. In the bleomycin IT model, it may be that microhemorrhage is a late event.

Overall, the single dose IT route and the chronic, repetitive injury appear to be two different mechanisms, each with its own distinctive pattern. The advantages of the single-dose IT bleomycin model are that it is well characterized, reproducible, straightforward in administration, has clinical relevance to some forms of fibrotic disease, and is an effective way to generate fibrosis. The disadvantages are that the disease may be self-limiting in mice, as well as the model having more in common with acute lung injury, than with the slowly progressing disease we see in our animals. The

next logical step would be intravenous administration of bleomycin in small, repetitive doses, which will be the focus of future studies.

5.6 Figures and legends

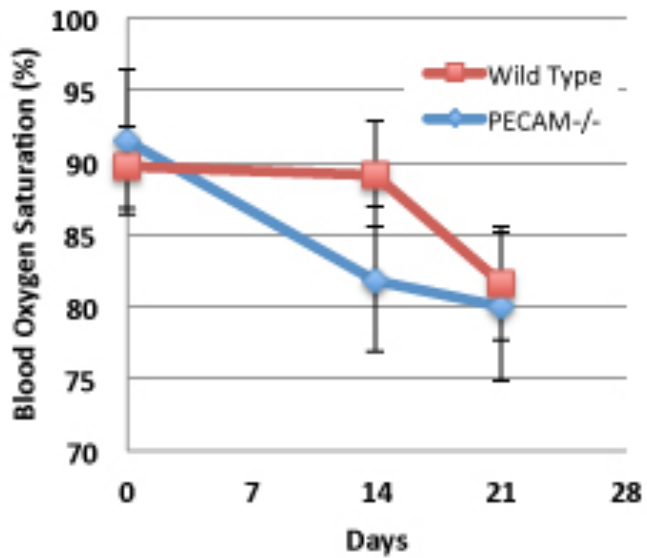


Fig. 5.1. 50% of WT and KO mice showed drop in SpO₂ only at highest dose (0.5U/mouse, full concentration). This indicates that 0.5U/mouse is LD₅₀ in FVB/n. LD₁₀₀ in C57 is 0.1U/mouse. No statistical differences between WT and PECAM KO (Kaplan-Meier, n = 5 for WT and n= 4 KO).

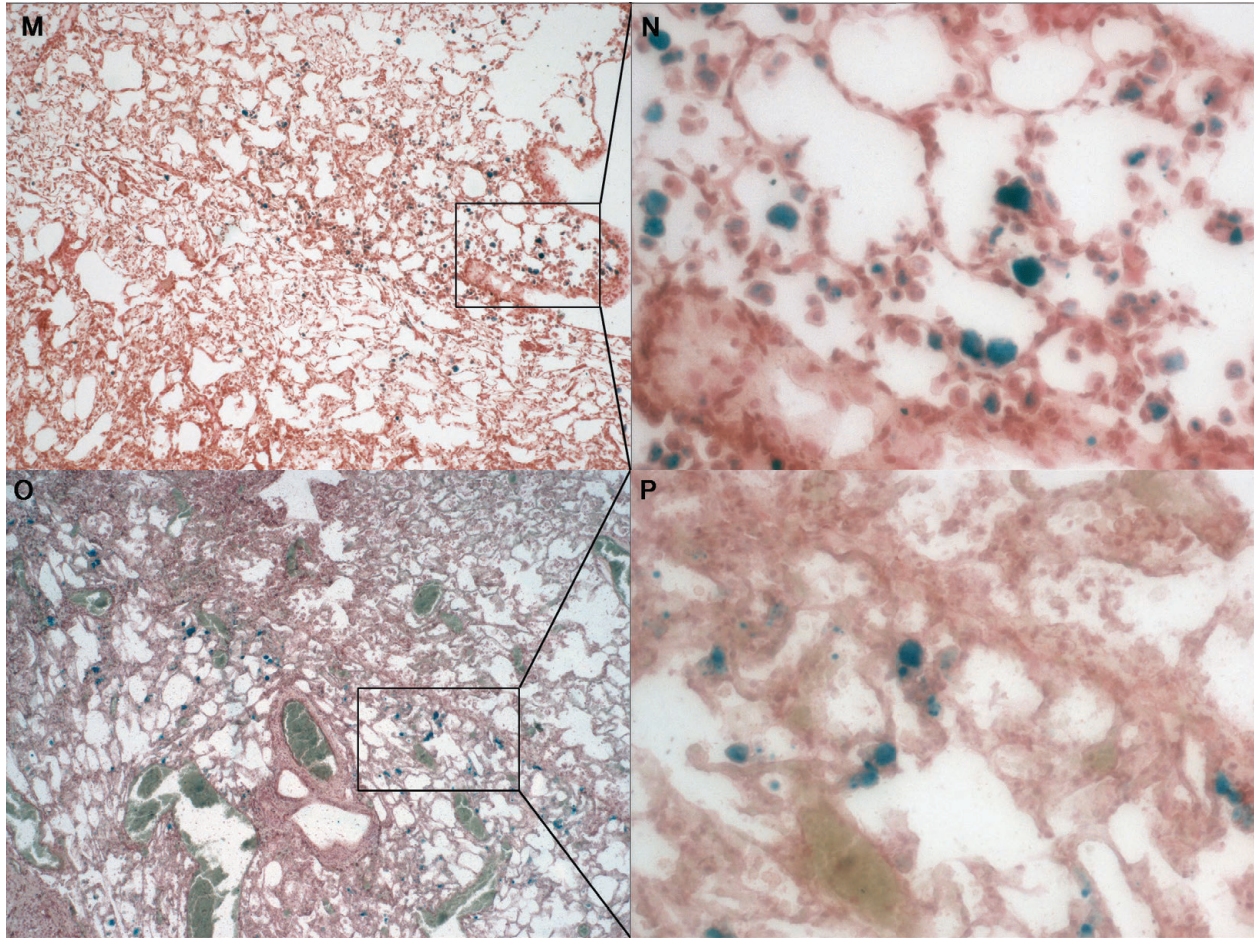


Fig. 5.2. Prussian Blue stain for hemosiderin-positive macrophages in PECAM-1 deficient and WT FVB/n mice at 0.01 U bleomycin single-dose IT treatment, visible in light to dark blue. M, PECAM-1 deficient FVB/n 4X. N, PECAM-1 deficient FVB/n 20X. O, WT FVB/n 4X. P, WT FVB/n 20X

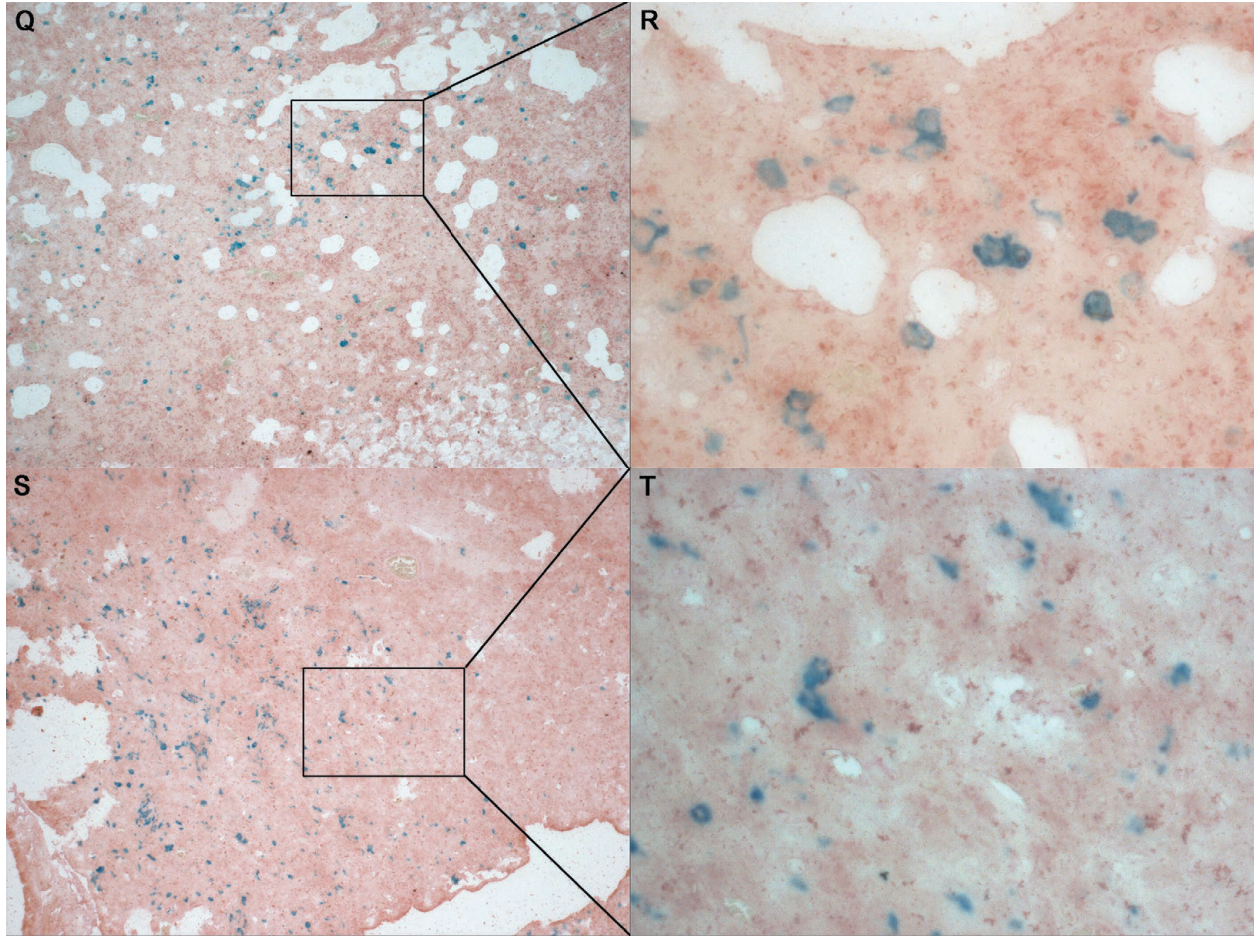


Fig. 5.3. Prussian Blue stain for hemosiderin-positive macrophages in PECAM-1 FVB/n mice at 0.5 U bleomycin single-dose IT treatment, visible in light to dark blue. All images taken at 4X and 20X.

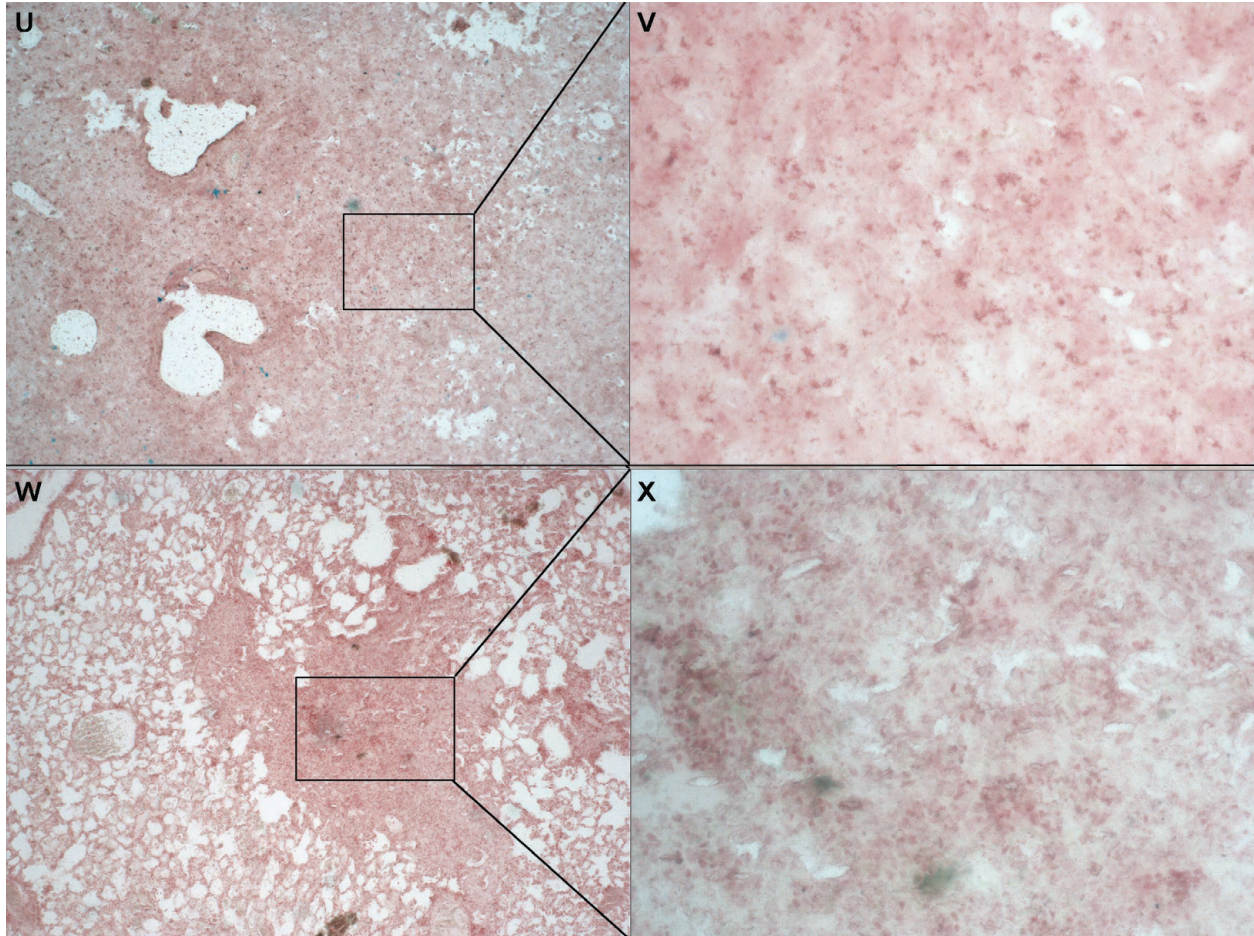


Fig. 5.4. Prussian Blue stain for hemosiderin-positive macrophages in WT deficient FVB/n mice at 0.5 U bleomycin single-dose IT treatment, visible in light to dark blue. All images taken at 4X and 20X.

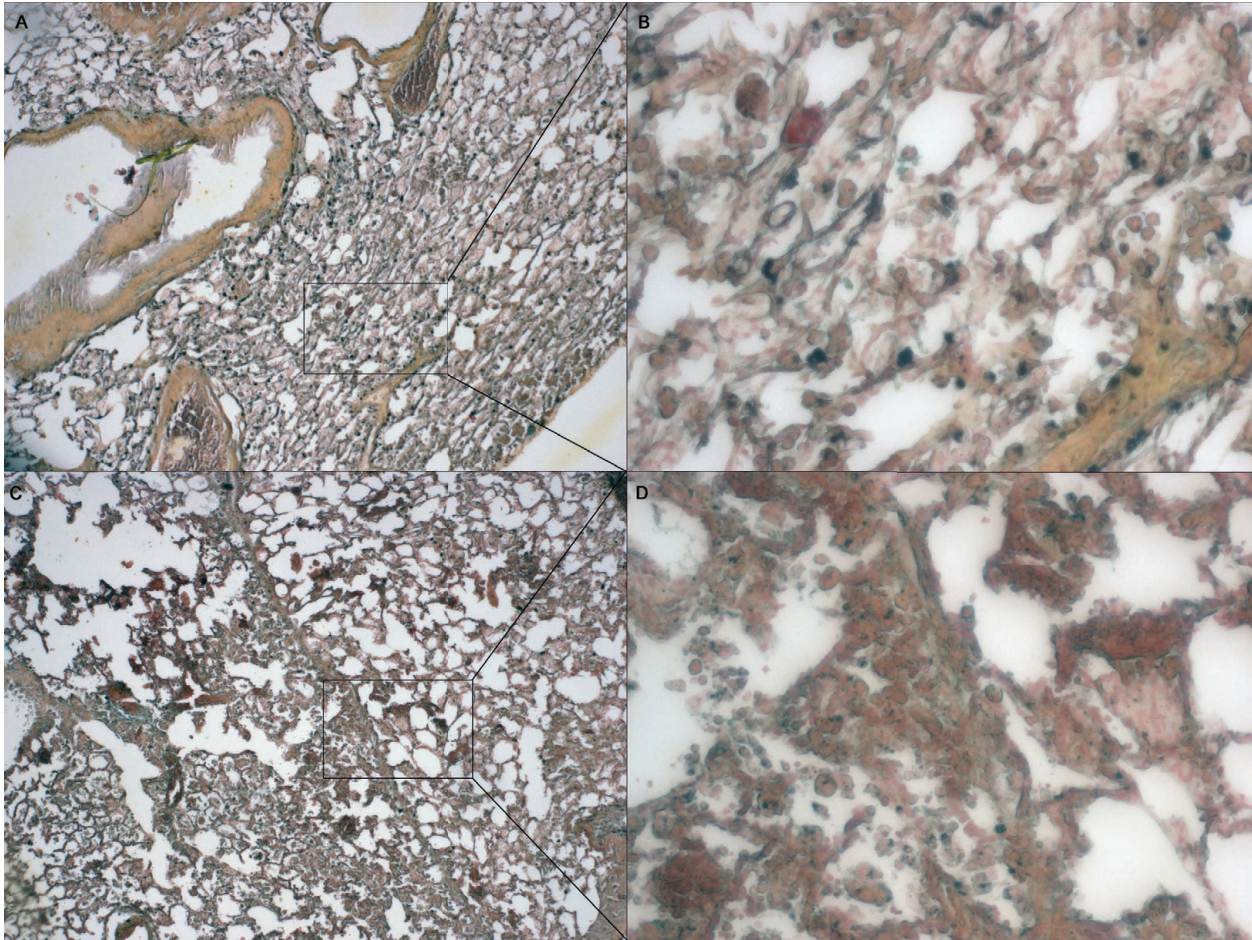


Fig. 5.5. Russell-Movat Pentachrome stain for fibrin in WT and PECAM-1 deficient, bleomycin-instilled FVB/n mice at 0.01U single-dose IT bleomycin treatment. Fibrin is stained in light pink to more intense red. A, PECAM-1 deficient FVB/n 4X. B, PECAM-1 deficient FVB/n 20X. C, WT FVB/n 4X. D, WT FVB/n 20X.

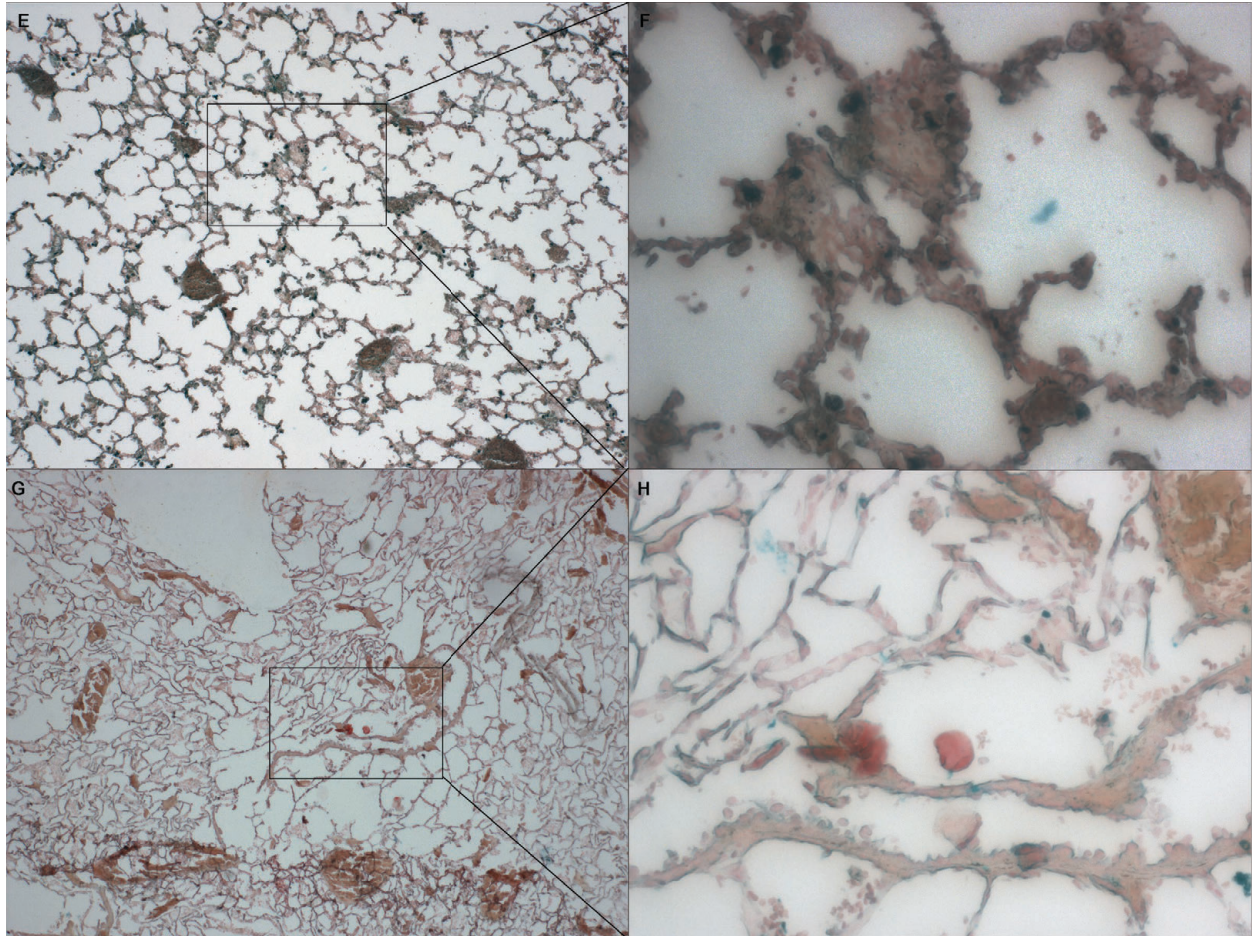


Fig. 5.6. Russell-Movat Pentachrome stain for fibrin in WT and PECAM-1 deficient, bleomycin-instilled FVB/n mice at 0.03U single-dose IT bleomycin treatment. Fibrin is stained in light pink to more intense red. E, PECAM-1 deficient FVB/n 4X. F, PECAM-1 deficient FVB/n 20X. G, WT FVB/n 4X. H, WT FVB/n 20X.

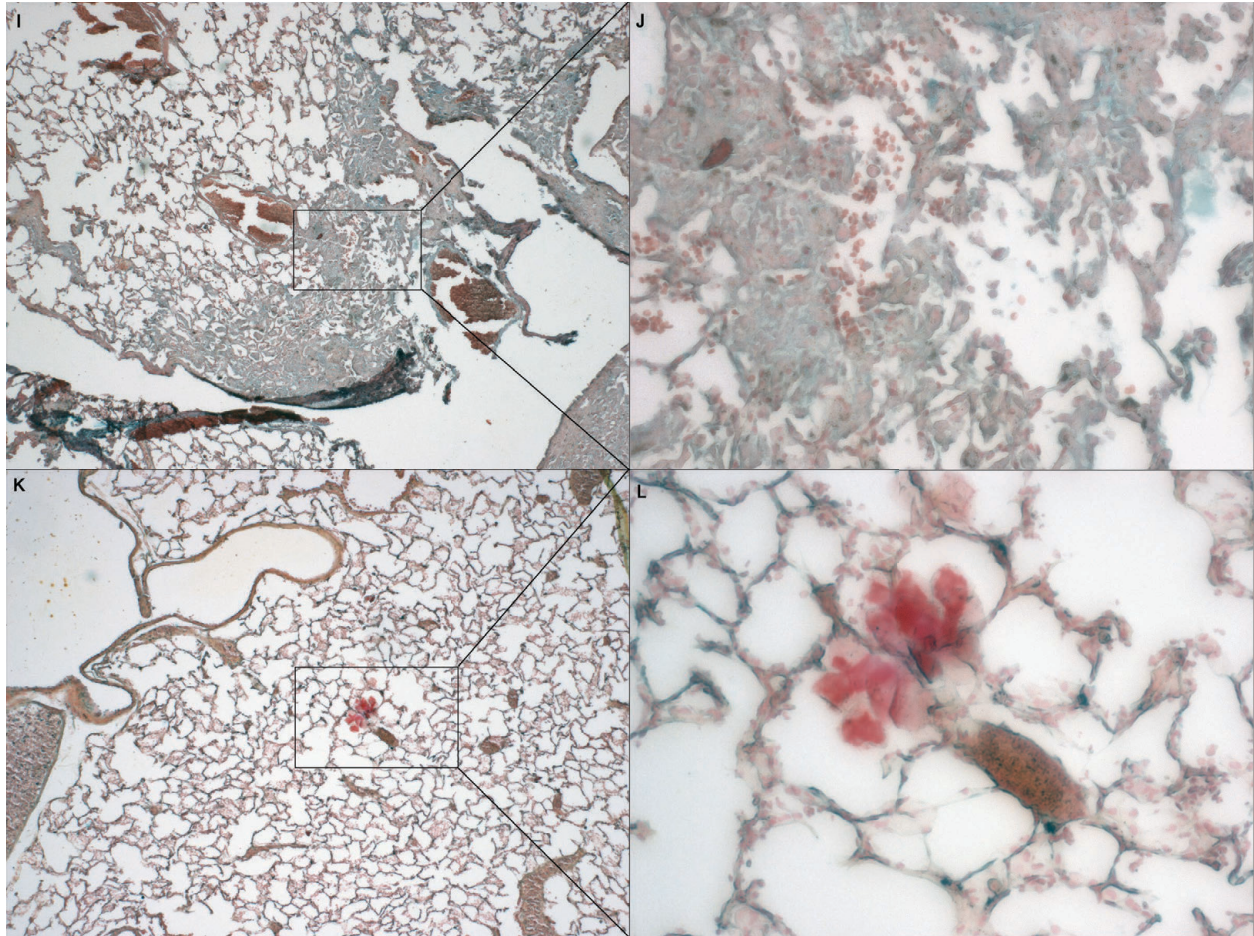


Fig. 5.7. Russell-Movat Pentachrome stain for fibrin in WT and PECAM-1 deficient, bleomycin-instilled FVB/n mice at 0.5U single-dose IT bleomycin treatment. Fibrin is stained in light pink to more intense red, with a more diffuse interspersion in the highly fibrotic areas.

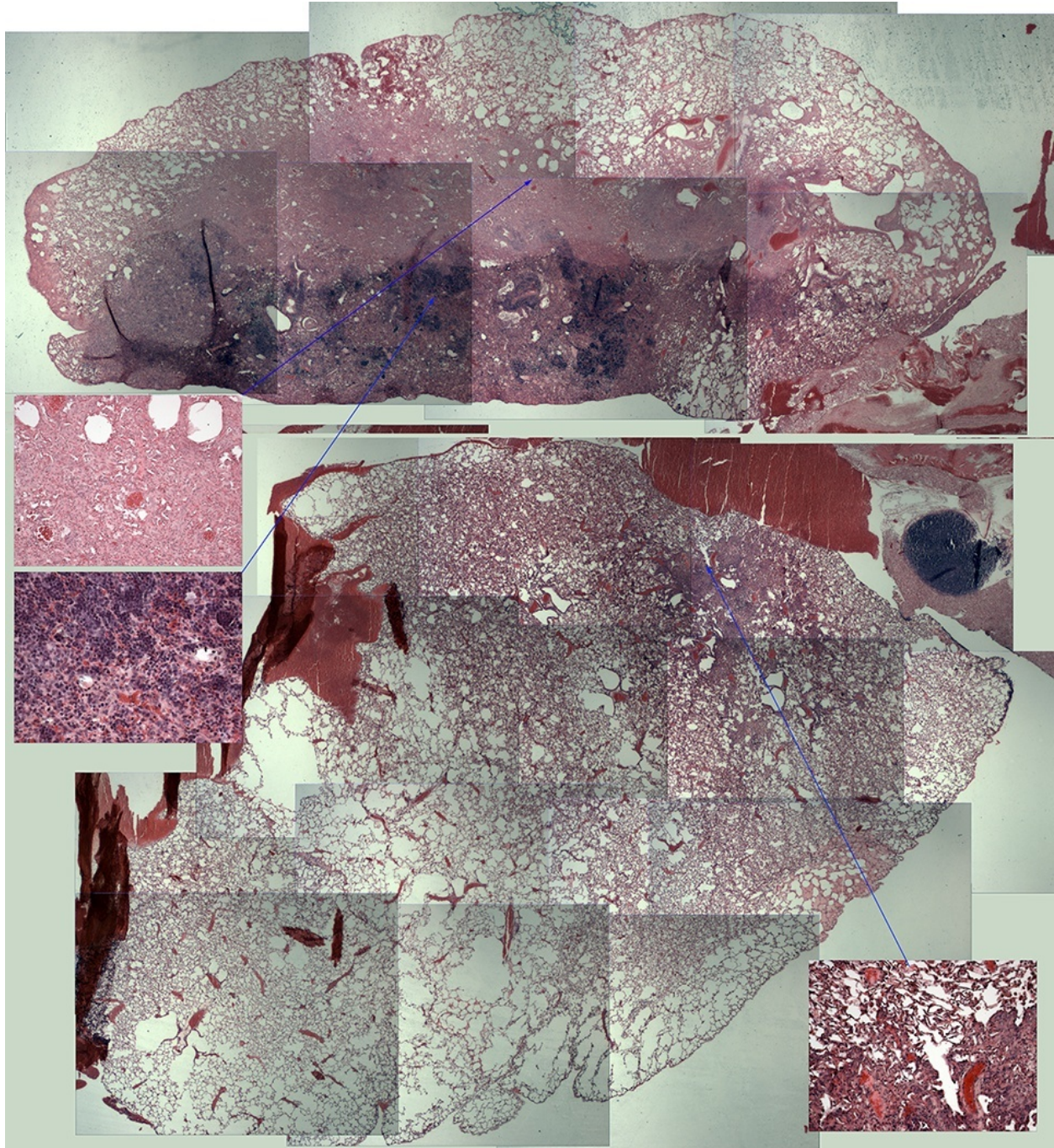


Fig. 5.8. Mosaic of Bleomycin-instilled PECAM-1 deficient FVB/n lung (top) and WT FVB/n lung (bottom) showing inflammatory infiltrate, areas of still preserved lung architecture, and areas of fibrosis at 0.5 U.

CHAPTER 6 - DISCUSSION AND FUTURE DIRECTIONS

These studies demonstrate microhemorrhaging into the alveoli to be an important step in initiation and progression of fibrotic disease in the lungs, thereby helping to further define the role of PECAM-1 in the regulation of pulmonary vascular barrier integrity.

One of the problems in diagnosing IPF in a clinical setting is that patients generally do not present with symptoms until IPF is already in its later stages, making treatment options even more limited. Likewise, our PECAM-1 deficient mice do not show clinical symptoms of pulmonary fibrosis until the later stages of the disease. The main goal of Specific Aim I was to test the sensitivity and accuracy of pulse oximetry in detecting the earliest disease stage. The importance of Specific Aim 1 lies in identifying the earlier stages of disease, where collagen deposition had either not yet occurred or is not yet extensive, and possible targets for drug intervention can be developed to preserve the normal lung architecture before it is replaced by scar tissue, which would be an easier proposition than trying to reestablish lung architecture that already has extensive collagen deposition.

Studies have shown that dysregulated coagulation plays a role in the development of pulmonary fibrotic disease. The Noth et al study has shown that anticoagulants, rather than helping, exacerbated the progress of disease in IPF patients to the point where the study had to be ended prematurely due to high morbidity/mortality [4]. At this time, IPF is not associated with PECAM-1 defects, however, given the data derived from PECAM-1 deficient FVB/n mice, sequencing human PECAM-1 would seem like a logical

step to see whether a particular human allele of PECAM-1 is associated with the IPF population. This project is being currently developed in our laboratory. If such an allele is identified, it may provide basis for genetic testing, early oxygenation monitoring, and possibly early drug intervention.

In 2003, a study of IPF patients, comprised of 8 women and 11 men, had found morphologic evidence of pulmonary capillary injury, with RBC extravasation and hemosiderin deposition identified by an iron stain, and fibrin deposition in intra-alveolar spaces, capillary walls, and/or lumens in all the patients in that study [104]. While Magro et al also believes the initiating events to start with an injury to the vascular endothelium, they propose a humoral-mediated mechanism for the initiation of vascular endothelial cell injury leading to endothelial cell apoptosis, while we propose that a possible defect in the functionality of PECAM-1 would lead to a weakness in vascular barrier, and possibly also increased apoptosis of endothelial cells, as PECAM-1 is inhibitory to apoptosis.

Hemosiderin-positive macrophages are also found in several other conditions. They are seen in the alveoli of individuals with left heart failure, where the left ventricle cannot handle the blood coming in from pulmonary veins, causing a backup, increasing the pressure in the alveolar capillaries, and leading to extravasated red blood cells, which are picked up by macrophages. They are also seen in people who chronically have pulmonary edema, since when the high pulmonary blood pressure is chronic, it forces red blood cell extravasation across the vascular barrier, and once more scavenging by

macrophages. Although hemosiderin-positive macrophages are present under those conditions, they are not exclusive to them. In general they are an indicator of a minor or a major hemorrhage - they are seen whenever macrophages engulf red blood cells and convert hemoglobin to hemosiderin for storage. One disease that is well-known for the presence of these cells is Idiopathic Pulmonary Hemosiderosis (IPH), which manifests mostly in children and usually shows reoccurring bouts of diffuse alveolar haemorrhage. It is associated with high mortality, and in many cases with resultant pulmonary fibrosis. It can also cause iron deficiency anaemia in addition to deposition of iron in the alveoli. Interestingly, this condition shows hemosiderin-positive macrophages in the alveoli without any evidence of nonspecific/granulomatous inflammation, or immunoglobulin deposition [133]. Corticosteroids and other immunosuppressants have been the mainstay treatment of IPH, although in recent years they have come under suspicion as being ineffective and possibly even detrimental [134, 135]. If IPH, like IPF, is connected to dysregulated repair, it may be that corticosteroids are pushing the macrophages towards the M2 and M2-like regulatory IL-10 upregulated phenotype, exacerbating the course of the disease.

Macrophages respond to signals of exposure to pathogens, signals of tissue damage, and signals from activated lymphocytes. They need to adaptively activate depending on what is needed - coordinated immune response, pathogen resistance, or tissue repair. In his 2009 review, Martinez et al describes increasing evidence for the plasticity of this cell type, which is now thought to oscillate in a range of activation status between the classic M1 and the alternative M2 [136]. Evidence shows that the M2 phenotype can

be induced by many additional stimulants, transforming growth factor beta- β , interleukin-10, and glucocorticoids [108]. Hemosiderin is particularly important here because it has been observed to affect macrophage polarization. Macrophages around areas of hemorrhages tend to skew towards the M2 phenotype, as in order to take up red blood cells they need upregulated expression of the receptors geared for iron uptake, transferrin receptor (TfR1) being one example, CD163 hemoglobin/haptoglobin receptor being another [114, 137].

Hemosiderin not only possibly affects macrophage polarization, but may also affect their signaling and communication with other cell types. M2 phenotype has lowered iron storage protein H ferritin, but upregulated expression of ferroportin, which is an iron exporter [114, 137]. Unlike the M1 phenotype, which sequesters iron to keep it unavailable to pathogens, the M2 phenotype is prone to release iron. Corna et al indicates that cytokines mediating macrophage polarization do in effect mediate iron usage, leading to either the M1 phenotype that holds on to its intracellular iron content (M1) and has low ability for iron uptake, or the M2 which has high capacity to take up and recycle iron [137]. Recalcati et al has shown that conditioned medium of M2 macrophages was supportive of faster growth in non-malignant and malignant cell lines. Since iron is an important co-factor for DNA synthesis, it may be that the alternatively activated macrophages might be releasing iron that is necessary for the tumor cells' high needs [138]. In a similar manner, it may be possible that the M2 macrophages are donating iron to fibroblasts/myofibroblasts for upregulation of collagen synthesis. Indeed, Prasse et al has shown that culture supernatants derived from alveolar

macrophages of IPF patients induced normal lung fibroblasts to increase collagen production [139]. Gibbons et al has shown that the human marker for alternative macrophage activation CD163 was not present on lung macrophages from healthy subjects, but was present on more than 90% of lung macrophages from IPF patients [140].

Additionally, Wynes et al has shown that M2 macrophages secrete insulin-like growth factor which protects myofibroblasts from apoptosis [141]. The M2 phenotype is well known to be a major producer and possibly main source of active TGF β [142], and Broekelmann et al has shown in a study with IPF patients, that TGF β_1 mRNA was present in macrophages that were around locations of fibroblastic activity, but that the locations themselves did not show signal for TGF β_1 mRNA [143]. It is possible that during the fibrotic process, the M2 phenotype secretes factors that promote both epithelial to mesenchymal transitioning, and fibroblast/myofibroblast survival [140]. In this way, the initial extravasation of red blood cells from compromised blood vessels could be providing a microenvironment that is conducive to M2 polarization, setting off a cascade of signaling events that are contributing to a dysregulated repair. This is also one of the reasons why steroid therapy has shown ineffective and even detrimental in the treatment of IPF, as glucocorticoids have been shown to polarize monocytes toward a M2 phenotype [144].

Hypoxia has been linked to increased IL-10 production, which possibly feeds into the vicious circle of: initial collagen deposition contributes to hypoxia, which raises levels of IL-10, leading to increased collagen deposition and further hypoxia.

One of the consequences of microhemorrhages is fibrin deposition. In a normal pulmonary environment, the vascular side tends to maintain an anti-coagulant environment, while the alveolar side support a pro-coagulant environment. There is also evidence that in the alveoli, alveolar macrophages themselves serve as sites of prothrombinase complexes assembly, thrombin generation and fibrin polymerization. In that, alveolar macrophages may be a significant source of fibrin deposition.

Interestingly, Takabayashi et al observed increased FXIII-A staining within M2 macrophages in their study of fibrin dysregulation and nasal polyps. They propose that overproduction of FXIII-A by M2 macrophages might contribute to the excessive fibrin deposition [145]

Fibrin deposition can contribute to pathology in multiple ways, such as occlusion of the vascular bed, rising pulmonary vascular resistance, and products of fibrin degradation serving as chemoattractants for fibroblasts in a dysregulated repair response which would be destructive to capillaries. Evidence in acute lung injury shows that within days the alveolar fibrin deposits become coated with fibronectin and possibly thrombospondin, which serves as in-signaling for migration and proliferation of fibroblasts in a well known repair response. Biopsies of ARDS patients and animals

studies show that this provisional matrix becomes replaced with collagen with 5 to 10 days post injury [120, 146].

Evidence from acute lung injury studies shows a consistent increase in procoagulant activity of alveolar macrophages, which may affect fibrin deposition by increased macrophage tissue factor expression, by availability of distal clotting factors, and/or increased permeability due to injury/vascular weakness. Studies from IPF patients have shown fibrin deposit accumulation around alveolar macrophages. It is still not clear how much increased macrophage procoagulant activity contributes to fibrin formation. Fibrinolytic activity appears reduced in the alveolar environments of IPF patients, which would favor formation, deposition, and ongoing buildup of fibrin [104].

In the disease of PECAM-1 deficient FVB/n mice, it ties in with our hypothesis of PECAM-1 being a critical molecule to the maintenance of vascular integrity and normal coagulation cascade, as the absence of PECAM-1 leads to microhemorrhages, which lead to accumulations of M2 macrophage populations, which leads to an increase in IL-10 secretion, which attracts fibroblastic cells, leading to collagen deposition, leading to hypoxic environment and further IL-10 upregulation, supporting the cycle; on the parallel path, microhemorrhages due to absence of PECAM-1 lead to fibrin deposition and degradation, which generates fibrin degradation products (FDP's), forming a provisional matrix and again attracting fibroblastic cells, leading to collagen deposition and further supporting a hypoxic environment.

To date, there is no known human PECAM-1 deficiency, although the question is whether such an occurrence would be a lethal mutation in humans, or on the contrary, that an individual with such a mutation would appear to be phenotypically normal. Heterozygous breeding in our animals produces an average of 10% FVB/n PECAM-1 deficient pups instead of the expected 25%. The DeLisser study demonstrated transiently-delayed alveolarization in the PECAM-1 deficient C57 mice [107], so there may be incomplete embryonic lethality during vascular and/or embryonal development. Incomplete embryonic lethality has been reported in association with other molecules [147], and in human this may be a lethal mutation as humans may lack murine compensatory mechanisms or there may be a difference in the need for tissue PECAM-1 expression. As the multifunctionality of PECAM-1 becomes more apparent, elucidating its role in embryonic development, fibrosis, coagulation, cancer signaling, immune function, and possibly many others will hopefully lead to new and personalized therapies for a number of human conditions,

6.1 Event timeline

PECAM-1 defect (or deficiency in our mice) leads to a weakness in endothelial cell adhesion and communication.

Under the right trigger (external as in particles in air, or internal such as an anticoagulant), it leads to a series of microhemorrhages in the lung -> red blood cells in alveoli.

The macrophages around the area of microhemorrhages - in the already anti-inflammatory environment of the lung - polarize towards M2 phenotype in order to efficiently ingest the red blood cells since iron left in tissue is toxic. In this way, iron is affecting their phenotype.

They store the iron as hemosiderin, but since they are not geared towards storage, they start using it to donate to the immediate microenvironment. External and internal exposure to iron/hemosiderin also possibly affects their signaling.

Being in this iron rich external and internal microenvironment, they are now solidly M2 phenotype, and upregulate production of IL-10 and TGF β , which attracts fibroblasts.

It is possible that as the M2 macrophages donate iron to their microenvironment, it is getting taken up by incoming fibroblasts and used to convert to a myofibroblast phenotype. In this way, iron may be affecting fibroblastic cell behavior.

As fibroblasts/myofibroblasts start collagen production, the lung becomes more stiff, there is more difficulty in respiration, and there is probably some degree of initial hypoxia.

Hypoxia has been shown to cause the M2s to increase IL-10 production. This may initially be taking place in small increments, one feeding the other, until there is more collagen deposited, leading to a more intense hypoxic environment, which perhaps

leads to a spike in IL-10 and a dramatic increase in repair activity. In this way it may build somewhat slowly at first, then increase, peak out, and plateau out when collagen deposition is very extensive.

The plateau may occur because extensive collagenation is not conducive to macrophage infiltration, so lessened numbers of macrophages lead to less of the products they manufacture. Perhaps that is why we observe more of them in the areas of still preserved lung architecture.

Fibrin deposition is a consequence of microhemorrhages, and the M2 macrophages may play a role here as well, having already been linked with increased fibrin deposition via increased Tissue Factor production.

Fibrin deposition contributes to pathology in the way of occlusion of the vascular bed, rising pulmonary vascular resistance, and most importantly - fibrin degradation products (FDPs) serving as additional chemoattractants for fibroblasts/myofibroblasts.

Fibrin deposition serves as basis for the formation of provisional matrix, which is when alveolar fibrin deposits become coated with fibronectin and possibly thrombospondin. Provisional matrix also serves as in-signaling for migration and proliferation of fibroblasts, as they aim to replace it with collagen.

Provisional matrix has been shown to be replaced with collagen in 5-10 days, in human and animal studies.

6.2 Issues and troubleshooting

One of the issues encountered in counting hemosiderin-positive macrophages stained with Prussian Blue stain is that the cells are often found in clusters, making it difficult to visualize each individual cell and making such analysis prone to user bias. To counter that, a method by Lezoray and Lecluse uses automatic classification of Prussian blue stained macrophages and additionally ranks them according to their Golde score, which is the degree of their hemosiderin content. The diagnosis of alveolar hemorrhage is made by increasing numbers of hemosiderin-positive macrophages [148]. Golde's score was established based on degree of hemosiderin content of macrophages stained with Prussian Blue stain [149, 150], where each macrophage is ranked on a scale of 0 to 4, with 0 = no stain, and 4 = heavy staining. The cells are then ranked on the scale of: 0 - no stain; 1 - pale blue stain in part of the cytoplasm; 2 - deep blue in a small portion of cell (appearance of a granule); 3 - deep blue throughout the cytoplasm; 4 - deep blue (sometimes almost black) permeating throughout. The total is then divided by two, generating the Golde score. An average of 200 cells is usually counted. Golde's score classifies alveolar hemorrhage as greater or equal to 20, and can be further classified as mild to severe when Golde's score is 20 to 100, or greater than 100 [151, 152]. Golde's score is best evaluated by automatic imaging software, to prevent qualitative evaluation error from human examiner. Most importantly, the automated imaging software method proposed by Lezoray and Lecluse separates and extracts clustered

cells, then ranks each cell according to the Golde score. The software works on the scheme of:

- A) Clustering - extracts the main features of the image according to color
- B) Spatial refinement - redefines the boundaries of clumped objects
- C) Cell separation - separates clumped or touching cells
- D) Cell classification - classifies cells according to their color and stain intensity and stain locale [153].

One of the challenges we have with our PECAM-1 deficient FVB/n model is its unpredictability. We presently do not know why some of the mice develop the disease and others do not, which makes for an uncontrolled experimental factor. Probably, there is an external or internal trigger we have not yet accounted for, which initiates the pathological events in these animals. Since mice have different levels of stress tolerance, and being that they are handled often, it may be that increased blood pressure and respiration in some of them triggers the events more so than in others. It may also be environmental triggers, such as microscopic particles present in their environment, where they may be exposed on a random basis. Although the environment at the animal housing facilities is clean, it is by no means sterile, and particulate matter can be brought in on the persons handling the animals.

Another challenge will lay in deciphering why PECAM-1 deficient C57BL/6 strain mice, unlike FVB/n strain mice, do not develop pulmonary disease. The PECAM-1 deficient C57BL/6 strain do demonstrate prolonged bleeding times and decreased vascular

integrity, as evidenced by several studies [9-11]. The C57BL/6 strain is capable of mounting a PECAM-1 independent inflammatory response, which maps to a region on chromosome 2 which contains several prostaglandin synthase genes [154], suggesting that prostaglandins may play a role in protection or susceptibility to pulmonary fibrotic development respectively in each strain.

Single-dose intratracheal bleomycin delivers an acutely damaging stimulus to the epithelium of the lung. Although many studies still hypothesize that the events are initiated by an inflammatory response to an epithelial damage, leading to epithelial to mesenchymal transition (EMT), leading to fibrotic response[155], others are investigating the alveolar structure as a whole microenvironment, with the damaging event stemming possibly from the vascular endothelium [1]. In light of the ineffectiveness of anti-inflammatory therapies as IPF treatment [156-159], current thinking is turning away from the inflammatory route towards the role of dysregulated coagulation - particularly focusing on the vascular endothelium, platelets, alveolar macrophages, and fibroblasts, and soluble clotting factors, with more of a supporting role from the epithelial cells (Chambers, 2008, Ruppert, *et al.*, 2008, Magro, *et al.*, 2006). Based on that it would seem more useful to administer a repeated low-dose IV bleomycin treatment to examine this inducer from the side of the endothelium rather than the epithelium. Provided there were enough animals, it would also be useful to add a group of vehicle control with both PECAM-1 deficient animals and the wild type mice. Prior to embarking on that, assessment of bleomycin hydrolase levels in these animals should be done, to compare it to other strains.

6.3 Current projects and future directions

6.3.1 Identification of cell type involvement in initiation and development of spontaneous pulmonary fibrosis in PECAM-1 deficient FVB/n mice.

The currently ongoing project that uses bone marrow chimeric mice and leukocyte depletion is being used to determine what role do endothelial cells versus bone marrow derived cells (leukocytes and platelets) play in the initiation and development of pulmonary disease in these animals.

6.3.2 Examine how PECAM-1 deficient FVB/n mice react to pollution-based pulmonary insult.

It is possible that in a genetically susceptible individual, environmental triggers may have more of a detriment than in non-susceptible population. In the disease initiation phase, the factor that is particularly important is to find the trigger that starts the disease process in these animals. Without it, this model suffers from an unpredictable experimental variable that is currently not under the control of the investigator. In trying to accomplish this, it may be important to look at both external and internal factors. Particulate matter 2.5 (PM 2.5), is an air pollutant composed of microscopic particles that are about two and one half microns wide. Particles of that size can permeate deeply into the lungs, and PM 2.5 has been shown to induce coagulation dependent fibrosis in SIRT1 deficient mouse model of pulmonary fibrosis [160]. The response of PECAM-1 deficient mice as compared to control WT could be ascertained by aerosol exposure of the animals to PM 2.5, to examine whether PM 2.5 would trigger

microhemorrhages in the PECAM-1 deficient animals. If PM 2.5 is consistently successful in triggering pulmonary fibrosis in PECAM-1 deficient mice, it would be interesting to see what effect it has on PECAM-1 reconstituted FVB/n mice.

6.3.3 Quantification of tissue Evans Blue concentration in lung tissue of PECAM-1 deficient FVB/N mice versus WT FVB/N mice

In order to test leakage in endothelial cell barrier function as a stimulus for the disease process in PECAM-1 deficient mice, we completed a series of low-dose instillations of histamine causing vascular leakage in the lung. Mice were injected (i.v.) with Evan's blue dye (100 μ l of 1% Evans blue dye in sterile saline) as an indicator. One hour later, the mice were anesthetized with ketamine/xylazine (i.p.) and treated intratracheally with 5 μ g or 500ng per kg of histamine hydrochloride in PBS. We were able to induce transient but measurable vascular leakage with histamine, as assessed by the presence of intravenous Evan's blue dye in broncho-alveolar lavage fluid. Higher doses of histamine were toxic as FVB/n mice are derived from a histamine sensitive strain (Jackson-Laboratory, 2009). However, this failed to induce disease in wild type and PECAM -/- mice, even with repeated doses, in long term studies. Therefore, we hypothesize that simple leakage is not enough to induce disease. However, simple fluid leakage of plasma does not contain the same components as a full capillary rupture (including cells, platelets, and thrombus formation).

It would be useful to employ this method, as described by Duan et al [161]. Briefly, Evans Blue dye binds with high affinity to serum albumin. In a case of compromised

vascular barrier, albumin-bound Evans Blue (30 mg/kg) relocates into pulmonary parenchyma and can thus be detected and quantified. For vascular leakage assessment in vivo, Evans blue dye can be injected into the external jugular vein X hours before euthanasia. Post euthanasia, the lungs are perfused of blood, dissected out, patted dry, weighed, and flash frozen in liquid nitrogen. The right lung is homogenized in PBS (1 ml/100 µg tissue), incubated in 2 volumes of formamide for dye extraction, centrifuged, and optical density of the supernatant can be read on spectrophotometer at 620 nm. Concentration of Evans Blue is then calculated against a standard curve in micrograms of Evans blue dye per gram of lung [161]. In that way, it can be assessed if there is any vascular leakage taking place slowly and naturally, without an inducing agent.

6.3.4 Quantification of BAL Evans Blue concentration in PECAM-1 deficient FVB/N mice versus WT FVB/N mice

In bronchoalveolar lavage, vascular leakage can be assessed by using the Bradford Assay to measure the total protein concentration in supernatants [161].

6.3.5 Identify coagulation mechanisms active in pulmonary fibrotic development.

Warfarin has been shown to exacerbate disease in IPF patients [4]. This trial would investigate how PECAM-1 deficient and WT FVB/n mice react to administration of warfarin.

6.3.6 Characterizing and quantifying macrophage populations

Macrophage polarization and marker expression is largely influenced by their environment [162]. Characterizing which macrophage phenotypic populations are present at each stage of disease in PECAM-1 deficient FVB/n mice and quantifying these populations would be important to establishing the role of these cells and their timeline in the disease process. Macrophage-specific surface markers combined with flow cytometry can be used to identify macrophages in tissue and to characterize their phenotype. For example, arginase I antibody could be used as a marker of M2 polarization, while iNOS antibody could be used as a marker for M1 polarization. Immunostaining and flow cytometry could be used to assess cell population numbers in BAL and tissue. ELISA immunoassay could be used to quantify cytokine levels.

6.3.7 Defining the role of M2 macrophages in the pulmonary environment

Clodronate-containing liposomes can be used to deplete alveolar macrophages, to assess the extent of their contribution to disease development. The advantage of this method is that it can be used in any mouse strain, and saves the time and financial expense of backcrossing mice onto a CD11b-DTR background. The disadvantage of this method is that clodronate-containing liposomes deplete both dendritic cells and all macrophages, so when looking for a specific scenario, other phenotypes need to be reconstituted by adoptive transfer. In that way, polarized macrophages can be derived *ex vivo* and transferred to mice via IV route [163].

6.3.8 Lineage tracing myofibroblast populations

Endothelial-mesenchymal transitioning (EndMT) has been implicated in various kinds of EndMT of fibrosis, specifically cardiac fibrosis and kidney fibrosis. Investigating whether endothelial cells may be significant contributors to myofibroblast populations in pulmonary fibrosis would be useful is determining the main source of these cells.

EndMT has also been implicated in the loss of endothelium, as has been documented in cases of spinal injury where vascular trauma at the place of injury creates lack of vascular support and generates secondary injury events that can lead to loss of tissue function. This cascade has been shown to strongly activate TGF β related signaling in endothelial cells [164]. Many approaches use EndMT induction agents such as TGF β . However, it would be informative to examine whether spontaneous EndMT is taking place in the spontaneously occurring disease of PECAM-1 deficient FVB/N mice, possibly due to increased TGF β signaling. Cell fate mapping methods can be used to trace EndMT in in this fibrosis model, and using multiple markers would differentiate myofibroblast populations per derivation. Since CD31 (PECAM-1) is usually most commonly used as an endothelial cell marker, and since that would not be possible to do in PECAM-1 deficient animals, two other markers unique to endothelial cells can be used, such as VE Cadherin (CD144), or thrombomodulin (CD141), to examine if they co-localize with α -SMA on myofibroblasts. Similarly, fibrocytes uniquely express the combination of CD45RO, 25F9, and S100A8/A9, but not PM-2K, and fibroblasts uniquely express the combination of CD90, cellular fibronectin, hyaluronan, and TE-7 [165].

6.4 Summary

The studies in this thesis use PECAM-1 deficient FVB/n mice as a novel model for characterizing the relationship between vascular barrier function, coagulation, and the development of pulmonary fibrosis. Chapter 3 shows a novel, non-invasive method for detecting disease in these animals, and shows the red blood cell presence in the alveoli and alveolar enlargement and early events in the fibrotic disease of these mice. Chapter 4 shows chronic microhemorrhaging into the alveolar spaces indicated by hemosiderin-positive macrophages, increasing as the disease progresses in these mice, indicating that PECAM-1 expression is important for the maintenance of normal vascular barrier function. Chapter 5 shows that PECAM-1 deficient and WT FVB/n mice were virtually the same in their resistance to single-dose IT bleomycin, indicating that the spontaneous disease in these animals is not a consequence of a single, large-scale inflammatory event. Since intratracheal instillation of bleomycin may depend on absorption and thus destroy the epithelium and not necessarily the endothelium, further studies are warranted using IV method of delivery to target the endothelium. These studies demonstrate microhemorrhaging into the alveoli to be an important step in initiation and progression of pulmonary fibrosis in the the absence of PECAM-1, showing the importance of studying PECAM-1 dysfunction in human pulmonary fibrosis.

CHAPTER 7 - REFERENCES

1. Strieter, R.M. and B. Mehrad, *New mechanisms of pulmonary fibrosis*. Chest, 2009. **136**(5): p. 1364-70.
2. Chambers, R.C., *Procoagulant signalling mechanisms in lung inflammation and fibrosis: novel opportunities for pharmacological intervention?* British Journal of Pharmacology, 2008. **153 Suppl 1**: p. S367-78.
3. Ruppert, C., et al., *Role of coagulation and fibrinolysis in lung and renal fibrosis*. Hamostaseologie, 2008. **28**(1-2): p. 30-2, 34-6.
4. Noth, I., et al., *A placebo-controlled randomized trial of warfarin in idiopathic pulmonary fibrosis*. American Journal of Respiratory and Critical Care Medicine, 2012. **186**(1): p. 88-95.
5. Moore, B.B. and C.M. Hogaboam, *Murine models of pulmonary fibrosis*. Am J Physiol Lung Cell Mol Physiol, 2008. **294**(2): p. L152-60.
6. Bringardner, B.D., et al., *The role of inflammation in the pathogenesis of idiopathic pulmonary fibrosis*. Antioxid Redox Signal, 2008. **10**(2): p. 287-301.
7. Early, M.A., et al., *Non-invasive diagnosis of early pulmonary disease in PECAM-deficient mice using infrared pulse oximetry*. Experimental and Molecular Pathology, 2009. **87**(2): p. 152-8.
8. Schenkel, A.R., et al., *Different susceptibilities of PECAM-deficient mouse strains to spontaneous idiopathic pneumonitis*. Experimental and Molecular Pathology, 2006. **81**(1): p. 23-30.

9. Graesser, D., et al., *Altered vascular permeability and early onset of experimental autoimmune encephalomyelitis in PECAM-1-deficient mice*. Journal of Clinical Investigation, 2002. **109**(3): p. 383-92.
10. Mahooti, S., et al., *PECAM-1 (CD31) expression modulates bleeding time in vivo*. American Journal of Pathology, 2000. **157**(1): p. 75-81.
11. Carrithers, M., et al., *Enhanced susceptibility to endotoxic shock and impaired STAT3 signaling in CD31-deficient mice*. American Journal of Pathology, 2005. **166**(1): p. 185-96.
12. Bogen, S., et al., *Monoclonal antibody to murine PECAM-1 (CD31) blocks acute inflammation in vivo*. Journal of Experimental Medicine, 1994. **179**(3): p. 1059-64.
13. Muller, W.A., *The role of PECAM-1 (CD31) in leukocyte emigration: studies in vitro and in vivo*. Journal of Leukocyte Biology, 1995. **57**(4): p. 523-8.
14. Ilan, N., et al., *PECAM-1 shedding during apoptosis generates a membrane-anchored truncated molecule with unique signaling characteristics*. FASEB Journal, 2001. **15**(2): p. 362-72.
15. Zocchi, M.R. and A. Poggi, *PECAM-1, apoptosis and CD34+ precursors*. Leukemia and Lymphoma, 2004. **45**(11): p. 2205-13.
16. Ming, Z., et al., *Lyn and PECAM-1 function as interdependent inhibitors of platelet aggregation*. Blood, 2011. **117**(14): p. 3903-6.
17. Aird, W.C., *Phenotypic heterogeneity of the endothelium: I. Structure, function, and mechanisms*. Circulation Research, 2007. **100**(2): p. 158-73.
18. Aird, W.C., *Endothelium as an organ system*. Critical Care Medicine, 2004. **32**(5 Suppl): p. S271-9.

19. Aird, W.C., *Endothelium in health and disease*. Pharmacol Rep, 2008. **60**(1): p. 139-43.
20. Aird, W.C., *Molecular heterogeneity of tumor endothelium*. Cell and Tissue Research, 2009. **335**(1): p. 271-81.
21. Aird, W.C., *Phenotypic heterogeneity of the endothelium: II. Representative vascular beds*. Circulation Research, 2007. **100**(2): p. 174-90.
22. Wilkinson, R., et al., *Platelet endothelial cell adhesion molecule-1 (PECAM-1/CD31) acts as a regulator of B-cell development, B-cell antigen receptor (BCR)-mediated activation, and autoimmune disease*. Blood, 2002. **100**(1): p. 184-93.
23. Albelda, S.M., et al., *EndoCAM: a novel endothelial cell-cell adhesion molecule*. Journal of Cell Biology, 1990. **110**(4): p. 1227-37.
24. Muller, W.A., et al., *A human endothelial cell-restricted, externally disposed plasmalemmal protein enriched in intercellular junctions*. Journal of Experimental Medicine, 1989. **170**(2): p. 399-414.
25. Newman, P.J., et al., *PECAM-1 (CD31) cloning and relation to adhesion molecules of the immunoglobulin gene superfamily*. Science, 1990. **247**(4947): p. 1219-22.
26. Sheibani, N., C.M. Sorenson, and W.A. Frazier, *Tissue specific expression of alternatively spliced murine PECAM-1 isoforms*. Developmental Dynamics, 1999. **214**(1): p. 44-54.
27. Jackson, D.E., *The unfolding tale of PECAM-1*. FEBS Letters, 2003. **540**(1-3): p. 7-14.

28. Muller, W.A., et al., *PECAM-1 is required for transendothelial migration of leukocytes*. Journal of Experimental Medicine, 1993. **178**(2): p. 449-60.
29. Newman, P.J., *Switched at birth: a new family for PECAM-1*. Journal of Clinical Investigation, 1999. **103**(1): p. 5-9.
30. Cao, M.Y., et al., *Regulation of mouse PECAM-1 tyrosine phosphorylation by the Src and Csk families of protein-tyrosine kinases*. Journal of Biological Chemistry, 1998. **273**(25): p. 15765-72.
31. Wang, Y. and N. Sheibani, *PECAM-1 isoform-specific activation of MAPK/ERKs and small GTPases: implications in inflammation and angiogenesis*. Journal of Cellular Biochemistry, 2006. **98**(2): p. 451-68.
32. Woodfin, A., M.B. Voisin, and S. Nourshargh, *PECAM-1: a multi-functional molecule in inflammation and vascular biology*. Arteriosclerosis, Thrombosis, and Vascular Biology, 2007. **27**(12): p. 2514-23.
33. Yan, H.C., et al., *Alternative splicing of a specific cytoplasmic exon alters the binding characteristics of murine platelet/endothelial cell adhesion molecule-1 (PECAM-1)*. Journal of Biological Chemistry, 1995. **270**(40): p. 23672-80.
34. Yan, H.C., et al., *Localization of multiple functional domains on human PECAM-1 (CD31) by monoclonal antibody epitope mapping*. Cell Adhesion and Communication, 1995. **3**(1): p. 45-66.
35. Piali, L., et al., *Endothelial vascular cell adhesion molecule 1 expression is suppressed by melanoma and carcinoma*. Journal of Experimental Medicine, 1995. **181**(2): p. 811-6.

36. Piali, L., et al., *CD31/PECAM-1 is a ligand for alpha v beta 3 integrin involved in adhesion of leukocytes to endothelium*. *Journal of Cell Biology*, 1995. **130**(2): p. 451-60.
37. Deaglio, S., et al., *Human CD38 (ADP-ribosyl cyclase) is a counter-receptor of CD31, an Ig superfamily member*. *Journal of Immunology*, 1998. **160**(1): p. 395-402.
38. Wong, C.W., et al., *PECAM-1/CD31 trans-homophilic binding at the intercellular junctions is independent of its cytoplasmic domain; evidence for heterophilic interaction with integrin alphavbeta3 in Cis*. *Molecular Biology of the Cell*, 2000. **11**(9): p. 3109-21.
39. Tanaka, Y., et al., *CD31 expressed on distinctive T cell subsets is a preferential amplifier of beta 1 integrin-mediated adhesion*. *Journal of Experimental Medicine*, 1992. **176**(1): p. 245-53.
40. Sheibani, N. and W.A. Frazier, *Thrombospondin-1, PECAM-1, and regulation of angiogenesis*. *Histology and Histopathology*, 1999. **14**(1): p. 285-94.
41. Berman, M.E., Y. Xie, and W.A. Muller, *Roles of platelet/endothelial cell adhesion molecule-1 (PECAM-1, CD31) in natural killer cell transendothelial migration and beta 2 integrin activation*. *Journal of Immunology*, 1996. **156**(4): p. 1515-24.
42. Piali, L., et al., *Murine platelet endothelial cell adhesion molecule (PECAM-1)/CD31 modulates beta 2 integrins on lymphokine-activated killer cells*. *European Journal of Immunology*, 1993. **23**(10): p. 2464-71.

43. Varon, D., et al., *Platelet/endothelial cell adhesion molecule-1 serves as a costimulatory agonist receptor that modulates integrin-dependent adhesion and aggregation of human platelets*. *Blood*, 1998. **91**(2): p. 500-7.
44. Zhao, T. and P.J. Newman, *Integrin activation by regulated dimerization and oligomerization of platelet endothelial cell adhesion molecule (PECAM)-1 from within the cell*. *Journal of Cell Biology*, 2001. **152**(1): p. 65-73.
45. Dangerfield, J., et al., *PECAM-1 (CD31) homophilic interaction up-regulates alpha6beta1 on transmigrated neutrophils in vivo and plays a functional role in the ability of alpha6 integrins to mediate leukocyte migration through the perivascular basement membrane*. *Journal of Experimental Medicine*, 2002. **196**(9): p. 1201-11.
46. Wee, J.L. and D.E. Jackson, *The Ig-ITIM superfamily member PECAM-1 regulates the "outside-in" signaling properties of integrin alpha(IIb)beta3 in platelets*. *Blood*, 2005. **106**(12): p. 3816-23.
47. DeLisser, H.M., et al., *Deletions in the cytoplasmic domain of platelet-endothelial cell adhesion molecule-1 (PECAM-1, CD31) result in changes in ligand binding properties*. *Journal of Cell Biology*, 1994. **124**(1-2): p. 195-203.
48. DeLisser, H.M., P.J. Newman, and S.M. Albelda, *Molecular and functional aspects of PECAM-1/CD31*. *Immunology Today*, 1994. **15**(10): p. 490-5.
49. Famiglietti, J., et al., *Tyrosine residue in exon 14 of the cytoplasmic domain of platelet endothelial cell adhesion molecule-1 (PECAM-1/CD31) regulates ligand binding specificity*. *Journal of Cell Biology*, 1997. **138**(6): p. 1425-35.

50. Sun, J., et al., *Contributions of the extracellular and cytoplasmic domains of platelet-endothelial cell adhesion molecule-1 (PECAM-1/CD31) in regulating cell-cell localization*. Journal of Cell Science, 2000. **113 (Pt 8)**: p. 1459-69.
51. Newman, D.K., C. Hamilton, and P.J. Newman, *Inhibition of antigen-receptor signaling by Platelet Endothelial Cell Adhesion Molecule-1 (CD31) requires functional ITIMs, SHP-2, and p56(lck)*. Blood, 2001. **97(8)**: p. 2351-7.
52. Newton-Nash, D.K. and P.J. Newman, *A new role for platelet-endothelial cell adhesion molecule-1 (CD31): inhibition of TCR-mediated signal transduction*. Journal of Immunology, 1999. **163(2)**: p. 682-8.
53. Newman, P.J., *The role of PECAM-1 in vascular cell biology*. Annals of the New York Academy of Sciences, 1994. **714**: p. 165-74.
54. Schimmenti, L.A., et al., *Platelet endothelial cell adhesion molecule, PECAM-1, modulates cell migration*. Journal of Cellular Physiology, 1992. **153(2)**: p. 417-28.
55. Gratzinger, D., M. Barreuther, and J.A. Madri, *Platelet-endothelial cell adhesion molecule-1 modulates endothelial migration through its immunoreceptor tyrosine-based inhibitory motif*. Biochemical and Biophysical Research Communications, 2003. **301(1)**: p. 243-9.
56. Kim, C.S., T. Wang, and J.A. Madri, *Platelet endothelial cell adhesion molecule-1 expression modulates endothelial cell migration in vitro*. Laboratory Investigation, 1998. **78(5)**: p. 583-90.
57. Lu, T.T., L.G. Yan, and J.A. Madri, *Integrin engagement mediates tyrosine dephosphorylation on platelet-endothelial cell adhesion molecule 1*. Proceedings

- of the National Academy of Sciences of the United States of America, 1996. **93** (21): p. 11808-13.
58. DiMaio, T.A. and N. Sheibani, *PECAM-1 isoform-specific functions in PECAM-1-deficient brain microvascular endothelial cells*. *Microvascular Research*, 2008. **75** (2): p. 188-201.
59. Kondo, S., et al., *PECAM-1 isoform-specific regulation of kidney endothelial cell migration and capillary morphogenesis*. *Am J Physiol Cell Physiol*, 2007. **292**(6): p. C2070-83.
60. Ilan, N., et al., *PECAM-1 (CD31) functions as a reservoir for and a modulator of tyrosine-phosphorylated beta-catenin*. *Journal of Cell Science*, 1999. **112 Pt 18**: p. 3005-14.
61. Albelda, S.M. and C.A. Buck, *Integrins and other cell adhesion molecules*. *FASEB Journal*, 1990. **4**(11): p. 2868-80.
62. Noble, K.E., et al., *Monocytes stimulate expression of the Bcl-2 family member, A1, in endothelial cells and confer protection against apoptosis*. *Journal of Immunology*, 1999. **162**(3): p. 1376-83.
63. Gao, C., et al., *PECAM-1 functions as a specific and potent inhibitor of mitochondrial-dependent apoptosis*. *Blood*, 2003. **102**(1): p. 169-79.
64. Brown, S., et al., *Apoptosis disables CD31-mediated cell detachment from phagocytes promoting binding and engulfment*. *Nature*, 2002. **418**(6894): p. 200-3.
65. Chimini, G., *Apoptosis: repulsive encounters*. *Nature*, 2002. **418**(6894): p. 139-41.

66. Newman, P.J., et al., *Activation-dependent changes in human platelet PECAM-1: phosphorylation, cytoskeletal association, and surface membrane redistribution.* Journal of Cell Biology, 1992. **119**(1): p. 239-46.
67. Kalra, V.K., et al., *Hypoxia induces PECAM-1 phosphorylation and transendothelial migration of monocytes.* American Journal of Physiology, 1996. **271**(5 Pt 2): p. H2025-34.
68. Rattan, V., et al., *Glucose-induced transmigration of monocytes is linked to phosphorylation of PECAM-1 in cultured endothelial cells.* American Journal of Physiology, 1996. **271**(4 Pt 1): p. E711-7.
69. Maas, M., et al., *Endothelial cell PECAM-1 confers protection against endotoxic shock.* Am J Physiol Heart Circ Physiol, 2005. **288**(1): p. H159-64.
70. Duncan, G.S., et al., *Genetic evidence for functional redundancy of Platelet/Endothelial cell adhesion molecule-1 (PECAM-1): CD31-deficient mice reveal PECAM-1-dependent and PECAM-1-independent functions.* Journal of Immunology, 1999. **162**(5): p. 3022-30.
71. Thompson, R.D., et al., *Platelet-endothelial cell adhesion molecule-1 (PECAM-1)-deficient mice demonstrate a transient and cytokine-specific role for PECAM-1 in leukocyte migration through the perivascular basement membrane.* Blood, 2001. **97**(6): p. 1854-60.
72. Solowiej, A., et al., *Lack of platelet endothelial cell adhesion molecule-1 attenuates foreign body inflammation because of decreased angiogenesis.* American Journal of Pathology, 2003. **162**(3): p. 953-62.

73. Tran, R., et al., *Biomechanics of haemostasis and thrombosis in health and disease: from the macro- to molecular scale*. J Cell Mol Med, 2013. **17**(5): p. 579-96.
74. Jones, K.L., et al., *Platelet endothelial cell adhesion molecule-1 is a negative regulator of platelet-collagen interactions*. Blood, 2001. **98**(5): p. 1456-63.
75. DeLisser, H.M., et al., *Involvement of endothelial PECAM-1/CD31 in angiogenesis*. American Journal of Pathology, 1997. **151**(3): p. 671-7.
76. Sheibani, N., P.J. Newman, and W.A. Frazier, *Thrombospondin-1, a natural inhibitor of angiogenesis, regulates platelet-endothelial cell adhesion molecule-1 expression and endothelial cell morphogenesis*. Molecular Biology of the Cell, 1997. **8**(7): p. 1329-41.
77. Kelleher, J.F., *Pulse oximetry*. Journal of Clinical Monitoring, 1989. **5**(1): p. 37-62.
78. Zisman, D.A., et al., *Prediction of pulmonary hypertension in idiopathic pulmonary fibrosis*. Respiratory Medicine, 2007. **101**(10): p. 2153-9.
79. Lama, V.N., et al., *Prognostic value of desaturation during a 6-minute walk test in idiopathic interstitial pneumonia*. American Journal of Respiratory and Critical Care Medicine, 2003. **168**(9): p. 1084-90.
80. Stephan, S., et al., *Oxygen desaturation during a 4-minute step test: predicting survival in idiopathic pulmonary fibrosis*. Sarcoidosis, Vasculitis, and Diffuse Lung Diseases, 2007. **24**(1): p. 70-6.
81. Newman, P.J. and D.K. Newman, *Signal transduction pathways mediated by PECAM-1: new roles for an old molecule in platelet and vascular cell biology*. Arteriosclerosis, Thrombosis, and Vascular Biology, 2003. **23**(6): p. 953-64.

82. Bird, I.N., et al., *Homophilic PECAM-1(CD31) interactions prevent endothelial cell apoptosis but do not support cell spreading or migration*. Journal of Cell Science, 1999. **112 (Pt 12)**: p. 1989-97.
83. Kiernan, J.A., *Histological and histochemical methods : theory and practice*. 3rd ed. 1999, Oxford ; Boston: Butterworth Heinemann. x, 502 p.
84. Chu, V., et al., *Method for non-invasively recording electrocardiograms in conscious mice*. BMC Physiol, 2001. **1**: p. 6.
85. Mitchell, G.F., A. Jeron, and G. Koren, *Measurement of heart rate and Q-T interval in the conscious mouse*. American Journal of Physiology, 1998. **274**(3 Pt 2): p. H747-51.
86. Murray, L.A., et al., *Deleterious role of TLR3 during hyperoxia-induced acute lung injury*. American Journal of Respiratory and Critical Care Medicine, 2008. **178** (12): p. 1227-37.
87. Grimm, P.C., et al., *Computerized image analysis of Sirius Red-stained renal allograft biopsies as a surrogate marker to predict long-term allograft function*. Journal of the American Society of Nephrology, 2003. **14**(6): p. 1662-8.
88. Junqueira, L.C., G. Bignolas, and R.R. Brentani, *Picrosirius staining plus polarization microscopy, a specific method for collagen detection in tissue sections*. Histochemical Journal, 1979. **11**(4): p. 447-55.
89. Junquiera, L.C., L.C. Junqueira, and R.R. Brentani, *A simple and sensitive method for the quantitative estimation of collagen*. Analytical Biochemistry, 1979. **94**(1): p. 96-9.

90. Whittaker, P., *Unravelling the mysteries of collagen and cicatrix after myocardial infarction*. Cardiovascular Research, 1995. **29**(6): p. 758-62.
91. Whittaker, P., et al., *Quantitative assessment of myocardial collagen with picrosirius red staining and circularly polarized light*. Basic Research in Cardiology, 1994. **89**(5): p. 397-410.
92. Chibbar, R., et al., *Nonspecific interstitial pneumonia and usual interstitial pneumonia with mutation in surfactant protein C in familial pulmonary fibrosis*. Modern Pathology, 2004. **17**(8): p. 973-80.
93. Jackson, D.E., et al., *Platelet endothelial cell adhesion molecule-1 (PECAM-1/CD31) is associated with a naive B-cell phenotype in human tonsils*. Tissue Antigens, 2000. **56**(2): p. 105-16.
94. Demeure, C.E., et al., *CD31 (PECAM-1) is a differentiation antigen lost during human CD4 T-cell maturation into Th1 or Th2 effector cells*. Immunology, 1996. **88**(1): p. 110-5.
95. Fornasa, G., et al., *TCR stimulation drives cleavage and shedding of the ITIM receptor CD31*. Journal of Immunology, 2010. **184**(10): p. 5485-92.
96. Bergom, C., et al., *An alternatively spliced isoform of PECAM-1 is expressed at high levels in human and murine tissues, and suggests a novel role for the C-terminus of PECAM-1 in cytoprotective signaling*. Journal of Cell Science, 2008. **121**(Pt 8): p. 1235-42.
97. Newton, J.P., et al., *Residues on both faces of the first immunoglobulin fold contribute to homophilic binding sites of PECAM-1/CD31*. Journal of Biological Chemistry, 1997. **272**(33): p. 20555-63.

98. Sun, Q.H., et al., *Individually distinct Ig homology domains in PECAM-1 regulate homophilic binding and modulate receptor affinity*. Journal of Biological Chemistry, 1996. **271**(19): p. 11090-8.
99. Boon, K., et al., *Molecular phenotypes distinguish patients with relatively stable from progressive idiopathic pulmonary fibrosis (IPF)*. PLoS One, 2009. **4**(4): p. e5134.
100. Bogatkevich, G.S., et al., *Thrombin differentiates normal lung fibroblasts to a myofibroblast phenotype via the proteolytically activated receptor-1 and a protein kinase C-dependent pathway*. Journal of Biological Chemistry, 2001. **276**(48): p. 45184-92.
101. Barbarin, V., et al., *Pulmonary overexpression of IL-10 augments lung fibrosis and Th2 responses induced by silica particles*. Am J Physiol Lung Cell Mol Physiol, 2005. **288**(5): p. L841-8.
102. Singh, S.R. and I.P. Hall, *Airway myofibroblasts and their relationship with airway myocytes and fibroblasts*. Proc Am Thorac Soc, 2008. **5**(1): p. 127-32.
103. Ina, K., et al., *Intestinal fibroblast-derived IL-10 increases survival of mucosal T cells by inhibiting growth factor deprivation- and Fas-mediated apoptosis*. Journal of Immunology, 2005. **175**(3): p. 2000-9.
104. Magro, C.M., et al., *Idiopathic pulmonary fibrosis related to endothelial injury and antiendothelial cell antibodies*. Human Immunology, 2006. **67**(4-5): p. 284-97.
105. Idell, S., *Coagulation, fibrinolysis, and fibrin deposition in acute lung injury*. Critical Care Medicine, 2003. **31**(4 Suppl): p. S213-20.

106. Privratsky, J.R., et al., *Relative contribution of PECAM-1 adhesion and signaling to the maintenance of vascular integrity*. Journal of Cell Science, 2011. **124**(Pt 9): p. 1477-85.
107. DeLisser, H.M., et al., *Loss of PECAM-1 function impairs alveolarization*. Journal of Biological Chemistry, 2006. **281**(13): p. 8724-31.
108. Mosser, D.M. and J.P. Edwards, *Exploring the full spectrum of macrophage activation*. Nat Rev Immunol, 2008. **8**(12): p. 958-69.
109. Edwards, J.P., et al., *Biochemical and functional characterization of three activated macrophage populations*. Journal of Leukocyte Biology, 2006. **80**(6): p. 1298-307.
110. Gordon, S. and F.O. Martinez, *Alternative activation of macrophages: mechanism and functions*. Immunity, 2010. **32**(5): p. 593-604.
111. Mora, A.L., et al., *Activation of alveolar macrophages via the alternative pathway in herpesvirus-induced lung fibrosis*. American Journal of Respiratory Cell and Molecular Biology, 2006. **35**(4): p. 466-73.
112. Shaykhiev, R., et al., *Smoking-dependent reprogramming of alveolar macrophage polarization: implication for pathogenesis of chronic obstructive pulmonary disease*. Journal of Immunology, 2009. **183**(4): p. 2867-83.
113. Vergadi, E., et al., *Early macrophage recruitment and alternative activation are critical for the later development of hypoxia-induced pulmonary hypertension*. Circulation, 2011. **123**(18): p. 1986-95.
114. Gaetano, C., L. Massimo, and M. Alberto, *Control of iron homeostasis as a key component of macrophage polarization*. Haematologica, 2010. **95**(11): p. 1801-3.

115. John, M., et al., *Inhaled corticosteroids increase interleukin-10 but reduce macrophage inflammatory protein-1alpha, granulocyte-macrophage colony-stimulating factor, and interferon-gamma release from alveolar macrophages in asthma*. American Journal of Respiratory and Critical Care Medicine, 1998. **157** (1): p. 256-62.
116. Hanzlick, R. and K. Delaney, *Pulmonary hemosiderin in deceased infants: baseline data for further study of infant mortality*. American Journal of Forensic Medicine and Pathology, 2000. **21**(4): p. 319-22.
117. Schluckebier, D.A., et al., *Pulmonary siderophages and unexpected infant death*. American Journal of Forensic Medicine and Pathology, 2002. **23**(4): p. 360-3.
118. Moeller, A., et al., *The bleomycin animal model: a useful tool to investigate treatment options for idiopathic pulmonary fibrosis?* International Journal of Biochemistry and Cell Biology, 2008. **40**(3): p. 362-82.
119. Meadors, M., J. Floyd, and M.C. Perry, *Pulmonary toxicity of chemotherapy*. Seminars in Oncology, 2006. **33**(1): p. 98-105.
120. Swaisgood, C.M., et al., *The development of bleomycin-induced pulmonary fibrosis in mice deficient for components of the fibrinolytic system*. American Journal of Pathology, 2000. **157**(1): p. 177-87.
121. Hoyt, D.G. and J.S. Lazo, *Murine strain differences in acute lung injury and activation of poly(ADP-ribose) polymerase by in vitro exposure of lung slices to bleomycin*. American Journal of Respiratory Cell and Molecular Biology, 1992. **7** (6): p. 645-51.

122. Phan, S.H., et al., *A comparative study of pulmonary fibrosis induced by bleomycin and an O₂ metabolite producing enzyme system*. *Chest*, 1983. **83**(5 Suppl): p. 44S-45S.
123. Phan, S.H., et al., *Effect of the beige mutation on bleomycin-induced pulmonary fibrosis in mice*. *American Review of Respiratory Disease*, 1983. **127**(4): p. 456-9.
124. Schrier, D.J., R.G. Kunkel, and S.H. Phan, *The role of strain variation in murine bleomycin-induced pulmonary fibrosis*. *American Review of Respiratory Disease*, 1983. **127**(1): p. 63-6.
125. Schrier, D.J., S.H. Phan, and B.M. McGarry, *The effects of the nude (nu/nu) mutation on bleomycin-induced pulmonary fibrosis. A biochemical evaluation*. *American Review of Respiratory Disease*, 1983. **127**(5): p. 614-7.
126. Harrison, J.H., Jr. and J.S. Lazo, *Plasma and pulmonary pharmacokinetics of bleomycin in murine strains that are sensitive and resistant to bleomycin-induced pulmonary fibrosis*. *Journal of Pharmacology and Experimental Therapeutics*, 1988. **247**(3): p. 1052-8.
127. Peters, L.J., et al., *Acute and late toxicity associated with sequential bleomycin-containing chemotherapy regimens and radiation therapy in the treatment of carcinoma of the nasopharynx*. *International Journal of Radiation Oncology, Biology, Physics*, 1988. **14**(4): p. 623-33.
128. Adamson, I.Y., *Pulmonary toxicity of bleomycin*. *Environmental Health Perspectives*, 1976. **16**: p. 119-26.

129. Weiner, R.E., et al., *Early detection of bleomycin-induced lung injury in rat using indium-111-labeled antibody directed against intercellular adhesion molecule-1*. Journal of Nuclear Medicine, 1998. **39**(4): p. 723-8.
130. Wynn, T.A., *Integrating mechanisms of pulmonary fibrosis*. Journal of Experimental Medicine, 2011. **208**(7): p. 1339-50.
131. Kolodsick, J.E., et al., *Prostaglandin E2 inhibits fibroblast to myofibroblast transition via E. prostanoid receptor 2 signaling and cyclic adenosine monophosphate elevation*. American Journal of Respiratory Cell and Molecular Biology, 2003. **29**(5): p. 537-44.
132. Oppenheimer-Marks, N., A.F. Kavanaugh, and P.E. Lipsky, *Inhibition of the transendothelial migration of human T lymphocytes by prostaglandin E2*. Journal of Immunology, 1994. **152**(12): p. 5703-13.
133. Ioachimescu, O.C., S. Sieber, and A. Kotch, *Idiopathic pulmonary haemosiderosis revisited*. European Respiratory Journal, 2004. **24**(1): p. 162-70.
134. Richeldi, L., et al., *Corticosteroids for idiopathic pulmonary fibrosis*. Cochrane Database Syst Rev, 2003(3): p. CD002880.
135. Papiris, S.A., et al., *Steroids in idiopathic pulmonary fibrosis acute exacerbation: defenders or killers?* American Journal of Respiratory and Critical Care Medicine, 2012. **185**(5): p. 587-8.
136. Martinez, F.O., L. Helming, and S. Gordon, *Alternative activation of macrophages: an immunologic functional perspective*. Annual Review of Immunology, 2009. **27**: p. 451-83.

137. Corna, G., et al., *Polarization dictates iron handling by inflammatory and alternatively activated macrophages*. *Haematologica*, 2010. **95**(11): p. 1814-22.
138. Recalcati, S., et al., *Differential regulation of iron homeostasis during human macrophage polarized activation*. *European Journal of Immunology*, 2010. **40**(3): p. 824-35.
139. Prasse, A., et al., *A vicious circle of alveolar macrophages and fibroblasts perpetuates pulmonary fibrosis via CCL18*. *American Journal of Respiratory and Critical Care Medicine*, 2006. **173**(7): p. 781-92.
140. Gibbons, M.A., et al., *Ly6Chi monocytes direct alternatively activated profibrotic macrophage regulation of lung fibrosis*. *American Journal of Respiratory and Critical Care Medicine*, 2011. **184**(5): p. 569-81.
141. Wynes, M.W., S.K. Frankel, and D.W. Riches, *IL-4-induced macrophage-derived IGF-I protects myofibroblasts from apoptosis following growth factor withdrawal*. *Journal of Leukocyte Biology*, 2004. **76**(5): p. 1019-27.
142. Sheppard, D., *Transforming growth factor beta: a central modulator of pulmonary and airway inflammation and fibrosis*. *Proc Am Thorac Soc*, 2006. **3**(5): p. 413-7.
143. Broekelmann, T.J., et al., *Transforming growth factor beta 1 is present at sites of extracellular matrix gene expression in human pulmonary fibrosis*. *Proceedings of the National Academy of Sciences of the United States of America*, 1991. **88**(15): p. 6642-6.
144. Vallelian, F., et al., *Glucocorticoid treatment skews human monocyte differentiation into a hemoglobin-clearance phenotype with enhanced heme-iron recycling and antioxidant capacity*. *Blood*, 2010. **116**(24): p. 5347-56.

145. Takabayashi, T., et al., *Increased expression of factor XIII-A in patients with chronic rhinosinusitis with nasal polyps*. Journal of Allergy and Clinical Immunology, 2013.
146. Matthay, M.A. and G.A. Zimmerman, *Acute lung injury and the acute respiratory distress syndrome: four decades of inquiry into pathogenesis and rational management*. American Journal of Respiratory Cell and Molecular Biology, 2005. **33**(4): p. 319-27.
147. Xue, J., et al., *Incomplete embryonic lethality and fatal neonatal hemorrhage caused by prothrombin deficiency in mice*. Proceedings of the National Academy of Sciences of the United States of America, 1998. **95**(13): p. 7603-7.
148. De Lassence, A., et al., *Alveolar hemorrhage. Diagnostic criteria and results in 194 immunocompromised hosts*. American Journal of Respiratory and Critical Care Medicine, 1995. **151**(1): p. 157-63.
149. Finley, T.N., et al., *Occult pulmonary hemorrhage in anticoagulated patients*. American Review of Respiratory Disease, 1975. **112**(1): p. 23-9.
150. Golde, D.W., et al., *Occult pulmonary haemorrhage in leukaemia*. British Medical Journal, 1975. **2**(5964): p. 166-8.
151. Moumouni, H., F. Lamotte, and P. Anthonioz, [*Sideroses of alveolar macrophages. Analysis of a continuous series of 360 bronchoalveolar lavages*]. Pathologie Biologie, 1993. **41**(7): p. 604-9.
152. Kahn, F.W., J.M. Jones, and D.M. England, *Diagnosis of pulmonary hemorrhage in the immunocompromised host*. American Review of Respiratory Disease, 1987. **136**(1): p. 155-60.

153. Lezoray, O.L.M., *Automatic Segmentation and Classification of Cells from Broncho Alveolar LAVAge*. Image Analysis and Stereology 2007. **26**(3): p. 111-119.
154. Seidman, M.A., et al., *PECAM-independent thioglycollate peritonitis is associated with a locus on murine chromosome 2*. PLoS One, 2009. **4**(1): p. e4316.
155. King, T.E., Jr., A. Pardo, and M. Selman, *Idiopathic pulmonary fibrosis*. Lancet, 2011. **378**(9807): p. 1949-61.
156. Selman, M. and A. Pardo, *Idiopathic pulmonary fibrosis: misunderstandings between epithelial cells and fibroblasts?* Sarcoidosis, Vasculitis, and Diffuse Lung Diseases, 2004. **21**(3): p. 165-72.
157. Selman, M., et al., *Idiopathic pulmonary fibrosis: pathogenesis and therapeutic approaches*. Drugs, 2004. **64**(4): p. 405-30.
158. Gauldie, J., M. Kolb, and P.J. Sime, *A new direction in the pathogenesis of idiopathic pulmonary fibrosis?* Respir Res, 2002. **3**: p. 1.
159. Raghu, G., *Idiopathic pulmonary fibrosis: guidelines for diagnosis and clinical management have advanced from consensus-based in 2000 to evidence-based in 2011*. European Respiratory Journal, 2011. **37**(4): p. 743-6.
160. Wu, Z., et al., *Sirt1 protects against thrombomodulin down-regulation and lung coagulation after particulate matter exposure*. Blood, 2012. **119**(10): p. 2422-9.
161. Duan, Y., et al., *Inhibition of Pyk2 blocks lung inflammation and injury in a mouse model of acute lung injury*. Respir Res, 2012. **13**: p. 4.
162. Guth, A.M., et al., *Lung environment determines unique phenotype of alveolar macrophages*. Am J Physiol Lung Cell Mol Physiol, 2009. **296**(6): p. L936-46.

163. Weisser, S.B., N. van Rooijen, and L.M. Sly, *Depletion and reconstitution of macrophages in mice*. J Vis Exp, 2012(66): p. 4105.
164. Benton, R.L., et al., *Transcriptional activation of endothelial cells by TGFbeta coincides with acute microvascular plasticity following focal spinal cord ischaemia/reperfusion injury*. ASN Neuro, 2009. 1(3).
165. Pilling, D., et al., *Identification of markers that distinguish monocyte-derived fibrocytes from monocytes, macrophages, and fibroblasts*. PLoS One, 2009. 4(10): p. e7475.